ROLE OF CXCL1 SIGNALING IN STROMA: EPITHELIUM INTERACTIONS DURING BREAST CANCER PROGRESSION

By

©2014

An Zou

B.S., Huazhong University of Science and Technology, 2008

Submitted to the graduate degree program in Pathology and Laboratory Medicine and the Graduate Faculty of the University of Kansas in partial fulfillment of the requirements for the degree of Doctor of Philosophy.

_____

Nikki Cheng, Ph.D.
Chairperson

_____

Benyi Li, Ph.D.

_____

Fariba Behbod, Pharm.D., Ph.D.

_____

Joan Lewis-Wambi, Ph.D.

_____

Timothy A. Fields, M.D., Ph.D.

Date Defended: August 29, 2014

The Dissertation Committee for An Zou

certifies that this is the approved version of the following dissertation:

ROLE OF CXCL1 SIGNALING IN STROMA: EPITHELIUM INTERACTIONS DURING BREAST CANCER PROGRESSION

_____

Nikki Cheng, Ph.D.
Chairperson

Date approved: August 29, 2014

Abstract

Enhanced expression of CXCL1 in tumor epithelium is associated with cell invasion and angiogenesis in melanoma, bladder, ovarian and breast cancer, yet CXCL1 expression in tumor associated stroma is largely undefined. In this dissertation, we show evidences that increased CXCL1 expression in breast cancer stroma correlates with poor patient prognosis, including increased rate of recurrence and shorter relapse-free survival, and co-localizes to alpha Smooth Muscle Actin (α-SMA) and Fibroblast Specific Protein 1 (FSP1) positive fibroblasts. Fibroblasts are important cellular components of the breast tumor microenvironment, and their accumulation correlates with invasive cancer progression and poor patient prognosis. However, the understanding of functional contribution of fibroblast secreted factors to breast tumor progression still remains limited. In this dissertation, we demonstrate that breast cancer associated fibroblasts (CAFs) overexpress CXCL1, which promotes luminal and basal-like breast cancer cell survival, invasion and mammary tumor progression through CXCR2-dependent mechanisms *in vitro* and *in vivo*. By candidate profiling, we have found the TGF-β signaling pathway as a regulator of CXCL1 expression in mammary fibroblasts. Mechanistically, we show that TGF-β suppresses CXCL1 expression through Smad2/3-dependent mechanisms, and, as a secondary mechanism, TGF-β suppresses CXCL1 expression through down-regulation of HGF/c-Met signaling. In summary, we document the prognostic relevance and significance of CXCL1 protein expression in breast cancer stroma, characterize the molecular mechanisms of CXCL1 expression in mammary fibroblasts in the context of TGF-β signaling, and demonstrate the functional contribution of fibroblast-derived paracrine CXCL1/CXCR2 signaling in mediating breast cancer cell survival, invasion and tumor progression.

Acknowledgements

This work was supported by NIH Grant (R00 CA127357-03, Cheng). I would like to first acknowledge all the people in the United States whose tax revenues make the medical research possible.

I would like to thank my mentor, Dr. Nikki Cheng to give me the opportunity to come to the U.S. and become a scientist. I enjoyed the five years working in your lab. You are a great mentor who is willing to help me when I was struggling and encourage me when I was frustrated. You taught me how to think, read, talk and write like a scientist. I will never forget the time you spent on guiding me how to critically read a paper and the moment you help me correct my writings side by side, word by word. Thank you for all your time, your patience, your guidance and your encouragement.

I also want to thank all my committee members: Dr. Benyi Li, Dr. Fariba Behbod, Dr. Joan Lewis-Wambi, Dr. Timothy Fields, and Dr. Charlotte Wines. I enjoyed the time talking with you during and after the committee meetings. The tough questions you have asked taught me how to think critically and pushed me to do better. The encouragement and help from you really help me on tract with the research, study and graduate study life.

Other faculty members in the department, Dr. Adam Krieg, Dr. Patrick Fields, Dr. Soumen Paul, I would like to give my acknowledgement to you too. You are always willing to help when I have technical and scientific questions.

In the lab, I thank all the current and former members Dr. Wei bin Fang, Dr. Benford Mafuvadze, Min Yao, Michael Portsche, Diana Lambert, Iman Jokar for your friendship and help. I enjoyed working and sharing with you all.

Especially, I want to thank my parents for their 100% support all the time. The distance does not attenuate your love but makes it even stronger.

I would also like to thank Wen who is coming to US after me and being my wife, for the love support and everything. Also, I want to thank Wen's parents for all the trust and support. You are also my family.

Table of Contents

List of Figures

List of Tables

List of Abbreviations

2SKO: TGF-β type II receptor knockout;

ADH: Atypical Ductal Hyperplasia;

AEC: Alveolar Epithelial Cells;

α-SMA: alpha Smooth Muscle Actin;

BRCF: Biospecimen Repository Core Facility;

CAFs: Carcinoma Associated Fibroblasts;

cAMP: cyclic Adenosine Monophosphate;

cat. no.: catalogue number;

C/EBP-β: CCAAT/Enhancer-Binding Protein-beta;

ChIP: Chromatin Immunoprecipitation (ChIP);

CK: Cytokeratin;

CKII: c-Met kinase inhibitor type II, also known as PHA665752;

Con: Control;

COPD: Chronic Obstructive Pulmonary Disease;

CREB: cAMP Response Element-Binding protein;

CT: Computerized Tomography;

DAB: 3,3'-Diaminobenzidine;

DAG: Diacylglycerol;

DCIS: Ductal Carcinoma In Situ;

DMEM: Dulbecco's modified Eagle medium;

DMSO: Dimethyl Sulfoxide;

ECM: Extracellular Matrix;

EDTA: Ethylenediaminetetraacetic Acid

EGFR: Epidermal Growth Factor Receptor;

ELISA: Enzyme-Linked Immunosorbent Assay;

ELR: Glutamic acid (E) - Leucine (L) - Arginine (R);

EMT: Epithelial-Mesenchymal Transition;

ER: Estrogen Receptor;

ERK1/2: Extracellular signal-Regulated Kinases 1/2;

FAP: Fibroblast Activating Protein;

FBS: Fetal Bovine Serum;

FSP1: Fibroblast Specific Protein 1;

FspKO: Fibroblast Specific Protein Knockout for the Tgfbr2 gene;

G Protein: Guanine nucleotide-binding Protein;

GPCRs: Guanine Protein Coupled Receptors;

GTP: Guanosine-5'-Triphosphate;

HER2/neu: Human Epidermal growth factor Receptor 2;

HGF: Hepatocyte Growth Factor;

HuR: Human antigen R;

IBC: Inflammatory Breast Cancer;

IDC: Invasive Ductal Carcinoma;

IgG: Immunoglobulin G;

IκB: Inhibitor of κB;

IKKα/β: IκB Kinase alpha/beta;

IP_3: Inositol trisphosphate;

MAPK: Mitogen-activated protein kinases;

MGSA-α: Melanoma Growth Stimulating Activity-alpha

MMPs: Matrix Metalloproteinases;

MMTV: Mouse Mammary Tumor Virus;

MRI: Magnetic Resonance Imaging;

NA: Not Available;

NAFs: Normal (tissue)-Associated Fibroblasts;

NAP3: Neutrophil Activating Protein 3;

NF-κB: Nuclear Factor kappa-light-chain-enhancer of activated B cells;

NGS: Next Generation Sequencing;

NOS: Not Otherwise Specified;

ns: not significant;

OA: Osteoarthritis;

PAI1: Plasminogen Activating Inhibitor 1;

Par: Parental;

PARP: Poly ADP Ribose Polymerase;

PET: Positron Emission Tomography;

PIP_2: Phosphatidylinositol-3,4-bisphosphate;

PIP_3: Phosphatidylinositol-3,4,5-trisphosphate;

PLC: Phospholipase C;

PR: Progesterone Receptor

PyVmT: Polyoma Middle T;

S100A8/9: S100 calcium binding protein A8/9;

SBE: Smad Binding Element;

SD: Standard Deviation;

SEM: Standard Error of the Mean;

shRNA: short hairpin RNA;

siRNA: small interfering RNA;

Stat3: Signal transducer and activator of transcription 3;

TGF-β: Transforming Growth Factor beta;

TGFBR2: TGF-β type II Receptor gene;

TIE: TGF-β Inhibitory Elements;

TMA: Tissue Microarray;

TNBC: Triple Negative Breast Cancer;

TNF-α: Tumor necrosis factor-alpha;

TNM: T (Tumor size), N (lymph Node involvement), and M (Metastasis);

VEGF: Vascular Endothelial Growth Factor;

WT: Wild Type;

Chapter I: Introduction

Preface

Breast cancer is the most commonly diagnosed cancer in females in the US and worldwide, with 232,670 estimated new cases domestically in 2014 and over 1.3 million new cases annually in the world (1-3). Also, it is estimated that 40,000 women will die from breast cancer in 2014, which accounts for 15% of all cancer-related death. Breast cancer is a disease develops from breast tissue, including milk ducts and lobules supplying ducts with milk. Among all patients diagnosed with breast cancer, 60% of patients are diagnosed with localized disease, and 32-38% with regional disease, which show 94% and 74% of five-year survival rate respectively. However, patients diagnosed with distant metastatic breast cancer, which accounts for less than 8% of cases, have less than 25% five-year survival rate. Current treatments include hormone deprivation therapy, surgery, chemotherapy and radiation therapy. However, these treatments are not effective against metastatic breast cancer and are toxic to normal tissues, leading to side effects that include cardiac toxicity, immune cell depletion, pain, fatigue and anemia (4, 5). Understanding the molecular mechanisms through which breast cancer cells survive and become metastatic is of fundamental significance in improving breast cancer treatment.

Breast cancer progression

Breast cancer is a complicated multi-step disease that begins as proliferation of normal cells in breast tissues, also referred as hyperplasia. The cells develop abnormalities that make them different from normal cells yet not cancerous (atypical hyperplasia) and may keep changing their morphology and evolving into non-invasive cancer (*in situ*) or invasive cancer eventually. Furthermore, invasive breast cancer may

lead to metastasis to lymph nodes and other distant organs, including bone, lungs, liver and brain through bloodstream or the lymphatic system.

Atypical hyperplasia, which is defined as accumulation of abnormal cells in breast duct [atypical ductal hyperplasia (ADH)] or lobule (atypical lobular hyperplasia) due to increased cell proliferation, is classified as a benign condition, but may increase the risk of subsequent invasive breast cancer by up to five times (6). ADH can evolve to ductal carcinoma *in situ* (DCIS), a heterogeneous noninvasive breast cancer in which abnormal cells are found in the lining of a breast duct (NIH definition). While gene expression profiles dramatically vary from normal cells to cancer cells in DCIS, there is no unique gene change from DCIS to invasive cancer cells (7). However, quantitative changes of gene expression associated with progression from DCIS to invasive carcinomas have been identified (7).

Breast cancer grade, stage and subtype

The grade of breast cancer is representative of the aggressive potential of the tumor and generally classifies the cancer as well differentiated (low-grade), moderately differentiated (intermediate-grade), and poorly differentiated (high-grade). Breast cancer can be graded in different ways, one of the most commonly used scoring system is the Nottingham Histologic (also called Elston-Ellis) Score system. In this system, breast cancer grading is based on the microscopic morphologies, including tubule formation, mitotic count and nuclear pleomorphism of the tumor. Each component is given a score from 1 to 3 and the sum of the three elements determines the grade of a tumor. A tumor with score of 3-5 is considered as low grade or grade 1. Cancer cells of grade 1 are well differentiated and have the closest features as normal breast epithelial cells. Intermediate grade or grade 2 breast cancer (score 6-7) is featured by moderately

differentiated cells, higher growth rate and moderate variation in size and shape. High grade or grade 3 breast cancer has a score of 8-9 and the cells are poorly differentiated with marked variation in size and shape, proliferate fast and have the tendency to spread. Generally, breast cancers with lower grade have more favorable prognosis, higher survival rate, and can be more effectively treated. It was reported that different tumor grades are associated with distinct gene expression profiles (7).

The stage of breast cancer describes the extent or severity of cancer in the body. The most commonly used staging system is TNM system, which classifies cancers based on their T (Tumor size), N (lymph Node involvement), and M (Metastasis). Staging of breast cancer is an important aspect for cancer classification and is always considered in combination with other classification aspects, such as receptor expression patterns in making appropriate treatment choices.

Breast cancer is classified to four major subtypes (Luminal A, Luminal B, Triple negative/basal-like, HER2 type) based on the presence of estrogen receptors (ER), progesterone receptors (PR) and HER2/neu. Receptor status determines the suitability of using targeted treatments, thus is essential assessment for all breast cancers.

Breast cancer prognostic marker

The use of prognostic markers ensures optimal treatments are applied to breast cancer patients. Traditional prognostic factors include tumor size, lymph node status, nuclear and histological grade (8). A few other biomarkers such as estrogen receptor (ER), progesterone receptor (PR), and human epidermal growth factor receptor 2 (HER2/neu) were established and applied to optimize personalized therapies. Also, recent studies have suggested the importance of other prognostic markers such as Ki67, cyclin D1, cyclin E, p53, BRCA1/2 and VEGF (9). Although these prognostic markers

have been proven to be effective in providing comparatively accurate prognostic outcomes and predicting effectiveness for certain specific targeted therapies such as ER+ breast cancer, there is currently no effective predictive marker for many of the ER- subtypes, and the general accuracy of current prognostic markers are still far from optimal. Previous studies primarily examined the prognostic significance of CXCL1 expression in tumor epithelium (10). Yet, biomarker expression patterns in the stroma and epithelium can have vastly different relationships to known prognostic factors and clinical outcomes (11). In Chapter II of this dissertation, we further characterized the expression patterns of CXCL1 in breast cancer stroma and determined the prognostic significance of stromal CXCL1 expression in the context of known prognostic markers.

Therapies for breast cancer

A variety of treatments have been adopted to treat breast cancer patients including surgery, radiation therapy, chemotherapy, and targeted therapies (12-14). The strategies for optimal treatment of breast cancer are partially determined by accurate classification of subtypes in combination with other prognostic markers. For example, ER+ breast cancer cell growth is estrogen-dependent, thus its growth can be effectively retarded by drugs that reduce either the level of estrogen (e.g., aromatase inhibitors) or the effect of estrogen (e.g., tamoxifen). In addition, HER2+ cancer cells are responsive to monoclonal antibody (e.g., trastuzumab) blockade of epidermal growth factor receptor 2 (EGFR2/HER2/neu) and can be effectively treated in combination with conventional chemotherapy (15).

Despite advances in treatment, patients with invasive breast carcinoma still face around 80% mortality rate, partially due to drug toxicity and drug resistant disease. Also, the understanding for basal-like / triple negative breast cancer (TNBC) progression is still

limited, leading to the lack of effective targeted therapies. Furthermore, although expression patterns of the known prognostic markers have been well characterized, treatment effectiveness is complicated by the presence of reactive stroma, which is associated with tumor invasiveness and drug resistance (16-19). In order to tailor treatments more effectively to individual patient, it may be important to define clearly the breast tumor stroma at a molecular level, which could contribute to the identification of novel breast cancer prognostic markers with enhanced predictive potential for ER-targeted therapies.

Tumor Microenvironment

The tumor microenvironment is composed of the tumor, surrounding blood vessels, immune cells, fibroblasts, signaling molecules, and the extracellular matrix (NCI Dictionary of Cancer Terms). Tumors recruit these components to facilitate their progression and metastasis through bidirectional talk between tumor cells and the microenvironment (20, 21). In contrast to the well-organized homeostasis of the normal cells, tumor microenvironment is deregulated at molecular and cellular levels.

Fibroblast in cancer

Fibroblasts are a major cell type in connective tissues throughout the body, which regulate multiple physiological processes including inflammation, wound healing and senescence (22). Fibroblasts normally play an important role in maintaining the structural integrity of connective tissues through secretion of extracellular matrix precursors including type I, type III and type V collagen, and fibronectin (23). In addition to deposition of extracellular matrix (ECM), fibroblasts play an essential role in

maintaining ECM homeostasis through secretion of ECM-degrading proteases such as matrix metalloproteinases (MMPs) as well (24).

As a key cellular component in breast stroma, fibroblasts normally get activated during mammary gland development to regulate ductal branching and morphogenesis (25, 26). Fibroblasts are also a major cellular component of the breast tumor microenvironment, yet the molecular signals that identify cancer associated fibroblasts (CAFs) still remain poorly understood. CAFs are not a uniform population of cells and may be derived from different origins, including embryonic mesenchyme, endothelial cells, macrophages and cancer cells (27). CAFs are generally identified by their spindle cell morphology and expression of mesenchymal markers, including Fibroblast Specific Protein 1 (Fsp1), alpha Smooth Muscle Actin (α-SMA), and Fibroblast Activating Protein (FAP) (27, 28). Accumulation of CAFs strongly correlates with tumor grade and poor patient prognosis (29-31). Recent studies demonstrated the importance of CAFs in chemo-resistance. Fibroblasts are more resistant to chemotherapy than cancer cells, including melanoma and squamous cell carcinoma (32). In animal models, Doxorubicin treatment results in increased CAF secretion of growth factors and cytokines involved in the development of drug-resistant prostate and colorectal cancers (33, 34). Targeting FAP-expressing CAFs in animal models has been shown to inhibit growth of invasive tumors and enhance chemo-sensitivity to Doxorubicin in colon and breast cancers (35, 36). Yet the use of FAP inhibitors has not been successful in clinical trials (37, 38). This result may be due in part to the complex identity of CAFs, as well as possible functional redundancy.

De-regulated growth and activity of fibroblast is associated with progression and poor patient prognosis of invasive breast cancer, which is characterized by the presence of dense collagenous tumor stroma and accumulation of activated fibroblasts (3,4). Activated fibroblasts exhibit enhanced secretion of extracellular matrix proteins,

proteases and growth factors, mediating tissue remodeling in tumor microenvironment. In animal studies, co-grafting of mammary CAFs with mammary carcinoma cells results in increased tumor growth, survival and metastasis (5-7). Conversely, breast tumor outgrowth and cellular invasiveness is inhibited by co-transplantation of normal tissue-associated fibroblasts (NAFs) (8,9). While NAFs and CAFs exhibit a uniform cell morphology, molecular profiling studies reveal that CAFs show increased expression of extracellular matrix proteins, growth factors and cytokines, which may contribute to tumor progression (10-12). Interestingly, metastatic carcinoma cells (Ki-67 positive) down-regulate E-cadherin expression at the periphery of cancer islands, where they are in direct contact with CAFs, leading to the hypothesis that CAFs not only promote tumor invasion but also facilitate metastases, either by co-metastasizing and/or being recruited to lymph nodes (39).

Epithelial cell: fibroblast interactions

Epithelial cell: fibroblast interactions are well known to contribute to the pathogenesis of fibrotic diseases in multiple organs including lung, kidney and liver, where fibroblasts and epithelial cells normally reside in close proximity. For example, mechanical injury to lung alveolar epithelial cells (AEC) provoke expression of α-SMA and type I and III collagen in co-cultured fibroblasts, which in turn amplify AEC injury and apoptosis through paracrine mechanisms (40).

Epithelial cell: fibroblasts interactions also play important roles in aging and cancer progression. Senescent stromal fibroblasts secret soluble factors including inflammatory cytokines, epithelial growth factors and matrix matalloproteinases (MMPs) that can disrupt the architecture and function of the surrounding tissues and regulate proliferation of neighboring cells including epithelial cells (41). In this way, senescent fibroblasts

create a tissue environment to facilitate epithelial senescence or malignancies (42, 43). Additionally, a number of studies provide strong evidence that cancer-associated fibroblasts (CAFs) enhance tumorigenic potential of prostate epithelial cells and gland-forming capability of prostate cancer stem cells, yet the molecular mechanisms remains to be elucidated (44, 45).

Chemokines

Chemokines, also referred to as chemotactic cytokines, are a family of small soluble proteins (8-10 kDa) secreted by a variety of cells, including neutrophils, monocytes, macrophages, epithelial cells and fibroblasts. While fibroblasts are commonly recognized to play a role in regulating recruitment of immune cell recruitment during inflammatory response, studies in the last decades have revealed important roles of chemokine signaling in many types of cancer (46-48). More than 50 chemokine ligands and 18 chemokine receptors have been identified so far in human. Chemokines are categorized into four distinct families based on the spacing of their first two N-terminal cysteine residues: C, CC, CXC, and CX3C in which a conserved cysteine motif may also include an amino acid in their NH2 terminal domain. The CXC chemokines can be further classified as Glu-Leu-Arg positive (ELR+) and ELR- based on the presence or absence of this motif before the first cysteine. ELR+ chemokines specifically induce the migration of neutrophils, and were found to be potent angiogenic factors (49-51). CXCL1 is a ELR+ member of the CXC subfamily and is also referred as GRO1 oncogene, GROα, KC, neutrophil-activating protein 3 (NAP-3) and melanoma growth stimulating activity, alpha (MGSA-α) (52). Other than CXCL1, there are currently 16 other CXC chemokine ligands identified, which bind promiscuously to 7 chemokine receptors (CXCR1, CXCR2, CXCR3, CXCR4, CXCR5, CXCR6, CXCR7).

Generally, chemokines bind to seven-transmembrane-domain receptors, which couple to G proteins and activate signaling pathways involved with cell migration and differentiation. The biological effects of CXCL1 are mediated through two class A, rhodopsin-like guanine-protein-coupled receptors (GPCRs): CXCR1 and CXCR2 (53). CXCR1 and CXCR2 have 78% identical amino acid sequences (54, 55), however, due to the differences in the receptor N-terminal sequences, CXCL1 predominantly binds to CXCR2 instead of CXCR1 under physiologic conditions (56). CXCR2 binds to multiple chemokine ligand in addition to CXCL1, including CXCL2, CXCL3, CXCL5, CXCL6, CXCL7 and CXCL8.

Chemokine signaling in cancer

Inflammatory chemokines such as CXCL1, CXCL8, CCL2, CCL5 are overexpressed in melanoma, ovarian, prostate cancers, correlating with poor diagnosis, shortened patient survival, increased angiogenesis (57-59). Interestingly, overexpression of chemokines is tissue specific, indicating their specific roles in tumor progression. For instance, CXCL3 is up-regulated in prostate cancer, whereas CXCL5 has been detected in lung and liver cancers (60, 61).

Generally, chemokines are known to promote tumor progression through recruiting immune cells such as neutrophils and macrophages to primary tumor sites, leading to inflammatory responses (62). Additionally, a number of studies suggest that chemokine signaling is essential in metastatic disease, in which specific expression patterns of chemokine ligands and receptors in tissues or regional lymph nodes may potently facilitate tumor dissemination at several key steps of metastasis, including adherence of tumor cells to endothelium, extravasation from blood vessels, metastatic colonization, angiogenesis, proliferation, and protection from the host response (63).

CXCL1/CXCR2 signaling in cancer

Increased expression of CXCL1 in tumors has been reported in multiple tumor types including prostate cancer, gastric cancer, renal cell carcinoma and melanoma (64, 65). In breast cancer, increased CXCL1 protein expression has been reported in HER2 positive metastatic breast cancer (66) and was associated with increased tumor growth and pulmonary metastasis of MDA-MB231 breast cancer cells grafted in the mammary fat pads of nude mice (67). Moreover, increased plasma levels of CXCL1 protein are associated with decreased survival of breast cancer patients with metastatic disease (68). Similarly, increased tumoral expression of CXCL1 RNA is associated with metastatic disease, correlating with tumor grade and decreased survival of patients with ER positive breast cancer (10).

Emerging studies have suggested important tumorigenic roles of chemokines in breast tumor stroma. For instance, CXCL12 derived from CAFs promotes tumor growth and angiogenesis through endocrine and paracrine mechanisms; CCL5 from mesenchymal stem cells acts in a paracrine fashion on cancer cells to enhance cell motility, invasion and metastasis (69, 70). However, the expression, clinical relevance of CXCL1 in breast tumor stroma and its role in breast cancer progression has not been fully characterized. Recently, it has been reported that a CXCL1 paracrine network links breast cancer chemo-resistance and metastasis via recruitment of myeloid cells, which enhance tumor cell survival through secretion of S100A8/9 (71). In this dissertation, we have systematically characterized the expression patterns of CXCL1 in breast cancer stroma, determined the prognostic significance of stromal CXCL1 expression in the context of other known prognostic factors, and identified factors affecting stromal CXCL1 expression in Chapter II. Additionally, in Chapter IV, we demonstrate that CXCL1 signals to its receptor CXCR2 to promote breast cancer cell survival and invasion

without influencing cell proliferation, suggesting a novel role for CXCL1/CXCR2 signaling in breast tumors. Furthermore, in Chapter IV, we have shown evidence that CXCL1 stimulates Akt and NF-κB signaling in breast cancer cells, indicating a potential role for these signaling pathways in CXCL1-induced cell invasion and survival.

Signal Transduction

CXCL1/CXCR2 signaling

Like many other GPCR-induced signaling pathways, binding of CXCL1 activates its receptor CXCR2, resulting in activation of the associated G protein (72). The G protein disassociates into the GTP-bound Gα-subunit and the Gβγ-complex, which activate different signaling molecules. The Gα-subunit either inhibits some isoforms of adenylyl cyclase leading to decrease of intracellular cAMP-levels and cAMP-dependent protein kinase activity or activates some small GTPases (73). The Gβγ-complex is able to activate PI3Kγ and β_2/β_3 isoforms of phospholipase C (PLC), which hydrolyzes phosphatidylinositol 4,5-bisphosphate to generate inositol trisphosphate (IP_3), followed by mobilization of calcium and diacylglycerol (DAG) and eventually activates Ca^{2+}-independent and Ca^{2+}-dependent protein kinase C. In addition, activation of PI3Kγ catalyzes conversion of phosphatidylinositol-3,4-bisphosphate (PIP_2) to phosphatidylinositol-3,4,5-trisphosphate (PIP_3), leading to activation of downstream signaling such as Akt (74, 75). In addition to activation by the Gα-subunit, Small GTPases of Rho family such as Rac1 and 2 can also be activated downstream of PI3K (76, 77).

TGF-β Signaling

Transforming Growth Factor-beta (TGF-β) signaling is an important regulator of fibroblast activity. TGF-β signals through TGF-β type I and II receptors on cell surface, which activate Smad2 and Smad3 proteins, resulting in a complexes with Smad4. These complexes translocate into the nucleus and regulate transcription of genes related to the cell cycle, adhesion and invasion (78).

TGF-β signaling in fibroblasts can be activated by tumor cells. For example, increased protease expression and plasmin generation by tumor cells enhances activation of TGF-β and degradation of the extracellular matrix, with a consequent release of TGF-β (79). TGF-β signaling plays an important role in regulating fibroblasts activity. *In vitro*, TGF-β induces anchorage-dependent growth of mouse fibroblasts (80). *In vivo*, TGF-β regulates desmoplastic responses by activating fibroblasts to acquire a myofibroblast state, characterized by spindle-shaped morphology and increased expression of α-SMA, growth factors, angiogenic factors, extracellular matrix proteins and proteases, corresponding with enhanced tumor growth and metastasis (81, 82).

Studies indicate that TGF-β signaling in fibroblasts either promotes or suppresses tumor progression in adjacent epithelia, depending on tissue of origin (83). To understand the role of TGF-β signaling in such epithelial-mesenchymal interactions, the TGF-β type II receptor gene was conditionally knocked out in mouse fibroblasts (Tgfbr2FspKO). Loss of TGF-β responsiveness in fibroblasts enhanced proliferation of both fibroblasts and adjacent epithelia and resulted in intraepithelial neoplasia in the prostate, and invasive squamous cell carcinoma in fore stomach, both associated with an increased abundance of stromal cells (84, 85).

In contrast, in the mammary gland, TGF-β signaling plays a tumor suppressive role. TGF-β signaling and HGF signaling play antagonistic roles in mammary gland

development and tumor progression. Female Tgfbr2FspKO mice exhibit severe defects in mammary gland development, including increased ductal epithelial cell turnover and increased fibroblast abundance. Transplantation of mammary carcinoma cells with Tgfbr2FspKO fibroblasts enhances mammary tumor growth and metastasis in MMTV-PyVmT transgenic mice and in co-transplantation models (86-88). Furthermore, Tgfbr2FspKO fibroblasts show increased expression of growth factors, including Transforming Growth Factor-α and Hepatocyte Growth Factor (HGF), which act on mammary carcinoma cells to promote epithelial cell growth and migration (87, 88). All these factors are similarly overexpressed in CAFs (80, 89), suggesting a link between decreased TGF-β signaling in breast CAFs and enhanced expression of tumor promoting factors. Interestingly, up-regulation of CXCL1 was identified in Tgfbr2FspKO fibroblasts by DNA microarray and by luciferase promoter activity assay in our preliminary studies, indicating a negative correlation of CXCL1 expression and TGF-β signaling. In chapter II, we have systematically characterized the expression pattern and prognostic significance of CXCL1 and TGF-β signaling components in breast tumor stroma. In chapter III, we provide strong evidences to address the hypothesis that TGF-β signaling coordinates with HGF signaling to regulate CXCL1 expression in mammary fibroblasts.

Summary

Taken together, our studies have for the first time revealed the clinical relevance and prognostic significance of up-regulated CXCL1 expression in breast tumor stroma and poor prognosis of breast cancer patients, identified the molecular mechanisms through which CXCL1 expression was regulated in mammary carcinoma-associated fibroblasts in the context of TGF-β signaling, and characterized the role of fibroblast-derived

paracrine CXCL1/CXCR2 signaling in promoting breast cancer cell survival, invasion and tumor progression. These studies provide new insights into the understanding of breast cancer progression at molecular levels, and underline the significance of blocking CXCL1/CXCR2 signaling-mediated epithelial cell: fibroblast interactions as a novel therapeutic strategies against breast cancer progression.

Chapter II: Elevated CXCL1 expression in breast cancer stroma predicts poor prognosis and is inversely associated with expression of TGF-β signaling proteins

Abstract

Fibroblasts are important cellular components of the breast tumor microenvironment; yet, the molecular signatures that identify cancer-associated fibroblasts (CAFs) remain poorly understood. In addition, CXCL1 is a chemotactic cytokine shown to regulate breast cancer progression and chemo-resistance. However, the prognostic significance of CXCL1 expression in breast cancer has not been fully characterized. Furthermore, recent studies indicate that stromal fibroblasts are potential sources of CXCL1 expression in breast tumors. The goals of these studies were to further characterize the expression patterns of CXCL1 in breast cancer stroma, to determine the prognostic significance of stromal CXCL1 expression, and to identify factors affecting stromal CXCL1 expression. Stromal CXCL1 protein expression was analyzed in 54 normal and 83 breast carcinomas by immunohistochemistry. RNA expression of CXCL1 was analyzed in breast cancer stroma through data mining in *www.Oncomine.org*. The relationships between CXCL1 expression and risk factors were analyzed by univariate analysis. Co-immunofluoresence staining for CXCL1, alpha Smooth Muscle Actin (α-SMA) and Fibroblast Specific Protein 1 (FSP1) was performed to analyze expression of CXCL1 in fibroblasts. By candidate profiling, the TGF-β signaling pathway was identified as a regulator of CXCL1 expression in fibroblasts. Expression of TGF-β and SMAD gene products were analyzed by immunohistochemistry and data mining analysis. The relationships between stromal CXCL1 and TGF-β signaling components were analyzed by univariate analysis. Carcinoma associated fibroblasts isolated from MMTV-PyVmT mammary tumors were treated with recombinant TGF-β and analyzed for CXCL1 promoter activity by luciferase assay, and protein secretion by ELISA. Elevated CXCL1 expression in breast cancer stroma correlated with tumor grade, disease recurrence and

decreased patient survival. By co-immunofluorescence staining, CXCL1 expression overlapped with expression of α-SMA and FSP1 proteins. Expression of stromal CXCL1 protein expression inversely correlated with the expression of TGF-β signaling components. Treatment of fibroblasts with TGF-β suppressed CXCL1 secretion and promoter activity. In conclusion, increased CXCL1 expression in breast cancer stroma correlates with poor patient prognosis. Furthermore, CXCL1 expression is localized to α-SMA and FSP1 positive fibroblasts, and is negatively regulated by TGF-β signaling. These studies indicate that decreased TGF-β signaling in carcinoma associated fibroblasts enhances CXCL1 expression in fibroblasts, which could contribute to breast cancer progression.

Introduction

Breast cancer remains to be the most common cancer diagnosed in women in the US and in the world, with over 1.3 million new cases annually (2, 3). 80% of all invasive breast cancers in the US are diagnosed as invasive ductal carcinoma (IDC). Current treatments include radiation, chemotherapy, hormone therapy and targeted HER2 therapy (12-14). Despite advances in treatment, patients with invasive breast carcinoma still face an 80% mortality rate, due in part to drug toxicity and drug resistant disease. Treatment effectiveness is complicated by the presence of reactive stroma, which is associated with tumor invasiveness and drug resistance (16-19). In order to tailor treatments more effectively to the individual patient, it may be important to define clearly the breast tumor stroma at a molecular level, which will enable us to identify biomarkers that will more accurately predict patient responsiveness to treatments.

Fibroblasts are key cellular components in breast stroma and are normally activated during mammary gland development to regulate ductal branching and morphogenesis

(25, 26). De-regulation of fibroblast growth and activity is associated with breast cancer. Carcinoma-associated fibroblasts (CAFs) are commonly identified by their spindle cell morphology and expression of mesenchymal markers including Fibroblast Specific Protein 1 (FSP1), alpha Smooth Muscle Actin (α-SMA), and Fibroblast Activating Protein (FAP) (27, 28). Accumulation of CAFs strongly correlates with tumor grade and poor patient prognosis (29-31). Co-transplantation studies and transgenic mouse studies have demonstrated that CAFs enhance breast tumor growth and invasion (70, 90, 91). Conversely, co-transplantation of normal fibroblasts with breast cancer cells inhibits cellular invasiveness and inhibits tumor progression (92). These studies indicate that fibroblasts may enhance or inhibit breast cancer progression depending on the tissue of origin.

Recent studies demonstrate the importance of CAFs in chemo-resistance. Fibroblasts are more resistant to chemotherapy than cancer cells, including melanoma and squamous cell carcinoma (32). In animal models, Doxorubicin treatment results in increased CAF secretion of growth factors and cytokines involved in the development of drug resistant prostate and colorectal cancers (33, 34). Targeting FAP expressing CAFs in animal models has been shown to inhibit growth of invasive tumors and enhance chemo-sensitivity to Doxorubicin of colon and breast cancers (35, 36). Yet the use of FAP inhibitors has not been successful in clinical trials (37, 38). This result may be due in part to the complex identity of CAFs. Fibroblasts are not a uniform population of cells. One type of CAF in breast cancer is the myofibroblast, which expresses α-SMA (93, 94). Another type of breast CAF expresses FSP1 but not α-SMA (95). Furthermore, fibroblasts may be derived from different origins including embryonic mesenchyme or endothelial cells (27). These studies indicate the presence of different populations of

CAFs. Currently, the molecular signatures that identify tumor-promoting fibroblasts remain incompletely understood.

Emerging studies indicate an important clinical significance for chemokine expression in cancer stroma. Chemokines are a family of small soluble proteins (8-10 KD) that regulate angiogenesis and immune cell recruitment during inflammation and cancer (46-48). Chemokines bind to seven transmembrane spanning receptors that couple to G proteins and activate signaling pathways involved with cell migration and differentiation. As a large family of molecules, chemokines are categorized into distinct families: C, C-C, C-X-C, and CX3C, in which a conserved cysteine motif may also include an amino acid (X) in their NH2 terminal domain. The C-X-C chemokine family is currently comprised of 17 ligands, which bind promiscuously to 7 chemokine receptors (CXCR1-7). A conserved glutamic acid-leucine-arginine (ELR) motif has been detected in a small subset of C-X-C chemokines (CXCL1,2,3,5,8), which is important for stimulating angiogenesis and regulating recruitment of neutrophils (50, 51). Up-regulated expression of ELR positive chemokines have been detected in various cancers, associated with increased angiogenesis and immune cell recruitment. CXCL3 is up-regulated in prostate cancer (96) while CXCL5 has been detected in lung and liver cancers (60, 61). Increased expression of CXCL1 has been reported in multiple tumor types including prostate cancer, gastric cancer, renal cell carcinoma and melanoma (64, 65). These studies indicate aberrant expression of C-X-C chemokines in cancer.

Recent reports have implicated a role for CXCL1 in breast cancer. Increased CXCL1 protein expression was associated with increased tumor growth and pulmonary metastasis of MDA-MB231 breast cancer cells grafted in the mammary fat pads of nude mice (67). Increased CXCL1 protein expression has been reported in HER2 positive metastatic breast cancer (66). Increased plasma levels of CXCL1 protein are associated

with decreased survival of patients with metastatic disease (68). Similarly, increased tumoral expression of CXCL1 RNA is associated with metastatic disease, correlating with tumor grade and decreased survival of patients with ER-α positive breast cancer (10). Recently studies have shown that CXCL1 expression is up-regulated in breast cancer associated fibroblasts (10), indicating that CXCL1 expression is not restricted to epithelial cells.

Previous studies primarily examined the prognostic significance of CXCL1 expression in tumor epithelium (10). Yet, biomarker expression patterns in the stroma and epithelium can have vastly different relationships to known prognostic factors and clinical outcomes (11). The goals of these studies were to characterize further the expression patterns of CXCL1 in breast cancer stroma, to determine the prognostic significance of stromal CXCL1 expression, and to identify factors affecting stromal CXCL1 expression. We used a combination of data mining analysis and immunohistochemistry staining of patient samples to investigate the RNA and protein expression patterns of CXCL1 RNA and protein in the breast cancer stroma. Our studies indicate that patient samples express high levels of CXCL1 RNA and protein in breast cancer stroma, correlating with tumor grade. CXCL1 RNA expression levels significantly associated with tumor recurrence and decreased patient survival. CXCL1 protein expression co-localized to FSP1 and α-SMA positive cells, indicating that CXCL1 is expressed in more than one population of CAFs. Increased CXCL1 in CAFs correlated with decreased TGF-β expression. Immunostaining analysis of breast tumor tissues indicated that increased CXCL1 expression inversely correlates with expression of TGF-β, phospho-SMAD2 and phospho-SMAD3. Treatment of cultured CAFs with TGF-β suppresses CXCL1 secretion and promoter activity. In summary, these studies indicate a prognostic significance for

CXCL1 expression in breast cancer stroma, showing that CXCL1 is localized to multiple fibroblast populations, and is negatively regulated by TGF-β signaling.

Materials and Methods

Patient samples used for immunohistochemistry analysis

Samples were collected from commercial and institutional resources (Table 2.1). Tissues microarrays (TMA) containing de-identified cores of 18 normal and 26 invasive breast ductal carcinoma samples were obtained from US Biomax (cat nos. 8032 and 241). Information included data on age, tumor grade and clinical diagnosis. Additional patient samples of normal, DCIS and IDC were obtained from the Biospecimen Repository Core Facility (BRCF), an IRB approved facility at the University of Kansas Medical Center. 14 normal, 5 DCIS and 13 IDC cases were obtained as individual specimens. Tissue microarrays were generated from an additional 22 normal, 20 DCIS and 14 IDC specimens. All tissues were obtained under a human subjects exemption policy. As these samples were collected within the last 4 years, no follow-up data was available. From the BCRF sample collection, 13 samples of normal tissues originated from adjacent breast tissues of cancer patients. 26 samples of normal tissues were collected from patients undergoing reduction mammoplasty. Tumor samples were collected under the following criteria: Patients were diagnosed with primary breast ductal carcinoma and had not been treated with radiation or chemotherapy before surgery and sample collection. Reports included data on biological risk factors, clinical diagnosis and histo- and cyto-pathology. The Van Nuys system was used to grade DCIS samples. IDC samples were graded according to the Scarff-Bloom and Richardson system. Characteristics of tumor samples are described in Table 2.1. Intensity of staining or percentage of positive cells were reported for BCL2, p53, ER, PR, Her2 and EGFR

Table 2.1. Characteristics of breast ductal carcinoma samples from US Biomax and the BRCF core.

Risk factor	no. of DCIS cases (percentage of total)	No. of IDC cases (percentage of total)
Histologic grade		
1	2 (9%)	10 (18%)
2	7 (32%)	24 (41%)
3	12 (59%)	24 (41%)
Tumor size		
≥2 cm	16 (70%)	10(36%)
<2cm	7 (30%)	18 (64%)
BCL2		
negative	4 (27%)	8 (42%)
positive	11 (73%)	11 (57%)
P53		
negative	7 (38%)	9 (36%)
positive	11 (62%)	16 (64%)
Ki67		
≥50%	3(16%)	5 (22%)
<50%	16(84%)	18 (78%)
ER		
negative	7 (38%)	9 (36%)
positive	11 (62%)	16 (64%)
PR		
negative	7 (38%)	11 (47%)
positive	11 (62%)	13 (53%)
HER2		
negative	0	7 (32%)
positive	18 (100%)	15 (68%)
EGFR		
negative	7 (38%)	10 (50%)
positive	11 (62%)	10 (50%)
Lymph node status	NA	
negative		12(52%)
positive		11(48%)

biomarkers, and are summarized as positive or negative. The number of samples with risk factor data is from a total of 25 DCIS samples and 58 IDC samples (US Biomax and BRCF samples combined). 100% of risk factor data from US Biomax samples, and risk factor data included in more than 55% of pathology reports from BRCF specimens are reported here. In total, normal tissues were collected from patients with median age of 48.6 years. Median age of patients with DCIS was 51 years. IDC patients had a median age of 50.5 years.

Ethics and Consent Statements

The tissues collected for these studies were categorized under the "Exemption Class", according to regulations set forth by the Human Research Protection Program (ethics committee) at the University of Kansas Medical Center (#080193). Written informed consent for tissue collection was obtained by the BRCF. Tissue samples were de-identified by the BRCF prior to distribution to the investigators. Existing medical records were used in compliance with the regulations of the University of Kansas Medical Center. These regulations are aligned with the World Medical Association Declaration of Helsinki.

Immunohistochemistry staining

CXCL1 protein expression was examined on patient samples obtained from US Biomax arrays and samples from the BRCF core. Expression of TGF-β, phospho-SMAD2 and phospho-SMAD3 proteins were primarily analyzed on patient samples obtained from the BRCF core. Tissue sections (5 μm) were de-waxed and rehydrated in PBS. Sections were subjected to antigen retrieval in 10 mM sodium citrate buffer pH 6.0 for 10 minutes at 100^{o}C and washed in PBS. Endogenous peroxidases were quenched in PBS containing 3% H_20_2 and 10% methanol for 30 minutes. After rinsing in PBS, samples were blocked in PBS containing 5% rabbit serum and incubated with antibodies

(1:100) to CXCL1 (cat. no. 1374, Santa Cruz Biotechnology), TGF-β (cat. no. MAB 240, R&D Systems), phospho-SMAD2 (Ser465/467) (cat. no. 3101, Cell Signaling Technologies), or phospho-Smad3 (Ser423/425) (cat. no. C25A9, Cell Signaling Technologies) overnight at 4^{o}C. Samples were washed in PBS and incubated with secondary goat biotinylated antibodies (1:500) (cat. no. BA-5000, Vector Labs), conjugated with streptavidin peroxidase (cat. no. PK-4000, Vector Labs) and incubated with 3,3'-Diaminobenzidine (DAB) substrate (cat. no. K346711, Dako). Sections were counterstained with Harris's hematoxylin for 5 minute, dehydrated and mounted with Cytoseal.

Quantification of Immunohistochemistry staining

Immunohistochemistry staining was imaged at 10 x magnification using a Motic AE 31 microscope with Infinity 2-1c color digital camera. Four fields were captured for each at 10 x magnification. To analyze biomarker expression in stromal tissues, we adapted methods described in previous studies (88, 97, 98). Images were first imported into Adobe Photoshop®. Hue and saturation of images were normalized using Auto-Contrast. Tumor epithelium was distinguished from stroma by differences in nuclear and cellular morphology, and tissue architecture. Using the lasso tool, epithelial tissues were selected and cropped out from the image, leaving the stromal tissues behind. These stromal tissues were labeled as " total stromal area". DAB chromogen staining (brown) was selected using the Magic Wand Tool in the Color Range Window, with a specificity range of 66. The selected pixels were copied and pasted into a new window and saved as a separate file. DAB positive images were opened in Image J and converted to greyscale. Background pixels resulting from luminosity of bright-field images were removed by threshold analysis. Images were then subjected to particle analysis.

Positive DAB staining and total stromal areas were expressed as particle area values of arbitrary units. Positive DAB values were normalized to total stromal values.

Immunofluorescence staining

Normal or breast cancer sections were de-paraffinized, and treated with sodium citrate as described for immunohistochemistry. Sections were permeabilized in PBS containing 10% Methanol for 30 minutes, washed in PBS and blocked for 1 hour with PBS containing 3% fetal bovine serum. Mouse IgGs were blocked using the M.O.M kit (cat. no. BMK-2202, Vector Labs) according to manufacturer's protocol. For co-immunofluorescence staining of CXCL1 and FSP1, sections were incubated with goat polyclonal antibodies to CXCL1 at a 1:100 dilution (cat. no. 1374, Santa Cruz Biotechnology) and with rabbit polyclonal antibodies to FSP1 (pre-diluted solution, cat. no. 27597, Abcam) in PBS/3% FBS overnight. For co-staining of CXCL1 and α-SMA, sections were incubated with antibodies to CXCL1, and mouse monoclonal antibodies to α-SMA (cat. no. ab134813, Abcam) at a 1:100 dilution. Sections were then washed with PBS and incubated with the following secondary antibodies at 1:500 dilution in blocking buffer for 1 hour: anti-goat-alexa-488 to detect CXCL1, anti-mouse-alexa-568 to detect α-SMA, or anti-rabbit-alexa-488 to detect FSP1. Sections were washed with PBS and countered with DAPI. Slides *were mounted in* Anti-Fade (cat. no. P36935, Invitrogen). Fluorescence images were taken at 20 x magnification using the Motic AE-31 microscope.

RNA expression analysis

RNA expression values in breast stromal samples were obtained from the microarray database in www.Oncomine.org, characterized by Finak et al. in previous studies (17, 99). Briefly, tissue samples were collected from 53 patients with invasive breast

carcinoma, of which 50 were diagnosed as IDC. Stromal samples were collected by laser capture micro-dissection and hybridized to microarrays. 6 normal samples were obtained from adjacent tissues of breast cancer patients. Patient samples included follow-up data, including information on recurrence within 5 years, and poor survival outcome. Poor survival outcome was defined as patients who died from disease at the time of follow-up. Median follow-up time was 3.58 years. The Finak database, provided as Log_2 median RNA expression values and prognostic information, including age, tumor grade and tumor size. The database did not include information on which cases were invasive lobular carcinoma, and were therefore included in the analysis.

Cell Culture

Primary mammary carcinoma-associated fibroblasts (CAFs) were isolated from transgenic mice (FVB) expressing the PyVmT oncogene under the control of Mouse Mammary Tumor Virus Promoter (MMTV) (100) at 12-16 weeks of age. Primary normal mammary tissue associated fibroblasts (NAFs) were isolated from wild-type C57/BL6 mice at 12-16 weeks of age. FspKO fibroblasts were isolated from FspKO knockout mice as described (88). Fibroblasts cell lines were generated by spontaneous immortalization of primary mammary fibroblasts and clonal populations of fibroblasts were obtained as described (88). Primary human fibroblasts were isolated from patient samples from reduction mammoplasty or invasive ductal carcinoma from the BRCF, using methods as described (88). Primary cells were cultured on 10-cm dishes coated with rat tail collagen I. All cells were cultured in Dulbecco's modified Eagle medium (DMEM) containing10% fetal bovine serum (FBS) (cat. no. FR-0500-A, Atlas Biological), 2 mM L-glutamine (cat. no. 25-005-CI, Cellgro) and 100 I.U/ml penicillin / 100 µg/ml of streptomycin (cat. no. 10-080, Cellgro).

ELISA

Cells were seeded in a 24-well plate at a density of 20,000 cells for 24 hours. Conditioned media was generated by incubating cells in 500 µl Opti-MEM media for 24 hours, and were centrifuged to eliminate cell debris. 100 µl of conditioned media generated from indicated cell lines was subjected to TGF-β ELISA (cat. no. DY1679, R&D Systems) or CXCL1 ELISA (cat. no. 250-11, Peprotech). Samples were analyzed according to manufacturer's protocol. Reactions were catalyzed using tetramethylbenzidine substrate (cat. no. 34028, Thermo Scientific) according to manufacturer's protocol. Reactions were stopped with 1M HCl, and absorbance was read at A_{450nm} using a 1420 multi-label plate reader (VICTOR3 TM V, PerkinElmer). All the samples were analyzed in triplicate.

Luciferase Assay

Cells were seeded in 6-cm dishes at a density of 150,000 cells for 24 hours, and then co-transfected with 8 µg of firefly luciferase plasmids (PGL3.luc.CXCL1) and 400 ng of Renilla luciferase plasmids (plasmid 12177: pIS2, Addgene) using 8.4 µl Lipofectamine LTX and 15 µl Plus reagents according to manufacturer's protocols (Invitrogen, life technologies). After 24 hours, cells were allowed to recover in Opti-MEM media containing 10% FBS for 24 hours. Cells were reseeded in 24-well plates at a density of 20,000 cells for 24 hours followed by incubation in serum free Opti-MEM media overnight. Cells were treated with Opti-MEM media containing 10% FBS in the presence or absence of 5 ng/ml TGF-β for 24 hours. Cell lysates were analyzed using Dual-Luciferase Reporter Assay system (cat. no. E1910, Promega) according to manufacturer's protocol. Cells were rinsed twice with PBS, lysed in 100 µl passive lysis buffer for 15 min at room temperature on a shaker. Cell lysates were sonicated for 10

seconds on ice, followed by centrifugation to eliminate cell debris. 20 µl lysates were assayed in triplicate in 96-well opaque plate (cat. no. 3912, Corning Costar) using the Veritas Microplate Luminometer (model no. 9100-202, Turner BioSystems).

Statistical Analysis

In vitro experiments were performed at minimum in triplicate. Data are expressed as Mean±SEM. Statistical analysis for *in vitro* experiments was determined using two-tailed *t* test or One-way ANOVAs with Bonferonni's post-test comparisons in Graphpad Software. Statistical Significance was determined as $p \leq 0.05$.

Sample populations did not fit a Gaussian distribution and were observed to be uneven. The uneven sample populations were due to two factors. Not all risk factors were consistently reported on pathology reports provided with the biospecimens. In addition, some tissue samples on tissue microarrays did not adhere to the slide during staining. Therefore, RNA and protein expression values and their relationships with risk factors were analyzed using non-parametric methods. Level of biomarker expression between two groups was analyzed by Wilcoxon Two-Sample Tests. Level of biomarker expression among more than 2 groups was analyzed by Kruskall-Wallis test with Dunn's post-*hoc* comparison between groups. Spearman rank correlation was used to analyze the relationship between biomarker expression and prognostic factors that were expressed as continuous variables. Wilcoxon Two-Sample Tests were used to analyze the relationship between biomarker expression and risk factors (such as tumor grade), which were expressed as discrete variables. Statistical significance was determined by confidence levels >95% and $p \leq 0.05$.

Results

Expression of CXCL1 RNA and proteins are elevated in breast cancer stroma

To assess the significance of CXCL1 expression in breast stroma, we compared protein and RNA levels of CXCL1 in breast cancer stroma. We first analyzed protein expression patterns in tissues from multiple stages of ductal carcinoma. Samples were collected from 54 normal breast tissues and 58 IDC tissues. We also collected 25 samples of DCIS, which is recognized as the immediate precursor to IDC (12, 101). Samples were subjected to immunohistochemistry staining for CXCL1 expression. Expression in the stromal tissues was quantified by software analysis using methods adapted from previous studies (97, 98). These methods were shown to be more reproducible and consistent compared to manual scoring. Consistent with previous studies (10, 71), CXCL1 was expressed in the tumor epithelium as well as stromal tissues (Figure 2.1A). By immunohistochemistry, 87% of normal samples and 100% of DCIS and IDC samples were positive for CXCL1 protein expression. CXCL1 expression was significantly higher in DCIS and IDC stroma compared to normal stroma (Figure 2.1B). Expression of CXCL1 in IDC stroma was higher than DCIS stroma; however, the differences were not significant. To determine RNA expression patterns of stromal CXCL1, we analyzed the microarray dataset on invasive breast cancer stroma generated by Finak et al., which consists of 53 cases of invasive breast carcinoma and 6 cases of normal breast samples (17). We observed that 33% of normal samples (n = 2) and 24% of IDC samples (n = 12) were positive for CXCL1 RNA expression (Figure 2.1C). In the subset of positive samples, mean intensity of expression in normal sample was 0.19 ± 0.07 (Mean ± SD) compared to 2.18 ± 1.23 in IDC stroma. Overall, these data indicate higher intensity of CXCL1 expression in breast cancer stroma compared to normal breast stroma. Breast ductal carcinoma is a heterogeneous disease, exhibiting

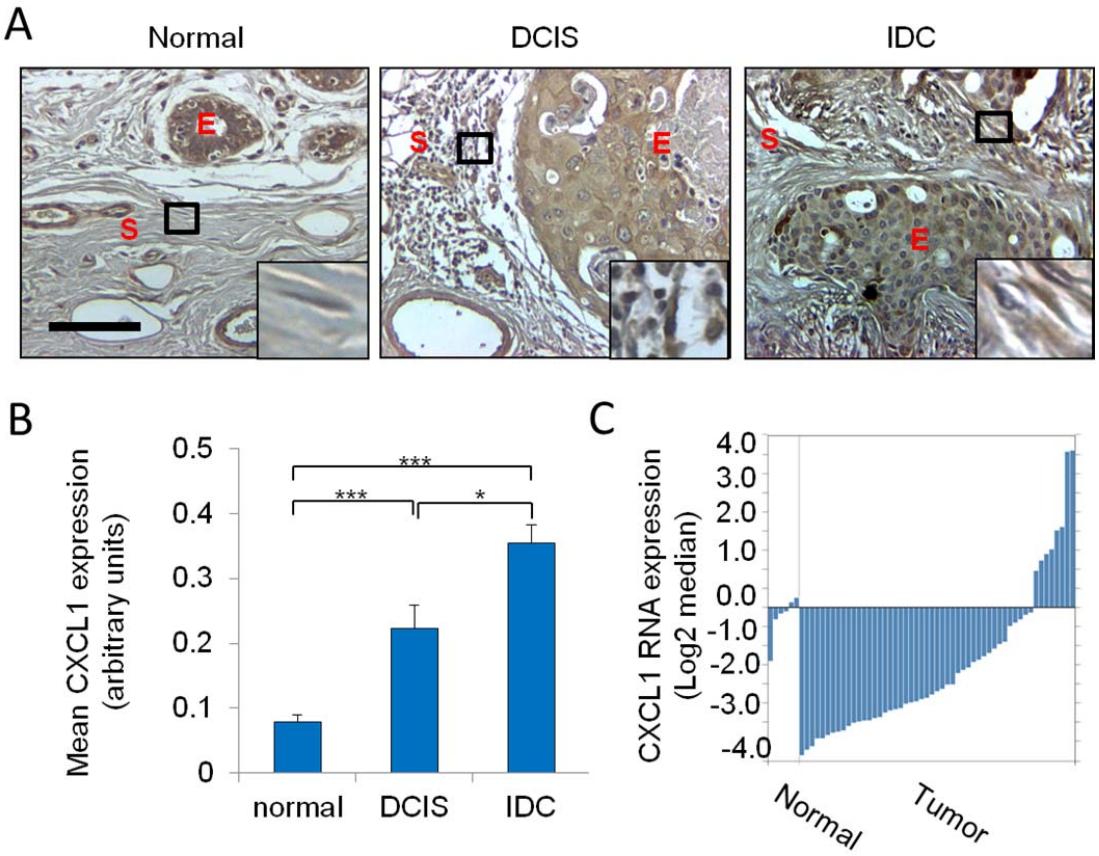
A
Normal
DCIS
IDC
E
S
B
Mean CXCL1 expression (arbitrary units)
0.5
0.4
0.3
0.2
0.1
0
***
***
*
normal
DCIS
IDC
C
CXCL1 RNA expression (Log2 median)
4.0
3.0
2.0
1.0
0.0
-1.0
-2.0
-3.0
-4.0
Normal
Tumor

Figure 2.1. CXCL1 expression is up-regulated in the stroma of breast ductal carcinomas.

(A). CXCL1 expression was analyzed by immunohistochemistry staining in normal (n=54), DCIS (n=25) or IDC (n=58) tissues. Representative staining shown. S= Stroma, E= epithelium. Arrows point CXCL1 positive staining in stroma. Scale bar= 50 microns. *(B).* Staining in stroma was quantified by Image J analysis. Statistical analysis was determined by Kruskall Wallis Test with Dunn's post-test comparison. *(C).* CXCL1 RNA expression values were obtained from the Finak microarray database. (Oncomine.org), and analyzed for expression among patient samples. *, $p<0.05$; ***, $p<0.001$. Values are expressed as Mean ± SEM. Error bars represent SEM.

different architectural patterns defined by histological analysis. Ductal carcinomas have been categorized into multiple histological subtypes. The most common form of ductal carcinoma is ductal carcinoma-not otherwise specified (NOS) (102). Less common subtypes include comedo and solid ductal carcinomas. Rarer subtypes include mucinous, micropapillary and cribribiform breast cancers. While the comedo subtype is associated with increased invasiveness, cribribiform, mucinous and papillary tumors are associated with a good prognosis. Ductal carcinomas with mixed histological subtypes have also been observed, complicating prognostic evaluation (102, 103). In these studies, we examined for differences in expression of stromal CXCL1 among the different subtypes. CXCL1 expression levels varied among groups. We found no significant differences in stromal CXCL1 expression among subtypes of DCIS and IDC. We were unable to draw conclusions on mucinous, micropapillary and micropappillary/solid tumors with only one sample provided in each group, reflecting the rarity of these subtypes (Figure 2.2 and 2.3). In these studies, we can only conclude that CXCL1 is expressed in the stroma of breast ductal carcinomas of multiple histologic subtypes.

Associations between stromal CXCL1 expression with risk factors and patient outcomes

To determine the factors affecting stromal CXCL1 expression, we examined for associations with commonly used prognostic markers through univariate analysis. We first analyzed the protein datasets. There were no significant associations between protein expression of CXCL1 among DCIS and IDC stroma with tumor size, BCL2 expression, p53 status, ER, PR, Her2 status, EGFR expression, lymph node status, Ki67 expression or age (Table 2.2). Increased stromal CXCL1 expression did not significantly correlate with grade of DCIS (Figure 2.4) but was significantly associated with IDC tumor

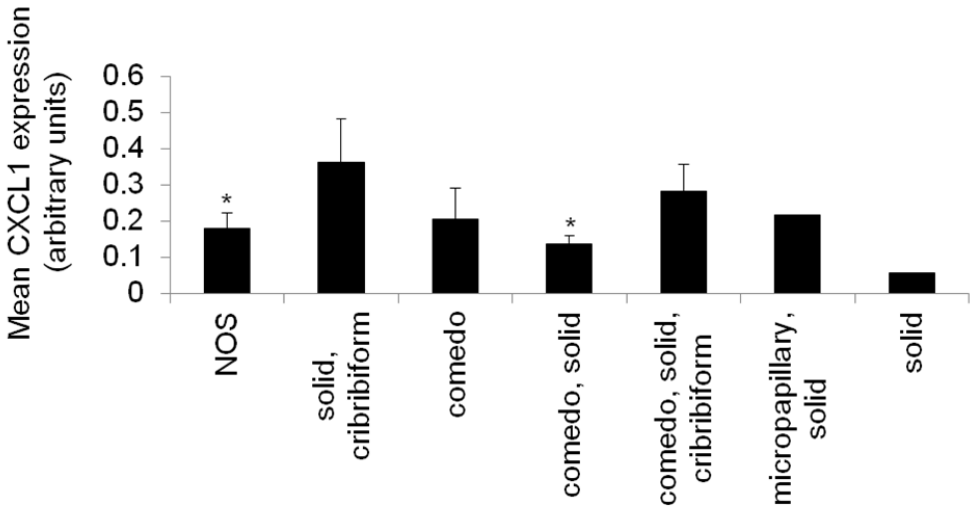

N	9	5	5	2	2	1	1 = 25
%	36	20	20	8	8	4	4 = 100

Figure 2.2. Expression of stromal CXCL1 in DCIS subtypes.

DCIS patient specimens were immunostained for CXCL1 protein expression and quantified for expression in the stroma among the different classified subtypes. Subtypes are organized in descending order of diagnosis. Statistical analysis among groups was performed using the Kruskall-Wallis test. Statistical significance determined by $p<0.05$. *, $p<0.05$ compared to all groups. Values are expressed as Mean$\pm$SEM.

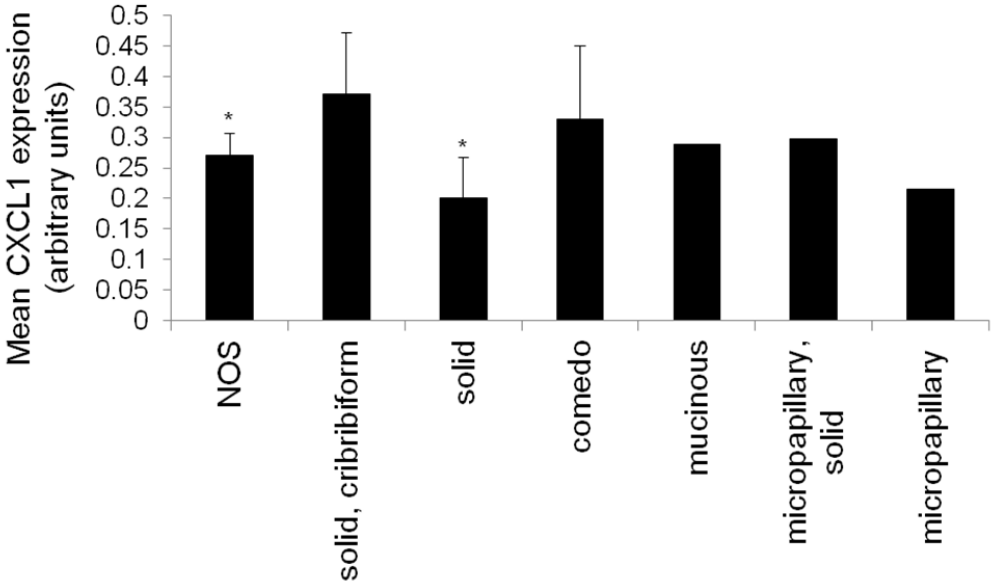

N	43	6	4	2	1	1	1 = 58
%	74	10	7	3	2	2	2 = 100

Figure 2.3. Expression of stromal CXCL1 in IDC subtypes.

IDC patient specimens were immunostained for CXCL1 and quantified for expression in the stroma among the different classified subtypes classified. Subtypes are organized in descending order of diagnosis. Statistical analysis among groups was performed using the Kruskall-Wallis test. Statistical significance determined by $p<0.05$. NOS= Not Otherwise Specified. *, $p<0.05$ compared to all groups. Values are expressed as Mean$\pm$SEM.

Table 2.2. Relationship between known prognostic factors and CXCL1 protein expression in breast cancer stroma.

Association between CXCL1 protein expression and commonly used prognostic markers was determined in DCIS and IDC stromal tissues using Spearman Correlation analysis. Significance was determined by $p<0.05$. r= correlation coefficient.

Factor	r	95% CI	p-value	n
Age	0.12	-0.03 to 0.40	0.08	79
tumor size	0.18	-0.11 to 0.44	0.19	51
BCL2	-0.06	-0.40 to 0.29	0.72	34
P53	0.08	-0.23 to 0.38	0.60	43
Ki67	0.25	-0.07 to 0.51	0.12	41
ER	-0.07	-0.37 to 0.24	0.70	42
PR	0.10	-0.22 to 0.40	0.51	42
HER2	0.14	-0.19 to 0.44	0.40	40
EGFR	0.07	-0.26 to 0.39	0.63	38
No. of lymph node metastases	0.17	-0.14 to 0.45	0.28	23

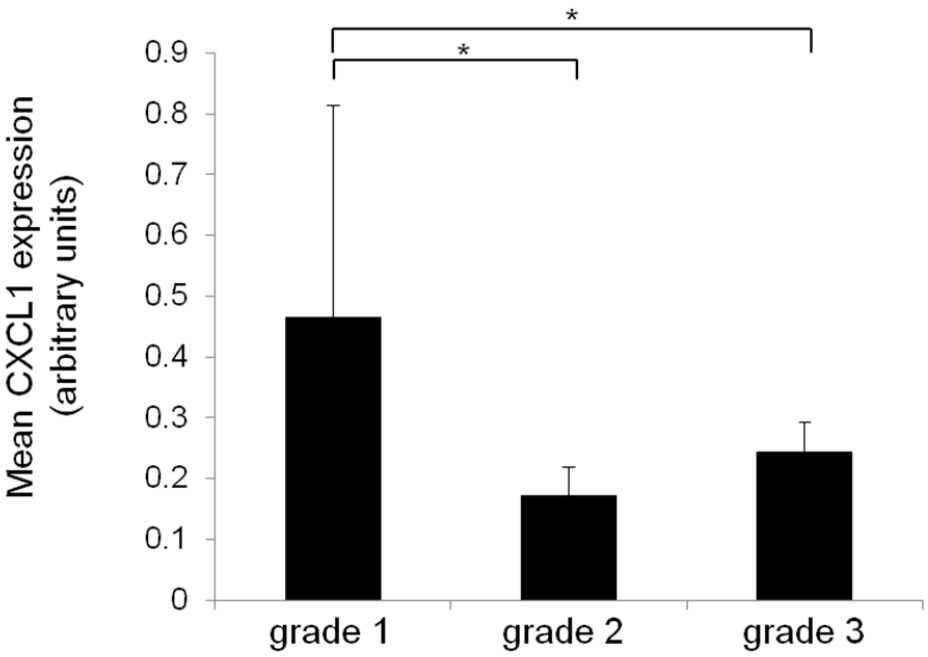
Mean CXCL1 expression
(arbitrary units)
0.9
0.8
0.7
0.6
0.5
0.4
0.3
0.2
0.1
0
*
*
grade 1
grade 2
grade 3

Figure 2.4. Stromal CXCL1 expression is not associated with grade of DCIS.

DCIS patient specimens were immunostained for CXCL1 protein expression and analyzed for association with histologic grade. N= 2 for DCIS grade 1, N=7 for DCIS grade 2 and N=13 for DCIS grade 3. Statistical analysis among groups was performed using the Kruskall-Wallis test. Statistical significance determined by $p<0.05$. *,$p<0.05$ compared to all groups. Values are expressed as Mean$\pm$SEM.

grade (Figure 2.5A). When we analyzed for associations between stromal CXCL1 RNA expression and risk factors, we also found a significant association with IDC grade (Figure 2.5B), but there was no significant association with age or tumor size (Table 2.3). In summary, these data indicate a statistically significant association between stromal CXCL1 expression and tumor grade, and modest association between stromal CXCL1 protein expression and age.

Patent samples used for immunohistochemistry analysis were collected within the last 4 years and therefore did not include outcome data. However, by RNA expression analysis in the Finak database, we found a significant correlation between increased CXCL1 RNA expression in breast cancer stroma and increased tumor recurrence and decreased patient survival (Figure 2.6). These data indicate that increased CXCL1 in the breast cancer stroma is associated with poor outcome.

Elevated expression of CXCL1 in stromal derived fibroblasts is associated with decreased TGF-β signaling

To identify the cellular components of the stroma that express CXCL1, we used immunofluorescence. CXCL1 has been shown to be induced in fibroblasts by melanoma cells (104). Breast CAFs were also positive for CXCL1 RNA expression (10). These studies indicate that cancer associated fibroblasts are a potential source of CXCL1 expression. Fibroblasts in breast cancer stroma show non-overlapping expression of a-SMA and FSP1, indicating the presence of different subsets of fibroblasts (95). To determine whether CXCL1 was expressed in particular fibroblast subsets in breast cancer, we performed co-immunoflourescence staining for CXCL1 expression with α-SMA or FSP1. Fluorescence expression of CXCL1 was positive in the tumor epithelium

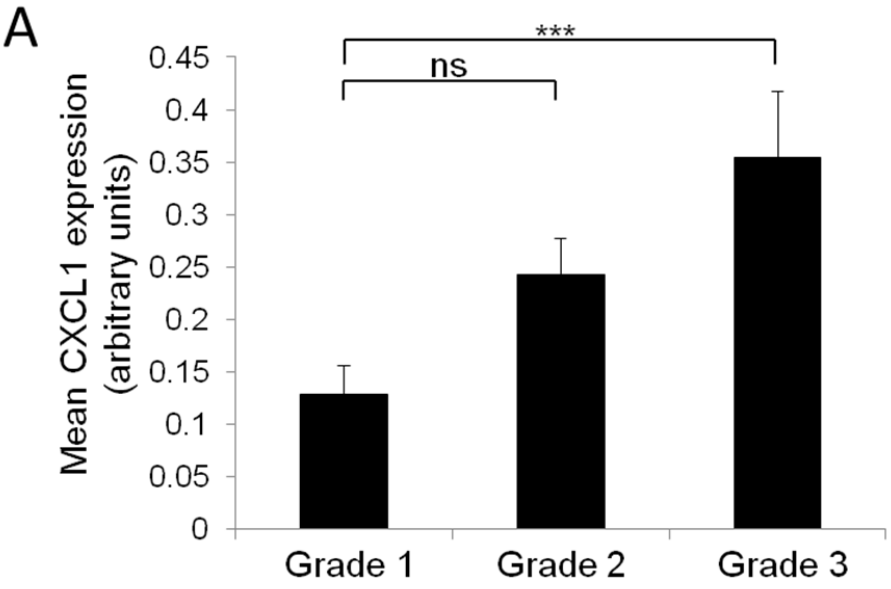
A
***
ns
Mean CXCL1 expression (arbitrary units)
0.45
0.4
0.35
0.3
0.25
0.2
0.15
0.1
0.05
0
Grade 1
Grade 2
Grade 3

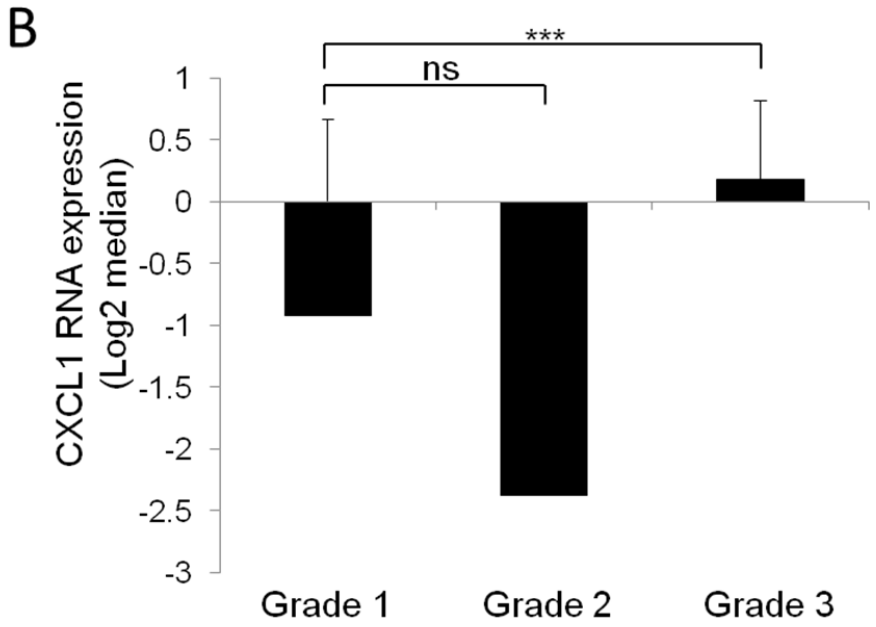
B
***
ns
CXCL1 RNA expression (Log2 median)
1
0.5
0
-0.5
-1
-1.5
-2
-2.5
-3
Grade 1
Grade 2
Grade 3

Figure 2.5. Associations between CXCL1 expression and tumor grade.

(A). Stromal CXCL1 protein expression was analyzed for associations with tumor grade of IDC by Kruskall Wallis Test, followed by Dunn's post-test comparison. *(B)*. CXCL1 RNA expression values were analyzed for associations for tumor grade. Statistical analysis was performed using Wilcoxon Two Sample T Test. Statistical significance determined by $p<0.05$. ns, $p>0.05$; ***$p<0.001$. Values expressed as Mean$\pm$SEM.

Table 2.3. Relationship between known prognostic factors and CXCL1 RNA expression in breast cancer stroma.

Associations were determined using Spearman Correlation analysis of data obtained from the Finak microarray database. Significance determined by $p<0.05$. r= correlation coefficient. N=53.

Prognostic factor	r	95% CI	*p*-value
Age	-0.13	-0.41 to 0.17	0.38
Tumor size	-0.004	-0.31 to 0.30	0.97

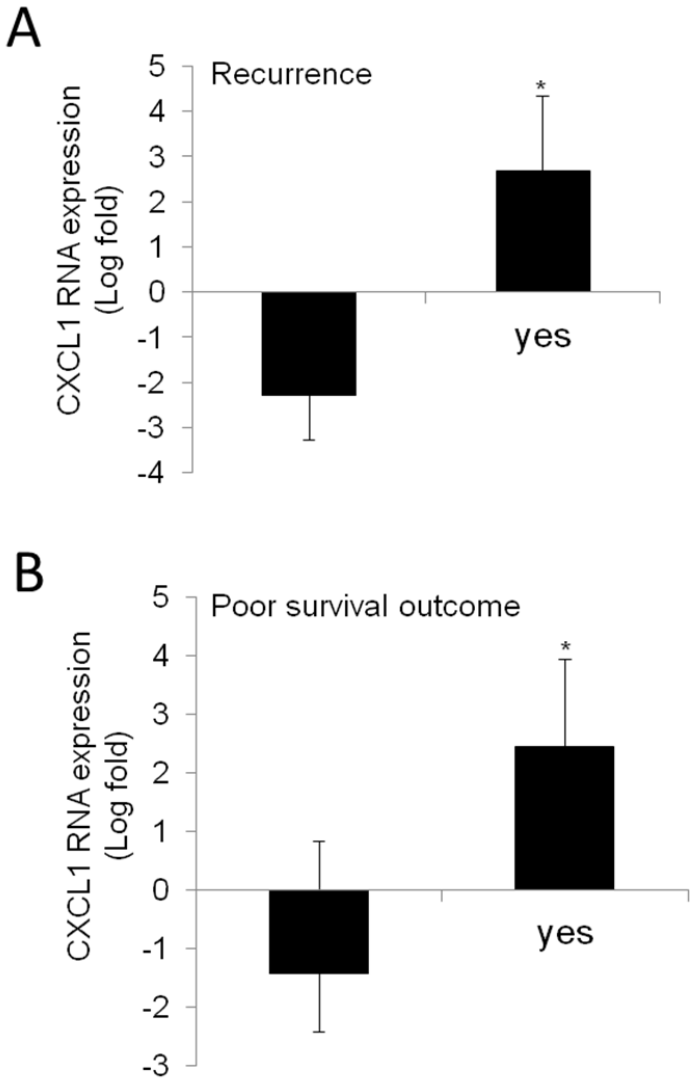
A
Recurrence
CXCL1 RNA expression (Log fold)
5
4
3
2
1
0
-1
-2
-3
-4
*
yes
B
Poor survival outcome
CXCL1 RNA expression (Log fold)
5
4
3
2
1
0
-1
-2
-3
*
yes

Figure 2.6. Increased RNA CXCL1 expression in breast stroma associated with poor prognosis.

CXCL1 RNA expression values were obtained from the Finak microarray database, and analyzed for associations with *(A).* Tumor Recurrence, and *(B).* Decreased survival. Mean±Stdev. Statistical analysis was performed using Wilcoxon Two Sample T Test. Statistical significance determined by $p<0.05$. *, $p<0.05$.

and stroma, consistent with DAB expression patterns. In particular, we observed that CXCL1 overlapped with both α-SMA and FSP1 expressing cells (Figure 2.7). The absence of CXCL1 expression was noted in some α-SMA and FSP1 expressing cells, indicating that these fibroblasts were not expressing CXCL1. In summary, these data indicate CXCL1 is expressed in both α-SMA and FSP1 positive fibroblasts in breast cancer stroma.

We had observed that stromal CXCL1 expression was independent of many known risk factors (Table 2.2), and that CXCL1 was localized to CAFs. We therefore analyzed for molecular factors affecting CXCL1 expression in fibroblasts. Transforming Growth Factor Beta signaling (TGF-β) is an important regulator of fibroblast activity. In cultured fibroblasts, TGF-β modulates cell proliferation and induces production of growth factors, angiogenic factors, extracellular matrix proteins and proteases, vital for mammary ductal branching and morphogenesis during mammary gland development (105). TGF−β carries out its functions by signaling through its TGF-β type II receptor to activate the Type I receptor, and downstream effectors including Smad2/3 transcription factors to regulate cellular behavior (105, 106). Dominant negative expression of the TGF-β type II receptor in mammary stroma of transgenic mice result in mammary hyperplasia, indicating that a tumor suppressive role for TGF-β signaling in mammary stroma (107). Cre-mediated deletion of exon 2 of TGF-β type II receptor gene (*Tgfbr2*) in mammary fibroblasts (FspKO) had been shown to inhibit TGF-β mediated suppression of fibroblast proliferation. Co-transplantation of FspKO fibroblasts with 4T1 and PyVmT mammary carcinoma cells in the sub-renal capsule of nude mice enhanced tumor progression. These tumor promoting phenotypes were associated with changes in paracrine signaling

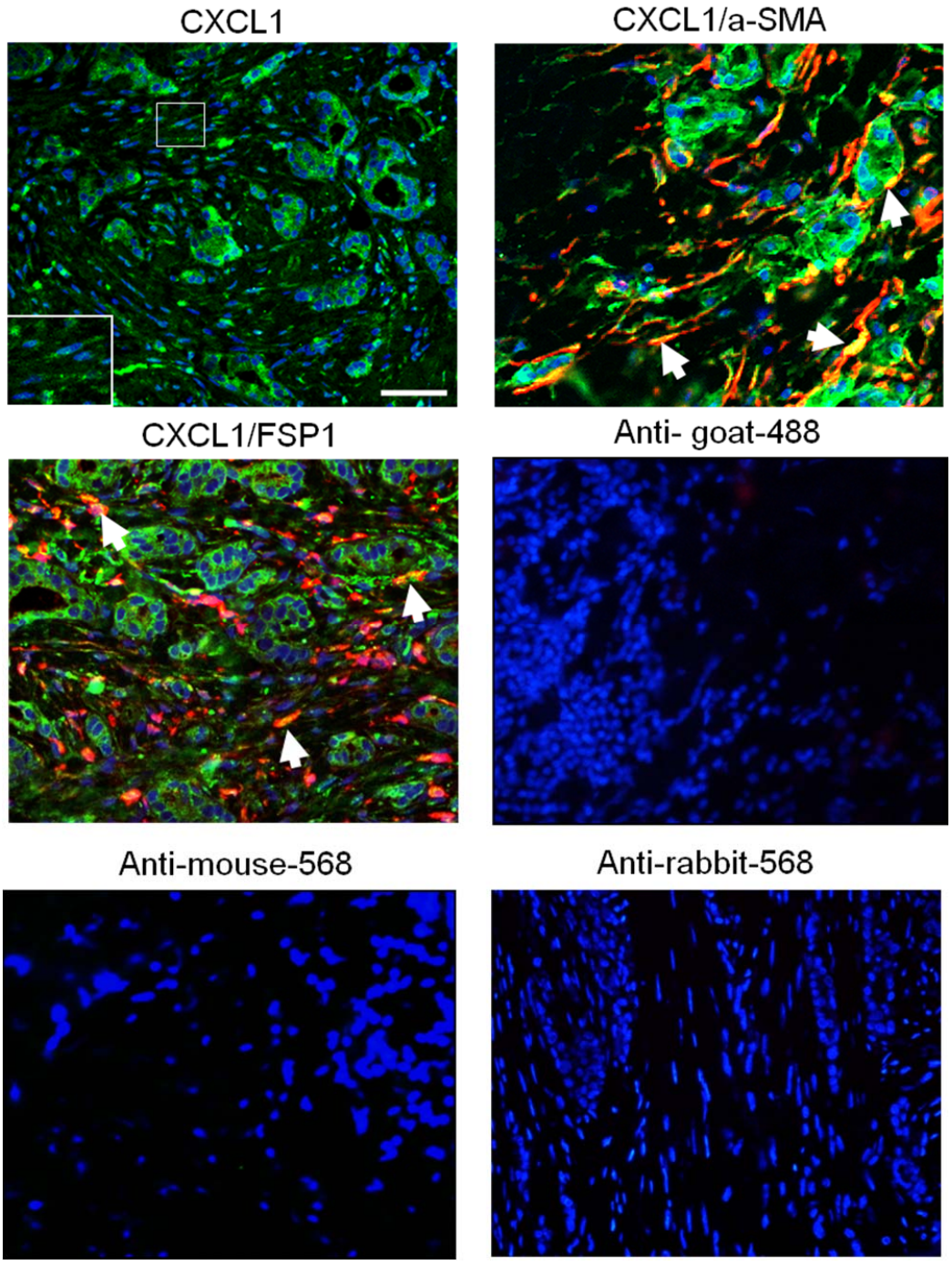
CXCL1
CXCL1/a-SMA
CXCL1/FSP1
Anti- goat-488
Anti-mouse-568
Anti-rabbit-568

Figure 2.7. CXCL1 co-localizes with α-SMA and FSP1 positive stroma.

Patient samples of breast ductal carcinoma were co-immunofluorescence stained for expression of CXCL1 (green), α-SMA and/or FSP1 (red). Representative samples of CXCL1, α-SMA, and FSP1 shown. Sections were counterstained with DAPI. Secondary antibody only controls are shown: anti-goat 488 for CXCL1, anti-mouse-568 for α-SMA and anti-rabbit-568 for FSP1. Arrows point to positive staining in fibroblastic cells. Scale bar= 100 microns.

and increased expression of growth factors and pro-metastasis factors (86-88). Given that TGF-β signaling in fibroblasts functioned to suppress tumor progression, we hypothesized that TGF-β would be negatively associated with CXCL1 expression in breast cancer stroma.

To determine the relationship between stromal CXCL1 and TGF-β signaling, we analyzed the protein expression patterns of TGF-β, and activation of downstream effectors, phosphorylated Smad2 and phosphorylated Smad3 in breast tumor samples. In order to perform pairwise correlation analysis, immunostaining was performed on tumor samples obtained from the BRCF core that were stained for CXCL1 expression. Decreased expression of TGF-β, phosphorylated Smad2 and phosphorylated Smad3 proteins were observed in DCIS and IDC stroma (Figure 2.8). Positive expression of stromal CXCL1 was inversely correlated with expression of TGF-β, phosphorylated Smad2 and phosphorylated Smad3 proteins (Table 2.4). These data indicate an inverse correlation between stromal CXCL1 protein expression and expression of TGF-β related proteins. We also analyzed the RNA expression patterns of CXCL1 and TGF-β related genes including *TGFB, TGFBR2, SMAD2* and *SMAD3*. By Spearman correlation analysis, we detected no significant associations with stromal *CXCL1* and *SMAD3* expression. *CXCL1* expression positively correlated with *TGFBR2* and *SMAD2* gene expression (Table 2.5). These data indicate a positive correlation between *CXCL1* and expression of TGF-β related genes.

Given the differences in association between CXCL1 RNA and protein with TGF-β related gene and protein expression, we performed further studies to clarify the role of TGF-β signaling on CXCL1 expression in fibroblasts. In previous studies, a conditional knockout mouse model (FspKO) was generated. In that model, exon2 of the Tgfbr2 gene

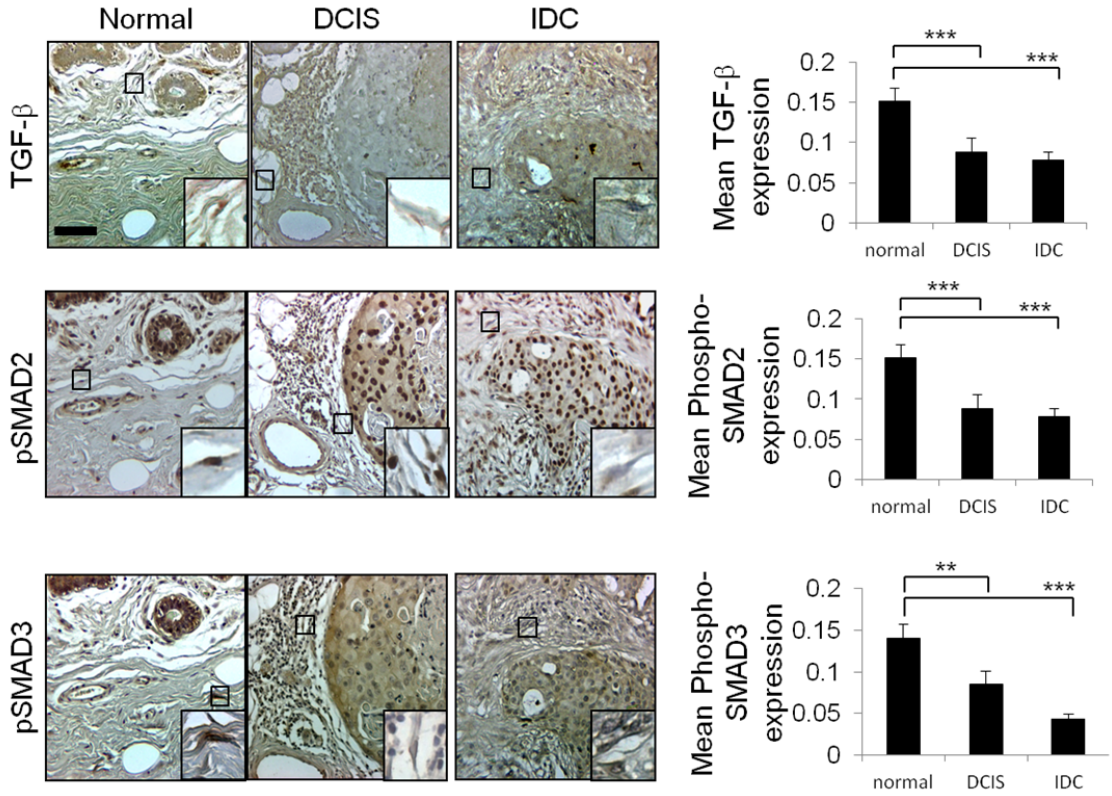
Normal
DCIS
IDC
TGF-β
pSMAD2
pSMAD3
Mean TGF-β expression
Mean Phospho-SMAD2 expression
Mean Phospho-SMAD3 expression
0.2
0.15
0.1
0.05
0
normal
DCIS
IDC
***
**

Figure 2.8. Expression patterns of CXCL1 and TGF-β signaling proteins in breast cancer stroma.

Adjacent sections of normal breast and invasive breast carcinoma on TMAs were subject to immunohistochemistry staining for TGF-β, phosphorylated Smad2 and phosphorylated Smad3 expression. Representative staining is shown. Expression was quantified by Image J, arbitrary units. Scale bar= 50 microns. Statistical analysis was performed using Kruskall Wallis Test, followed by Dunn's post-test comparison. Statistical significance determined by $p<0.05$. **, $p<0.01$; ***, $p<0.001$. Values are expressed as Mean±SEM.

Table 2.4. Protein expression of TGF-β signaling components inversely correlate with CXCL1 expression in breast stroma.

Association between expression of CXCL1 and expression of TGF-β signaling components in normal and breast cancer stroma was determined by Spearman Correlation analysis. Significance determined by $p<0.05$. r= correlation coefficient.

Signaling Component	r	95% CI	*p*-value	n
TGF-β	-0.33	-0.52 to -0.09	0.01	69
p-Smad2	-0.25	-0.44 to -0.027	0.02	80
p-Smad3	-0.32	-0.50 to -0.10	<0.01	81

Table 2.5. Correlation between RNA expression of CXCL1 and gene expression of TGF-β signaling components.

Association between CXCL1 protein expression and expression of TGF-β signaling components was determined using Spearman Correlation analysis of normal and breast cancer stroma. Significance determined by $p<0.05$. r= correlation coefficient.

Signaling Component	r	95% CI	*p*-value
TGFB1	0.19	-0.09 to 0.45	0.18
TGFBR2	0.12	-0.16 to 0.39	0.12
SMAD2	0.33	0.06 to 0.57	0.01
SMAD3	0.11	-0.17 to 0.38	0.42

was deleted by cre, placed under the control of the Fsp1 promoter. Mammary fibroblasts isolated from FspKO mice and control mice (Flox/Flox) were isolated and immortalized. Immortalized fibroblasts were shown to be genetically stable and behave similarly to primary fibroblasts in vitro and when transplanted into mice (88). These studies demonstrate a reliable model to study the role of TGF-β signaling on CXCL1 expression in mammary fibroblasts. In FspKO fibroblasts, a significant increase in CXCL1 protein secretion was detected by ELISA, compared to control fibroblasts (Figure 2.9A). The increased protein secretion corresponded to elevated luciferase activity of the CXCL1 promoter in FspKO fibroblasts (Figure 2.9B). To determine whether FspKO fibroblasts phenocopied CAFs, we analyzed for CXCL1 expression in mammary fibroblasts isolated from MMTV-PyVmT transgenic mice. CXCL1 expression was significantly higher in CAF cell lines compared to normal fibroblasts and corresponded to lower levels of TGF-β expression in CAFs (Figures 2.9C-D). Furthermore, treatment of TGF-β inhibited CXCL1 secretion in the fibroblast cell lines (Figure 2.9E). These data demonstrate that TGF-β signaling negatively regulates expression of CXCL1 in CAFs.

Discussion

Empirical studies in animal models and human tissues have established the importance of stromal derived fibroblasts on cancer progression (27, 108). However, the idea of the “tumor promoting” fibroblast has been unclear. While recent studies have shown that the CXCL1 chemokine is expressed in tumor epithelial cells and stromal cells, the relevance of stromal CXCL1 expression has remained poorly understood. The goals of these studies were to characterize the protein and gene expression patterns of CXCL1 in breast cancer stroma, and identify factors affecting stromal CXCL1 expression. Here we report that elevated CXCL1 expression in breast cancer stroma is associated

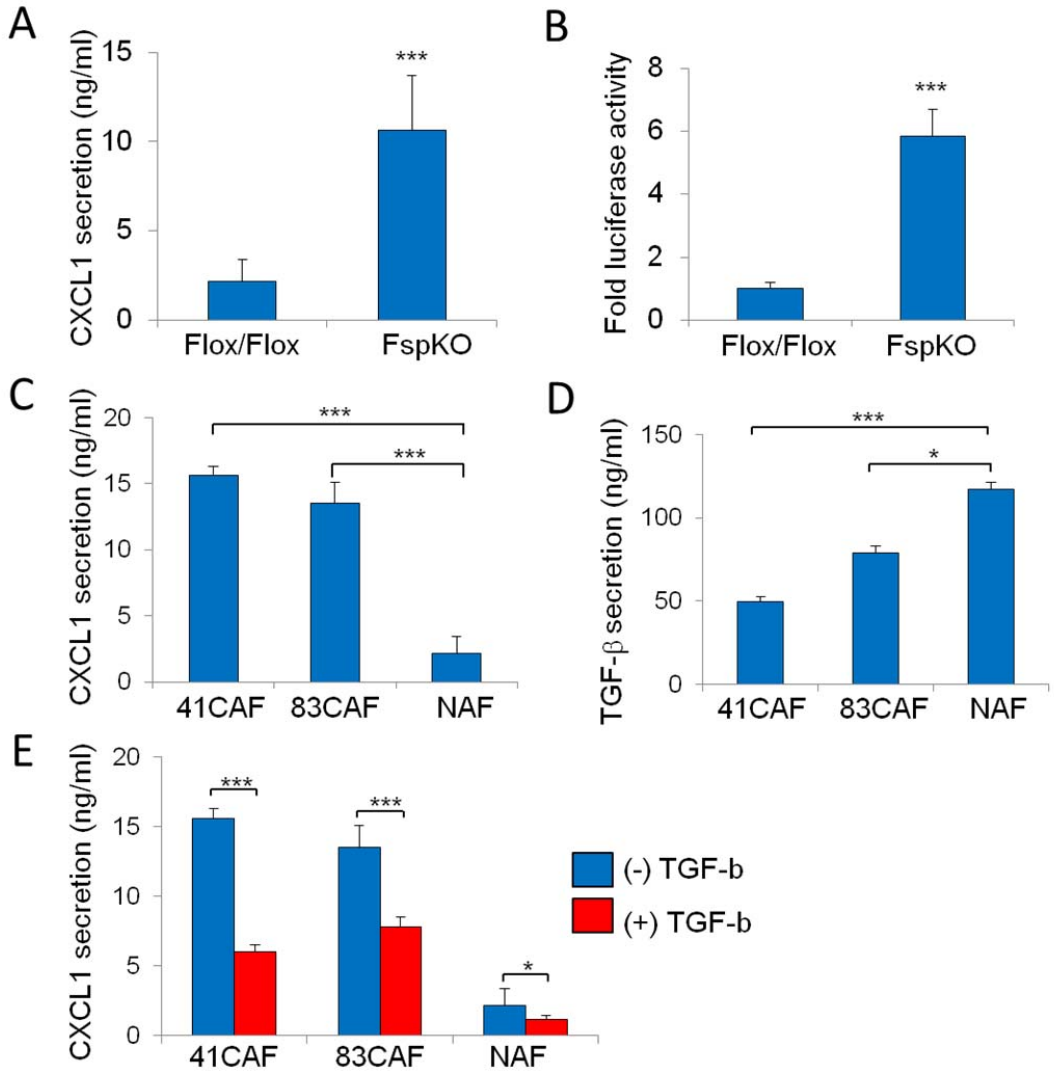
A
CXCL1 secretion (ng/ml)
15
10
5
0
***
Flox/Flox
FspKO
B
Fold luciferase activity
8
6
4
2
0
***
Flox/Flox
FspKO
C
CXCL1 secretion (ng/ml)
20
15
10
5
0
***
***
41CAF
83CAF
NAF
D
TGF-β secretion (ng/ml)
150
100
50
0
***
*
41CAF
83CAF
NAF
E
CXCL1 secretion (ng/ml)
20
15
10
5
0
***
***
*
41CAF
83CAF
NAF
(-) TGF-b
(+) TGF-b

Figure 2.9. CXCL1 expression is inversely associated with TGF-β signaling in mammary fibroblasts.

(A). Conditioned media from Flox/Flox or FspKO fibroblasts were analyzed for CXCL1 secretion by ELISA. *(B).* Flox/Flox control or FspKO fibroblasts were co-transfected with CXCL1 firefly and Renilla luciferase reporter constructs and analyzed for luciferase activity. Values are normalized to Renilla. *(C-D).* Conditioned medium of cultured Carcinoma associated fibroblast cell lines (41CAF, 83CAF) or normal fibroblasts (NAF) were analyzed by ELISA for CXCL1 (C) or TGF-β secretion *(D). (E).* Fibroblasts were treated with 5 ng/ml TGF-β for 48 hours and analyzed for CXCL1 secretion by ELISA. Statistical analysis was determined by two-tailed student *t*-test. Statistical significance determined by $p<0.05$. *,$p<0.05$; ***, $p<0.001$. Values are expressed as Mean ± SEM.

with tumor recurrence and decreased patient survival. We also show that CXCL1 is localized to α-SMA and Fsp1 expressing fibroblasts, and is negatively regulated by TGF-β signaling. These studies contribute to the definition of the tumor promoting fibroblast, identify similarities and differences in the RNA and protein expression patterns, and provide insight into the prognostic value of examining biomarker expression in cancer stroma.

Previous studies have reported elevated CXCL1 RNA expression in breast cancer, stroma (10). Some studies have shown significant correlations between RNA and protein expression in simple organisms such as yeast and E. Coli (109). High correlations of RNA and protein levels in mammalian cells referred to genes involved in structural and cellular homeostasis (110). Other studies have reported variations between RNA and protein levels in biomarker studies in various cancer cell lines of various origins (lymphoid, myeloid, melanoma, glioma, sarcoma, neuronal, and endometrial, colorectal and bladder carcinomas) through microarray and protein arrays over 1000 gene products (111). In our studies, we observed some similarities between stromal CXCL1 protein and RNA expression levels in breast stromal tissues. Intensity of RNA and protein expression levels were higher in breast tumors compared to normal breast tissues. Elevated expression levels of stromal CXCL1 RNA and protein were associated with tumor grade, but there were no significant differences in association with the other risk factors examined.

These studies indicate some associations between RNA levels and protein expression in breast cancer stroma. Yet, we also observed several differences in RNA and protein expression. Incidence patterns differed, with stromal CXCL1 protein expression expressed in all tumors examined, while the RNA was expressed in a small subset of breast tumor samples. In addition, the stromal CXCL1 protein expression inversely

correlated with expression of TGF-β, phosphor-Smad3 and phospho-Smad2. In contrast, CXCL1 RNA levels positively correlated with TGFBR2 and SMAD2 gene expression. It is highly possible that multiple post-transcriptional and post-translational mechanisms contribute to the differences in RNA and protein expression in breast cancer stroma. Studies have shown that NF-kB, PARP and CREB binding proteins positively regulate CXCL1 transcription, while CAAT displacement proteins negatively regulate CXCL1 transcription. Their activities have been reported in breast cancer and could affect CXCL1 transcript levels (112, 113). It would be of interest to examine the transcriptional mechanisms of CXCL1 expression in stromal cells. Post-transcriptional mechanisms active in breast cancer include RNA stabilization through RNA binding protein activity (114) and microRNAs (115) or up-regulated (mir 143) (116). However, studies have shown that RNA binding protein HuR regulates stability of CCL2 and CCL8 chemokines, but not CXCL1 (117). Mir7641 has been shown to regulate CXCL1 expression in endothelial cells (118). Mir200 has been shown to modulate CXCL1 mRNA expression in invasive breast cancers (119). These studies indicate that microRNA levels in breast tumor tissues may affect CXCL1 expression. The post-translational mechanisms for CXCL1 are less clear, studies have reported biochemical binding between CXCL1 and heparin normally present in extracellular matrix to enhance CXCL1 protein half-life (120). Thus, it is possible for stromal CXCL1 protein expression levels to be sustained in the absence of RNA expression. It would be of interest to further study post-transcriptional and post-translational mechanisms in the context of breast stromal tissues and fibroblasts to understand how RNA and protein levels are modulated.

We report here that CXCL1 is elevated in breast CAFs and is associated with increased tumor recurrence and tumor grade. As the binding receptors CXCR1 and CXCR2 are expressed on myeloid derived cells and carcinoma cells, CXCL1 expression

in CAFs may serve to regulate paracrine signaling interactions with immune cells and cancer cells to chemo-resistance and tumor progression. This hypothesis is supported by previous studies in which CXCL1 expression in MMTV-PyVmT transgenic mouse model functioned to recruit myeloid immune suppressor cells that enhanced survival and invasion of mammary tumors. Treatment of mammary tumors with Doxyorubicin, a commonly used chemotherapy, resulted in the selection of drug resistant mammary carcinoma cells with elevated CXCL1 expression in cancer cells (71). Studies have shown that chemotherapies do not efficiently target CAFs for cell death but rather enhance the tumor promoting activities through enhanced secretion of growth factors and cytokines (33, 34). It is possible that CXCL1 expression in CAFs is retained or further elevated after chemotherapy treatment, serving to promote the survival and selection of chemoresistant tumor cells. It would of interest in future studies to conduct further expression studies on stromal CXCL1 on breast tumor tissues from patients treated with chemotherapies, followed by studies in animals to clarify the role of CAF-derived CXCL1 on breast cancer progression and tumor recurrence.

A few studies have been conducted to report the prognostic significance of TGF-β signaling protein expression in breast stroma. One study reported that increased TGF-β type II receptor in breast cancer stroma (121) but did not identify the specific stromal cell type. In these studies, we report decreased expression of TGF-β, phosphorylated Smad2 and phosphorylated Smad3 in CAFs, which are associated with positive CXCL1 expression. These studies indicate that CAFs exhibit decreased TGF-β signaling, and that TGF-β signaling in fibroblasts may function as tumor suppressor. These observations are consistent with previous studies showing that TGF-β signaling deficient fibroblasts enhanced progression of 4T1 and PyVmT mammary carcinoma cells in the subrenal capsule model (87, 88). In breast tumor epithelial cells, TGF-β signaling

functions as both a tumor suppressor and tumor promoter (122-124). While it is recognized that expression of TGF-β related proteins are clinically significant in breast cancer, studies have reported opposing results, with some studies reporting that positive expression of TGF-β or phospho-Smad proteins is related to longer patient survival and decreased recurrence (125, 126), Other studies have reported the opposite associations (125, 127-129). Expression of TGF-β signaling proteins in cancer cells may be dependent on biological factors such as age and clinical factors including mutation status and stage of disease (125, 127). With different factors regulating TGF-β expression, it is possible that TGF-β signaling in stromal derived fibroblasts would be independent from the epithelium. In support of this hypothesis, TGF-β expression has been shown to be regulated by an autocrine feedback loop in mouse embryonic fibroblasts and lung carcinoma cells (130, 131). As fibroblasts are more genetically stable than cancer cells (132), it is possible that mechanisms other than genetic mutations would down-regulate TGF-β signaling in CAFs. Stat3, MAPK and NF-κb inhibit TGF-β signaling (133, 134) and may contribute to decreased TGF-β expression and phosphorylated Smad2 or Smad3 expression in stromal derived CAFs. In addition, epigenetic mechanisms, including methylation of TGF-β and Smad promoters to silence gene expression have been demonstrated in ovarian and breast cancer (135, 136). It would be of interest to further study how TGF-β signaling is regulated in the context of breast stromal tissues, in order to further define breast CAFs.

In summary, we report that elevated CXCL1 expression in breast cancer stroma is associated with poor patient prognosis. We provide further insight into the clinical significance of stromal derived CXCL1 expression, and demonstrate that multiple types of breast CAFs are sources of CXCL1 expression. In addition, we also demonstrate that CXCL1 expression in breast CAFs is in part, determined by TGF-β signaling. As CXCL1

is increasingly shown to play important roles in tumor recurrence and chemo-resistance, further studies on the impact of CXCL1 expression on the breast tumor microenvironment will aid in the development of novel anti-cancer therapies to combat drug resistant tumors.

Chapter III: Up-regulated CXCL1 expression in mammary carcinoma associated fibroblasts is negatively regulated by TGF-β signaling through Smad2,3-dependent mechanisms and through HGF/c-Met-dependent mechanisms.

Abstract

Fibroblasts are important cellular components of the breast tumor microenvironment, whose accumulation correlates with invasive cancer progression and poor patient prognosis. We previously demonstrated that breast cancer associated fibroblasts (CAFs) overexpress CXCL1, a chemotactic cytokine involved in cancer progression and chemo-resistance. In order to understand the molecular mechanisms regulating CXCL1 expression in CAFs, we examined the role of TGF-β, a key modulator of fibroblast activity in breast cancer. In time course studies, TGF-β inhibited CXCL1 mRNA and protein expression in CAFs within 24 hours, and continuing through 120 hours. The early reduction in CXCL1 expression correlated with TGF-β phosphorylation of Smad2/3 proteins. siRNA knockdown studies revealed that Smad2 and Smad3 were important for suppressing CXCL1 promoter activity in CAFs. Chromatin Immunoprecipitation (ChIP) assays revealed that Smad2 and Smad3 proteins bind to the CXCL1 promoter region which contains potential binding sites at -249 bp to -246 bp and -144 bp to -141 bp, relative to the transcriptional start site. These Smad binding elements are proximal to binding sites for C/EBP-β, a trans-activator of CXCL1 expression. siRNA knockdown studies showed that C/EBP-β activity was repressed by Smad3, but not Smad2. Long-term suppression of CXCL1 by TGF-β correlated with decreased expression of the growth factor, HGF. siRNA knockdown and pharmacologic inhibition studies revealed that HGF signaled through c-Met receptors expressed on CAFs to positively regulate CXCL1 expression through NF-κB dependent mechanisms. HGF expression was found to be negatively regulated by TGF-β signaling. These studies provide novel insight into how TGF-β and HGF signaling coordinate CXCL1 chemokine expression in CAFs.

Introduction

Fibroblasts are a major cell type in connective tissues throughout the body, that regulate multiple biological processes including inflammation, wound healing and tumor progression (27, 81, 82). Fibroblasts are normally quiescent, and become activated in response to inflammatory cytokines. Activated fibroblasts enhance secretion of extracellular matrix proteins, proteases and growth factors, which regulate tissue remodeling. In breast cancer, the accumulation of fibroblasts correlates with invasive cancer progression and poor patient prognosis (23, 27). In animal studies, co-grafting of carcinoma associated fibroblasts (CAFs) with breast carcinoma cells results in increased tumor growth, survival and metastasis (70, 80, 90). Breast tumor outgrowth is inhibited by co-transplantation of normal fibroblasts (NAFs) (83, 92). While NAFs and CAFs exhibit a uniform cell morphology, molecular profiling studies reveal that CAFs show increased expression of extracellular matrix proteins, growth factors and cytokines, which may contribute to tumor progression (17, 137, 138). Transforming Growth Factor-beta (TGF-β) signaling is an important regulator of fibroblast activity. TGF-β signals through TGF-β type I and type II receptors, which activate Smad2 and Smad3 proteins resulting in complexes with Smad4. This complexes translocate into the nucleus to regulate transcription of genes related to the cell cycle, adhesion and invasion (78). Studies indicate that TGF-β signaling in fibroblasts can promote or suppress tumor progression, depending on the cancer type. In prostate cancer, increased TGF-β expression enhances fibroblast proliferation, contributing to tumor progression (84, 85). In breast cancer, TGF-β signaling in fibroblasts is tumor suppressive. Inactivation of TBRII mammary fibroblasts through cre-lox mediated deletion (Tgfbr2FspKO) enhances mammary tumor growth and metastasis in MMTV-PyVmT transgenic mice and in co-transplantation models (86-88). Tgfbr2FspKO fibroblasts show increased expression of

growth factors, including Transforming Growth Factor-α and Hepatocyte Growth Factor (HGF), which act on mammary carcinoma cells to promote epithelial cell growth and migration (88, 89). These factors are similarly overexpressed in CAFs (80, 89), suggesting a link between decreased TGF-β signaling in breast CAFs and enhanced expression of tumor promoting factors. CXCL1 is a tumor promoting factor recently shown to be up-regulated in CAFs. CXCL1 is a member of the chemokine family, normally involved in regulating recruitment of bone marrow derived cells during wound healing and inflammation (64, 139, 140). In melanoma and breast cancer, CXCL1 recruits myeloid cells to primary tumors to promote cancer cell survival, invasion and drug resistance (71, 141). CXCL1 expression is de-regulated in a number of cancers, including: melanoma, prostate cancer, and bladder cancer (64, 142, 143). In breast cancer, CXCL1 overexpression is associated with metastasis of the HER2 overexpressing subtype (66). Recent studies show that breast CAFs express high levels of CXCL1, correlating with tumor recurrence and poor patient survival (10). CXCL1 levels expression in CAFs correlates with decreased expression of Transforming Growth Factor-β as described in Chapter II, revealing an inverse relationship between CXCL1 expression and TGF-β signaling. It has been unclear how CXCL1 expression is regulated in CAFs. Using mammary CAF cell lines isolated from Polyomavirus Middle T (PyVmT) transgenic mice, we characterized the mechanisms regulating expression of CXCL1. Through siRNA knockdown studies, we showed that TGF-β activated Smad2/3 proteins, which repressed CXCL1 promoter activity, contributing to an early reduction in CXCL1 levels. Through siRNA and pharmacologic inhibitor studies, we showed that TGF-β treatment of CAFs blocked expression of HGF, a positive regulator of CXCL1, contributing to a long-term reduction in CXCL1 levels. These studies reveal novel insight into how TGF-β and HGF signaling coordinate CXCL1 chemokine expression in CAFs in

a temporal manner, enhancing our understanding how expression of soluble factors are regulated in the cancer stroma.

Materials and methods

Cell culture

Primary CAFs (41CAF, 83CAF, 232CAF) were isolated from transgenic mice (FVB) expressing the PyVmT oncogene under the control of Mouse Mammary Tumor Virus Promoter (MMTV), at 12-16 weeks of age. Primary normal mammary tissue associated fibroblasts (NAFs) (311NAF, 4f NAF) were isolated from wild-type C57BL/6 mice at 12-16 weeks of age. Tgfbr2FspKO fibroblasts were isolated from Tgfbr2FspKO mice as described (88). Fibroblasts cell lines were generated by spontaneous immortalization of primary mammary fibroblasts and clonal populations of fibroblasts were obtained as described (88). Cells were cultured in Dulbecco's modified Eagle medium (DMEM) containing 10% fetal bovine serum (FBS)/ MEM nonessential amino acids/ 2 mM L-glutamine/ 100 I.U/ml penicillin/ 100 µg/ml streptomycin/ 0.5 µg/ml amphotericin B.

siRNA silencing

Negative control siRNAs (cat. no. AM4613) were obtained from Ambion. siRNAs targeting Smad2 (cat. no. sc-38375), Smad3 (cat. no. sc-38377), and HGF (cat. no. sc-37112) were obtained from Santa Cruz Biotechnology. Transfection of siRNA into the cells was performed according to manufacturer's protocols. Briefly, cells were seeded in a 24-well plate at a density of 20,000 cells per well and cultured for 24 hours. Cells were then rinsed with PBS and Opti-MEM (Gibco cat. no. 11058-021), and incubated in Opti-MEM with complexes of 12 pmol siRNA and 2.4 µl Lipofectamine TM 2000 reagent

(Invitrogen Life technologies) for 24 hours. The medium was replaced with Opti-MEM/10%FBS for 24 hours prior to stimulation or starvation.

Luciferase assay

The firefly luciferase reporter construct containing the CXCL1 promoter region between position -701 to +30 (PGL3.luc.CXCL1) was kindly provided by Katherine Roby, Ph.D (University of Kansas Medical Center, Kansas City, KS). Renilla luciferase reporter plasmid was obtained from Addgene (plasmid 12177: pIS2). The firefly luciferase reporter construct containing the NF-κB promoter (pNFκB-luc) was obtained from Agilent Technologies (cat. no. 219078). The firefly luciferase reporter contruct containing the pC/EBP-β promoter (pC/EBP-β.luc) was obtained from Agilent Techologies (cat. no. 24011). The Smad2/3 firefly luciferase reporter, 3TP-lux (144) was kindly provided by Harold L. Moses, M.D (Vanderbilt University, Nashville, TN). Cells were seeded in 6 cm-dishes at a density of 150,000 cells and cultured for 24 hours. Cells were then co-transfected with 8 µg firefly luciferase plasmids and 400 ng Renilla luciferase plasmids for 24 hours using 8.4 µl Lipofectamine LTX and 15 µl Plus reagents according to manufacturer's protocol (Invitrogen Life technologies). Cells were recovered in Opti-MEM/10% FBS for an additional 24 hours. Cells were re-seeded into 24-well plate, 20,000 cells/well for 24 hours prior to siRNA knockdown. After stimulation, cell lysates were analyzed using the Promega Dual-Luciferase Reporter Assay system (cat. no. E1910). Cells were rinsed twice with PBS, lysed in100 µl passive lysis buffer for 15 min at room temperature on shaker. Cell lysates were sonicated for 10 seconds on ice and centrifuged to eliminate cell debris. 20 µl lysates were assayed in triplicate in 96-well opaque plate (Corning Costar, cat. no. 3912) using a Veritas Microplate Luminometer (Turner BioSystems, model number 9100-202).

Site-directed mutagenesis

Site-directed mutagenesis for Smad Binding Elements (SBE) were generated using QuickChange Lightning Site-Directed Mutagenesis Kit (cat. no. 210518, Agilent) following manufacturer's protocol. The firefly luciferase reporter plasmids containing the CXCL1 promoter region between position -701 to +30 (PGL3.luc.CXCL1) was used as DNA templates. SBE1 (from -249 bp relative of TSS) was mutated from 5'-GTCTC-3' to 5'-TGAGA-3' using primers of:

SBE1_mut sense (5' to 3') cctgagcactggagactctgaatgagaactactcctccccccccca,

SBE_mut anti-sense (5' to 3') tgggggggggaggagtagttctcattcagagtctccagtgctcagg.

SBE2 (from -144bp relative of TSS) was mutated from 5'-GTCTA-3' to 5'-TGAGC-3' using primers of:

SBE2_mut sense (5' to 3') ccccccttgctccactcccaaggatgctcatctgggatttttgctttttgcccc,

SBE2_mut anti-sense (5' to 3') ggggcaaaaagcaaaaatcccagatgagcatccttgggagtggagcaaggggg.

SBE1 and SBE2 double mutant was generated by mutating SBE2 using generated SBE1 mutant as DNA template. All mutated plasmids was sequenced using primers of:

SBE mutagenesis sequencing sense (5' to 3') CCACCTCACGTGGGATAAGA.

Inhibitor reagents

c-Met kinase inhibitor II (cat. no.448102) and NF-κB cell-permeable inhibitor peptide SN50 (cat. no. 481480) were obtained from Calbiochem.

ELISA

Cells were seeded in 24-well plate at a density of 20,000 cells per well and cultured for 24 hours prior to treatment. To generate conditioned media, cells were incubated in

500 µl Opti-MEM/10%FBS media for 24 hours for TGF-β treatment experiments, or in 500ul Opti-MEM media for 24 or 48 hours for all other experiments. Conditioned media was collected and centrifuged to eliminate cell debris. For HGF ELISA, 100 µl of conditioned media was analyzed for HGF expression according to manufacturer protocol (capture antibody cat. no. AF2207; detection antibody cat. No. BAF2207, R&D Systems). For *CXCL1 ELISA*, 20 µl conditioned media was diluted in 80 µl Opti-MEM media and analyzed by CXCL1 ELISA kit following manufacturer's instructions (cat. no. 900-K27 for mouse CXCL1; cat. no. 900-K38 for human CXCL1, Peprotech). For TGF-β ELISA, 100 µl conditioned media was analyzed for TGF-β expression according to the manufacturer's protocol (cat. no. DY1679, R&D Systems) Reactions were catalyzed using tetramethylbenzidine substrate (cat. no. 34028, Thermo Scientific). Reactions were stopped using 50 µl/well of 2N HCl and read at *A*450nm using a 1420 multi-label counter (VICTOR3 TM V, PerkinElmer). All samples were analyzed in triplicate.

Immunoblot analysis

Cells were rinsed with PBS twice and lysed in RIPA buffer containing 10 mM Tris-HCl, pH 8.0, 0.1 mM EDTA, 0.1% sodium deoxycholate, 0.1% SDS, and 140 mM NaCl, supplemented with a Sigma cocktail of protease and phosphatase inhibitors (cat. no. P8340) and 10 mM of sodium orthovanadate (cat. no. S6508). 80 µg of protein were resolved by 10% SDS-PAGE. The proteins were transferred to nitrocellulose membranes and then probed with antibodies (1:1000) to Smad2 (cat. no.610843, BD Biosciences), Smad3 (cat. no. 9523, Cell Signaling Technology), phospho-Smad2 (Ser-465/467, Cell Signaling Technology, cat. no.3101), phospho-Smad3 (Ser-423/425, cat. no.9520, Cell Signaling Technology), c-Met (cat. no. 4560, Cell Signaling Technology), phospho-c-Met (Tyr-1234/1235, cat. no. 3077, Cell Signaling Technology), or pan-actin (cat. no. 4698, Cell Signaling Technology). Specific immunoreaction was detected with

rabbit or mouse secondary antibodies conjugated to horseradish peroxidase and West Pico ECL Western blotting substrate (cat. no. 34080, Thermo SCIENTIFIC)

Flow cytometry analysis

Cells were cultured in complete medium in 10 cm dishes to 80% of sub-confluence. To detach cells from the plastic, cells were rinsed with PBS twice followed by incubation with 3 mM EDTA at 37℃ for 10-15 min. Cells were washed with 10 ml of complete medium twice, and fixed by neutral formalin buffer (VWR) for 10 min. To remove traces of formalin, cells were washed with PBS twice. For combined extracellular and intracellular c-Met staining, 500,000 cells were permeabilized with 0.2% of Tween 20 / PBS at 37℃ for 15 min (180), followed by wash with 0.1% Tween/PBS three times. Cells were incubated with Alexa Fluor 488 conjugated-c-Met antibody (cat. no. 11-8854-80, eBiosciences) at 1: 100 dilution in PBS on ice for 30 min. Cells were washed with 0.1% Tween/PBS three times and filtered in PBS prior to analysis. Cells were compared with unstained control and secondary antibody-only controls. CXCR2 expression was analyzed on an LSRII flow cytometer (BD Biosciences).

qRT-PCR

41CAFs (20,000 cells) were treated with or without recombinant TGF-b for indicated time periods. Total RNA was extracted using E.Z.N.A.® Total RNA Kit I (cat. no. R6834, Omega) following manufacturer's protocol. One microgram of total RNA was reverse transcribed with the following in a total of 30μl volume: 4 μl of 25 mM MgCl2, 2 μl of 10 x PCR buffere II, 1 μl of 10 mM dNTPs (cat. no. 18427-013, Invitrogen), 1 μl of RNAse inhibitor (cat. no. EN0531, Thermo Scientific), 1 μl of random primers (cat. no. 48190-011, Invitrogen) and 1 μl SuperScript® II Reverse Transcriptase (cat. no. 18064-014, Invitrogen). PCR reactions were performed at 25°C for 10 minutes, 42°C for 45 minutes

and 99 °C for 5 minutes. Approximately 2% of each reverse transcription reaction mixture was added to reactions containing the following in a total volume of 50 µl: 25 µl 2 X SYBR green master mix (cat. no. 4309155, Applied Biosystems) and 1µl of 10µM forward and reverse primers for mouse CXCL1 gene. PCR primers were obtained from IDT (http://www.idtdna.com):

mouse CXCL1 sense (5'-3') TCCCCAAGTAACGGAGAAAGAA,

mouse CXCL1 anti-sense (5'-3') AGCCAGCGTTCACCAGACA,

mouse GAPDH sense (5'-3') CTGGCATGGCCTTCCGTG,

mouse GAPDH anti-sense (5'-3') GAAATGAGCTTGACAAAG.

The PCR reactions were performed at 95°C for 15 seconds, 60°C for 1 minute for 40 cycles using using StepOne™ System (cat. no. 4376357, Applied Biosystems). Samples were assayed in triplicate.

Chromatin immunoprecipitation (ChIP)

The ChIP method was previously detailed in (144), with the following modifications. Cells were treated with 5 ng/ml TGF-β for 6 hours in 10% FBS / Opti-MEM. DNA was fragmented to 200-1000 bp by sonicating 24 times for 10 sec each using a Vibra Cell Sonicator set at 30% output. Sonicated samples were incubated overnight at 4°C with 1.2 µg of antibody to Smad2 (Cell Signaling, cat. no. 5339), 0.96 µg of antibody to Smad3 (Cell Signaling, cat. no. 9523), or corresponding amounts of rabbit IgG. 30 µl of ChIP grade Protein G magnetic beads (Cell Signaling, cat. no. 9006) was added to the samples and incubated at 4°C for 2 hours. Beads were captured using a DynaMag-2 magnetic rack (Life Technologies). Samples were eluted with 400 µl of elution buffer and incubated at 65°C for 15 minutes. To prepare input controls for analysis, 350 µl of elution

buffer and 16 µl of 5 M NaCl were added to 50 µl of sonicated lysates. Samples were de-crosslinked at 95°C for 30 min and cooled down to room temperature. 40 µg of RNAase (cat. no. EN0531, Thermo Scientific) was added to each tube, and the samples were incubated at 37°C for 20 min. DNA was purified using QIAquick PCR purification kit (cat. no. 28104, QIAGEN Science) according to manufacturer's instructions. A total of 4 µl of each immunoprecipitate was assayed by real time PCR using primers recognizing 2 different regions of interest on the mouse CXCL1 or PAI-1 promoters. CXCL1_p1 primers amplified the promoter region from position from -271 to -123 upstream of the transcriptional start site (TSS). CXCL1_p2 primers amplified the promoter region from position -212 to -62. PAI_p primers amplified the promoter region at position -800 to -637. The following primers were synthesized by IDT Technologies:

CXCL1p_1 sense (5' to 3'): CCTGAGCACTGGAGACTCTG,

CXCL1p_1 anti-sense (5' to 3'): TGCTCCACTCCCAAGGATTA,

CXCL1p_2 sense (5' to 3'): CACTTGTCCAGCGAAGCAC,

CXCL1p_2 anti-sense (5' to 3'): GGAAATTCCCGGAGTACAGG,

PAI_p sense (5' to 3'): CAGTCATCTCAGGCTGCTGT,

PAI_p anti-sense (5' to 3'): GGCTCGCTCTTTGTGTCAAT.

PCR reactions were performed at 95°C for 15 seconds, 60°C for 1 minute for 40 cycles using using StepOne™ System (cat. no. 4376357, Applied Biosystems). Samples were run in triplicate, and the signals were normalized to signals obtained from input control samples.

Statistical Analysis

Experiments were performed in a minimum of triplicate. Values are expressed as Mean ± SEM. Statistical analysis was performed by Two-tailed student t-test or One-Way ANOVA with Bonferroni post-test as indicated. Statistical significance was

determined by $p<0.05$. not significant (ns); *, $p<0.05$; **, $p<0.01$; ***, $p<0.001$. StepOne™ System (Applied Biosystems, cat. no. 4376357). Samples were run in triplicate. In ChIP assays the signals were normalized to signals obtained from input control samples.

Results

TGF-β suppresses CXCL1 expression in mammary carcinoma associated fibroblasts over time

In chapter II, we reported that increased CXCL1 expression in breast cancer stroma inversely correlated with expression of TGF-β, indicating a possible functional relationship between TGF-β signaling and CXCL1 expression. Consistently, mammary CAF cell lines derived from PyVmT mammary tumors (86), 41CAF and 83CAF, showed increased expression of CXCL1 and decreased expression of TGF-β protein compared to the normal mammary fibroblast cell line, 311NAF (Chapter II). These mammary fibroblast lines represented physiologically relevant models to characterize the molecular mechanisms of CXCL1 expression. To determine the role of TGF-β signaling on CXCL1 expression in CAFs, we first examined the effects of TGF-β treatment on CXCL1 expression in time course studies using the 41CAF cell line. By real-time PCR, we observed a 20% reduction in CXCL1 mRNA expression 2 hours after TGF-β treatment. TGF-β continued to inhibit CXCL1 mRNA levels 24 hours after treatment, maximally inhibiting CXCL1 mRNA levels by 60%, 12 hours after treatment (Figure 3.1A). By ELISA analysis, TGF-β significantly inhibited CXCL1 protein expression by 50% at 24 hours post treatment, and maximally inhibiting expression by 85% after 120 hours of treatment (Figure 3.1B). The results show that TGF-β inhibits mRNA expression of CXCL1, followed by a reduction in CXCL1 protein levels over time in mammary CAFs.

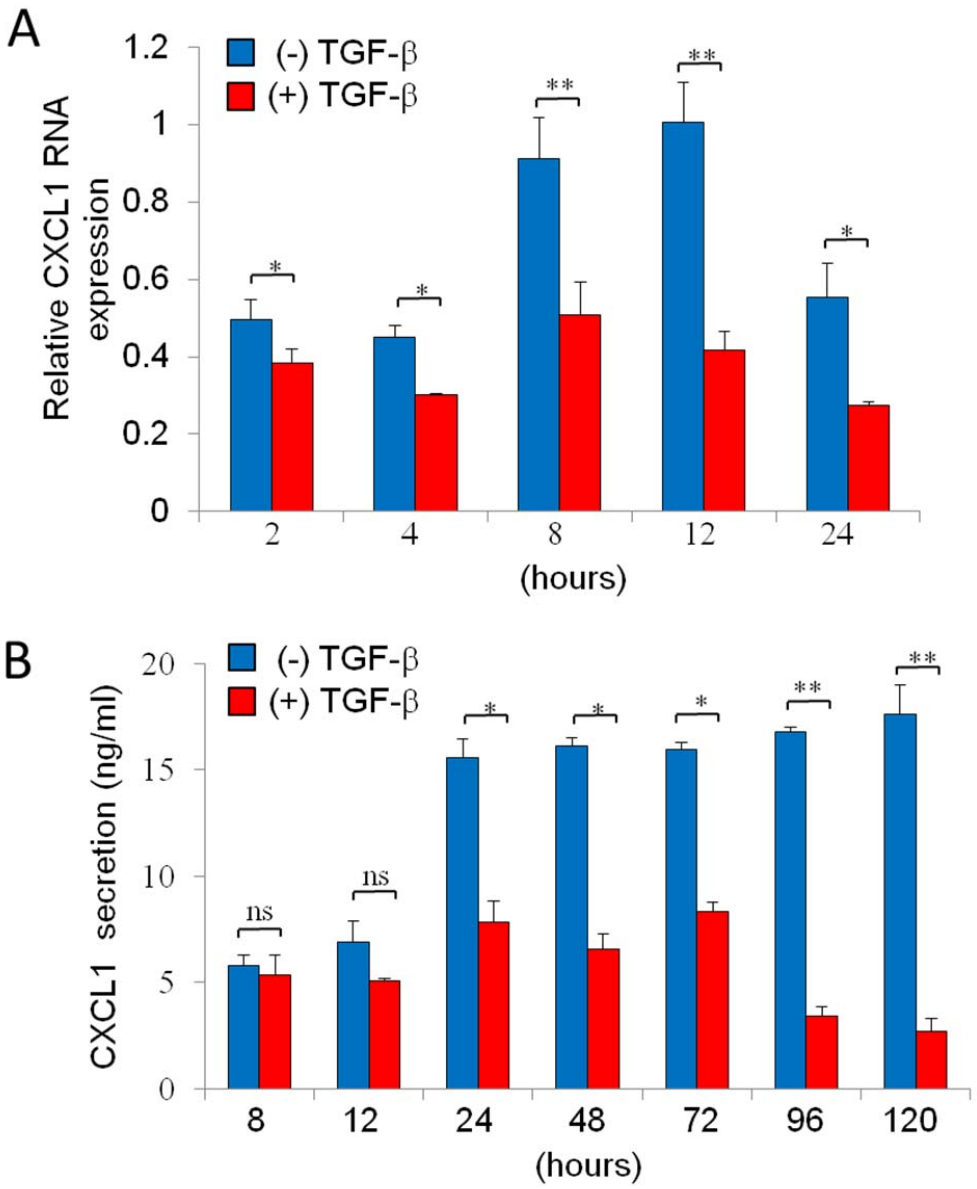
A
(-) TGF-β
(+) TGF-β
Relative CXCL1 RNA expression
1.2
1
0.8
0.6
0.4
0.2
0
*
*
**
**
*
2
4
8
12
24
(hours)
B
(-) TGF-β
(+) TGF-β
CXCL1 secretion (ng/ml)
20
15
10
5
0
ns
ns
*
*
*
**
**
8
12
24
48
72
96
120
(hours)

Figure 3.1. TGF-β suppresses CXCL1 expression in mammary carcinoma associated fibroblasts.

41CAFs were treated with 5 ng/ml of TGF-β for the indicated time points and analyzed for *(A).* CXCL1 mRNA expression by real time PCR, *(B).* CXCL1 secretion in conditioned media by ELISA. Statistical significance was determined by $p<0.05$. not significant (ns), $p>0.05$; *, $p<0.05$; **, $p<0.01$; ***, $p<0.001$. Values are expressed as Mean ± SEM.

Smad2 and Smad3 are required for TGF-β mediated suppression of CXCL1 expression in mammary carcinoma associated fibroblasts

TGF-β signaling activates Smad2 and Smad3 transcription factors, which form heterotrimeric complexes with Smad4 to positively or negatively regulate the expression of genes encoding extracellular matrix proteins, proteases and cell cycle proteins (105). Smad2 and Smad3 can also function independently of each other, forming Smad2/4 or Smad3/4 heteromeric complexes to regulate transcription (145-147). Given the importance of Smad2 and Smad3 in mediating TGF-β signaling, we determined the functional contribution of Smad2 and Smad3 in suppressing CXCL1 expression in mammary CAFs by siRNA knockdown studies. By western blot analysis, transfection of siRNAs to Smad2 or Smad3 in 41CAFs decreased expression of Smad2 by 80% or Smad3 by 86%, and significantly inhibited expression of phosphorylated proteins (Figure 3.2A). siRNA knockdown inhibited transcriptional activity mediated by Smad2 and Smad3, as determined by luciferase assay using the 3TP_lux promoter, a well characterized promoter region for Smad2/3 binding, which contains three consecutive tetradecanoylphorbol acetate response elements and a portion of the plasminogen activator/inhibitor promoter region (144) (Figure 3.2B). 41CAFs expressing control siRNAs, or siRNAs to Smad2, Smad3 were transfected with a luciferase reporter under the control of the CXCL1 promoter (148). In control siRNA expressing cells, TGF-β significantly inhibited CXCL1 promoter activity, as determined by luciferase assay. Knockdown of Smad2 or Smad3 enhanced luciferase activity in TGF-β treated cells (Figure 3.2C). By ELISA, TGF-β treatment decreased CXCL1 expression in control siRNA expressing cells, while knockdown of Smad2 or Smad3 resulted in a modest increase in CXCL1 protein expression with TGF-β treated cells (Figure 3.2D). These

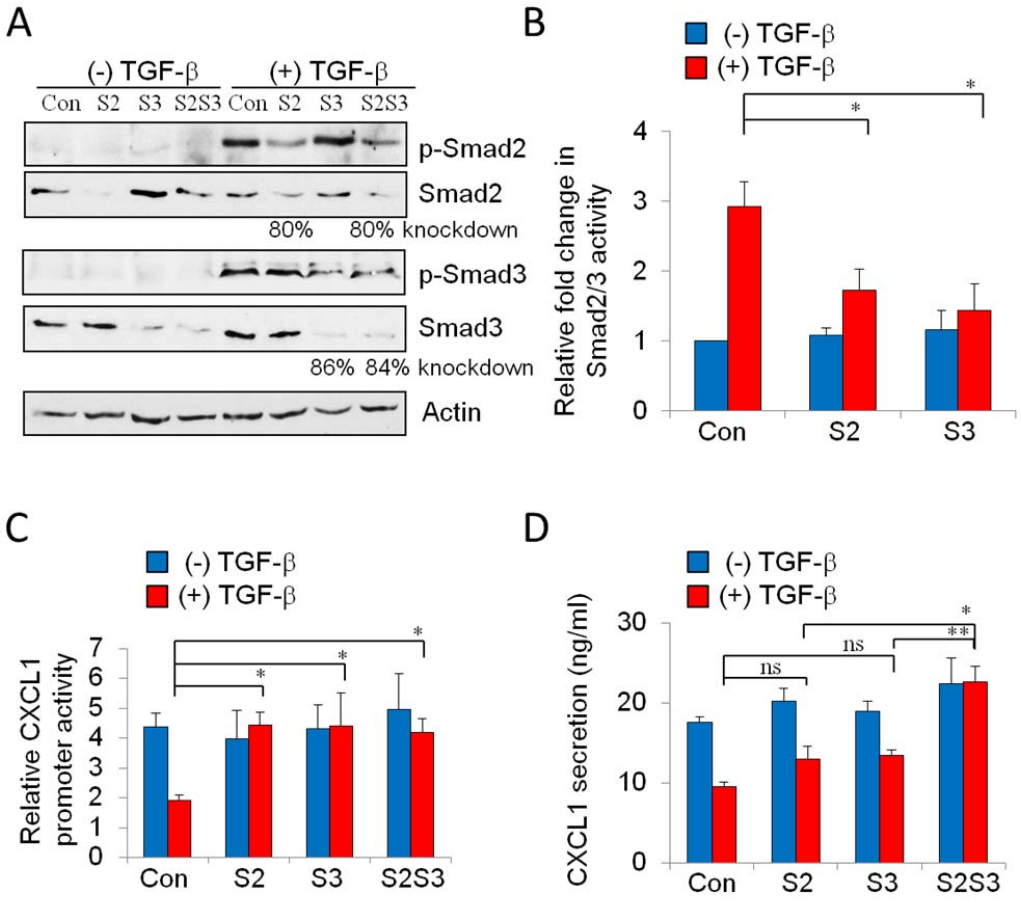
A
(-) TGF-β
(+) TGF-β
Con S2 S3 S2S3 Con S2 S3 S2S3
p-Smad2
Smad2
80% 80% knockdown
p-Smad3
Smad3
86% 84% knockdown
Actin
B
(-) TGF-β
(+) TGF-β
Relative fold change in Smad2/3 activity
0 1 2 3 4
Con S2 S3
C
(-) TGF-β
(+) TGF-β
Relative CXCL1 promoter activity
0 1 2 3 4 5 6 7
Con S2 S3 S2S3
D
(-) TGF-β
(+) TGF-β
CXCL1 secretion (ng/ml)
0 10 20 30
ns
ns
**
Con S2 S3 S2S3

Figure 3.2. siRNA knockdown of Smad2 and Smad3 up-regulates CXCL1 promoter activity and protein expression in mammary carcinoma-associated fibroblasts.

(A) 41CAFs were transfected with control siRNA (Con), siRNAs to Smad2 (S2), Smad3 (S3) or both (S2S3), treated with 5 ng/ml of TGF-β for 1 hour, and analyzed by western blot for expression of the indicated proteins. Expression levels of Smad2 and Smad3 were normalized to actin through densitometry analysis. *(B)* 41 CAFs co-expressing 3TP_lux and Renilla luciferase reporter constructs were transfected with siRNAs, treated with 5 ng/ml of TGF-β for 24 hours, and analyzed for TGF-β responsiveness by luciferase assay. (*C-D*) 41CAFs co-expressing PGL3.luc.CXCL1 firefly and Renilla luciferase reporter constructs were transfected with siRNAs, treated with TGF-β for 24 hours, and assayed for luciferase activity *(C),* or analyzed by ELISA for CXCL1 expression in conditioned medium *(D).* Firefly luciferase values are normalized to Renilla luciferase. Statistical significance was determined by $p<0.05$. not significant (ns), $p>0.05$; *, $p<0.05$; **, $p<0.01$; ***, $p<0.001$. Values are expressed as Mean ± SEM.

data indicate that Smad2 and Smad3 are important for TGF-β suppression of CXCL1 promoter activity. To determine whether Smad2 or Smad3 functioned independently to suppress CXCL1 expression, Smad2 and Smad3 were simultaneously knocked down in 41CAFs by co-transfection of Smad2 and Smad3 siRNAs. If Smad2 and Smad3 functioned independently to inhibit CXCL1 promoter activity, we would anticipate that dual knockdown of Smad2 and Smad3 would inhibit CXCL1 promoter activity more significantly than knockdown of individual Smad proteins. Co-transfection of Smad2 and Smad3 siRNAs resulted in 80% knockdown for Smad2 and an 84% knockdown in Smad3, demonstrating similar levels of knockdown (Figure 3.2A). By luciferase assay, dual knockdown of Smad2 and Smad3 did not further enhance CXCL1 promoter activity in TGF-β treated cells, compared to knockdown of Smad2 or Smad3 (Figure 3.2C). In contrast, by ELISA, knockdown of both Smad2 and Smad3 further enhanced CXCL1 protein expression compared to single knockdown of Smad2 or Smad3 (Figure 3.2D). Interestingly, in the absence of TGF-β, Smad3 knockdown enhanced Smad2 protein expression (Figure 3.2A) but did not significantly affect CXCL1 promoter activity or protein levels (Figure 3.2C-D). Similar effects of Smad2 and Smad3 inhibition on CXCL1 expression and promoter activity was also observed in other mammary CAFs and NAFs (83CAF, 311NAF), as well as cultured human breast ductal carcinoma associated fibroblasts (huCAF) (Figure 3.3). These results indicate that both Smad2 and Smad3 are required for TGF-β suppression of CXCL1 promoter activity and protein expression in mammary carcinoma associated fibroblasts.

Smad2 and Smad3 bind to the CXCL1 promoter to modulate transcriptional activity

Knockdown of Smad2 and Smad3 enhanced CXCL1 promoter activity in TGF-β treated cells to similar levels, and dual knockdown of Smad2 and Smad3 did not further

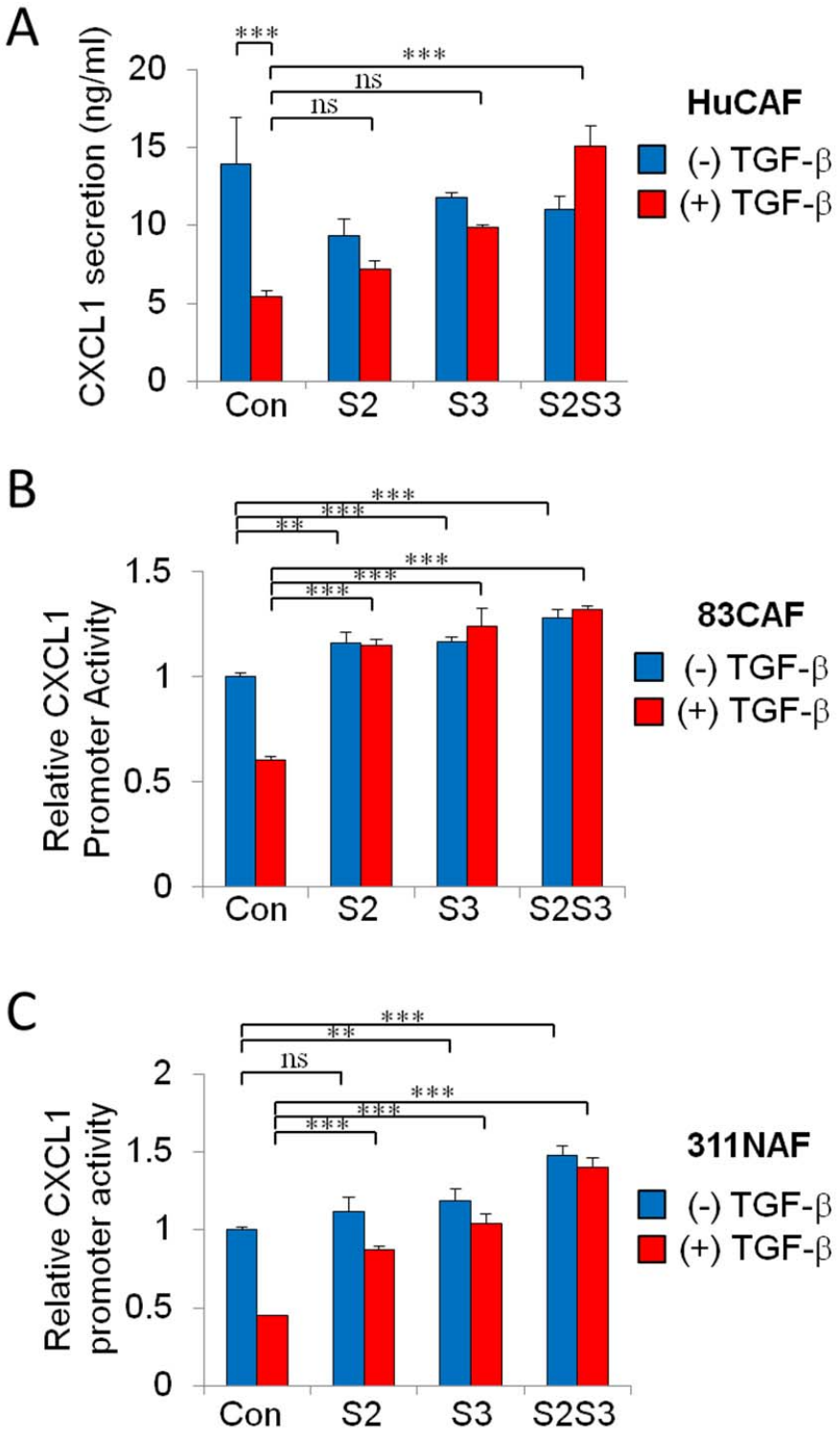
A
CXCL1 secretion (ng/ml)
20
15
10
5
0
***
***
ns
ns
Con
S2
S3
S2S3
HuCAF
(-) TGF-β
(+) TGF-β
B
Relative CXCL1
Promoter Activity
1.5
1
0.5
0
***
***
**
***
***
***
Con
S2
S3
S2S3
83CAF
(-) TGF-β
(+) TGF-β
C
Relative CXCL1
promoter activity
2
1.5
1
0.5
0
***
**
ns
***
***
***
Con
S2
S3
S2S3
311NAF
(-) TGF-β
(+) TGF-β

Figure 3.3. TGF-β suppress CXCL1 promoter activity and protein expression in Smad2- and Smad3-dependent manner in human breast ductal carcinoma associated fibroblasts (HuCAF), and other mouse mammary fibroblasts.

(A) HuCAF were transfected with control siRNA (Con), siRNAs to Smad2 (S2), Smad3 (S3) or both (S2S3), and treated with 5 ng/ml of TGF-β for 24 hours. Conditioned media was analyzed by ELISA. *(B-C)* 83CAF, 311NAF co-expressing PGL3.luc.CXCL1 firefly and Renilla luciferase reporter constructs were transfected with siRNAs, treated with TGF-β for 24 hours, and assayed for luciferase activity. Firefly luciferase values are normalized to Renilla luciferase. Statistical significance was determined by $p<0.05$. not significant (ns), $p>0.05$; *, $p<0.05$; **, $p<0.01$; ***, $p<0.001$. Values are expressed as Mean ± SD.

affect CXCL1 promoter activity. These data indicated that Smad2 and Smad3 functioned together to suppress CXCL1 gene expression. As the mechanisms of Smad2/3 binding to the CXCL1 promoter had not been clearly investigated, we searched for possible DNA binding sites in the CXCL1 promoter. Smad2/3 binding could suppress CXCL1 gene expression by binding to TGF-β inhibitory elements (TIE) (149, 150), or could bind to canonical Smad binding elements (SBEs), enabling Smad2/3 proteins to interact and suppress the activity of nearby cofactors (78, 151). We searched the upstream region sequence of the mouse CXCL1 TSS but did not identify the putative TIE sequence: 5'-GGCTT-3' (149, 150). Two SBEs with the sequence 5'- GTCT-3' (152, 153) were identified in the CXCL1 promoter region at -249 to -246 and - 144 to -141 relative to the TSS. In order to determine whether Smad2/3 proteins bound to the SBEs in the CXCL1 promoter, Chromatin Immunoprecipitation assays (ChIP) were performed. 41CAFs were treated with TGF-β for 6 hours, allowing sufficient time for Smad2/3 to translocate to the nucleus and suppress CXCL1 mRNA expression, as determined in earlier studies (Figure 3.1A). Cell lysates were immunoprecipitated with antibodies to Smad2, Smad3, or rabbit IgG as an isotype negative control. Real time PCR analysis was performed on immunoprecipitated DNA using 2 different sets of primers. One set of primers (CXCL1_p1) amplifies a 148 bp fragment containing both SBEs at -249 to -246 and -144 to -141. A second set of primers (CXCL1_p2) amplifies a 150 bp fragment containing only the SBE at -144 to - 141, enabling us to determine the relative importance of both SBEs to Smad2/3 binding. We predicted that if both SBEs were important for Smad2/3 binding, we would observe lower level PCR amplification with CXCL1_p2 primers. As a positive control, a set of primers was designed to amplify Smad2/3 binding regions on the Plasminogen Activating Inhibitor 1 promoter (PAI1_p), which is activated with TGF-β treatment of fibroblasts (154, 155). CXCL1_p1 primers amplified DNA that was immunoprecipitated with Smad2 or Smad3 antibodies, and which were from untreated

cells. PCR expression levels were further increased in samples treated with TGF-β (Figure 3.4A-B). Interestingly, amplicon levels with CXCL1_p1 primers were significantly higher than the positive control (Figure 3.4A-B). CXCL1_p2 primers amplified DNA from samples immunoprecipitated with Smad2 or Smad3 antibodies, but at lower levels than samples using CXCL1_p1 primers. Amplicon levels were increased in samples treated with TGF-β (Figure 3.4A-B). To further validate the functional contribution of the two identified SBEs, we performed site-directed mutagenesis for SBE1 (-249bp to -246bp), SBE2 (-144bp to -141bp), and both sites. Studies have shown that mutagenesis of "GTCT" to "TGAG" in SBEs results in complete loss of TGF-β responsiveness (156). We mutated "GTCTC" in SBE1 to "TGAGA", "GTCTA" in SBE2 to "TGAGC". As shown in Figure 3.4C, either SBE1 or SBE2 mutation significantly blunted responsiveness to TGF-β. Interestingly, while mutating SBE2 in addition to SBE1 mutation further blunted TGF-β responsiveness, mutating SBE1 in addition to SBE2 mutation did not achieve additive effect. These results indicate that in the absence of TGF-β, Smad2/3 proteins bind to SBEs identified in the CXCL1 promoter, and that TGF-β treatment promotes additional Smad2/3 binding to these elements.

As ChIP assays revealed binding of Smad2 and Smad3 to the CXCL1 promoter without a TIE sequence, we hypothesized that Smad2/3 proteins would inhibit CXCL1 gene transcription by blocking activity of adjacent co-factors. C/EBP-β is a possible co-factor positively regulating CXCL1 transcription in mammary CAFs. A C/EBP-β binding motif (5'-TGGAGCAAG-3') was identified at position -128 to -120 in the mouse CXCL1 promoter, proximal to the SBEs. C/EBP-β has been shown to positively regulate CXCL1 gene transcription in lung epithelial cells and mesenchymal stem cells. Smad3 and Smad4 have also been shown to complex and repress C/EBP-β transcriptional activity in glioma cells and mouse 3T3 fibroblasts (157, 158). To determine whether Smad2 or Smad3 suppressed C/EBP-β activity in mouse CAFs, 41CAFs co-expressing Renilla

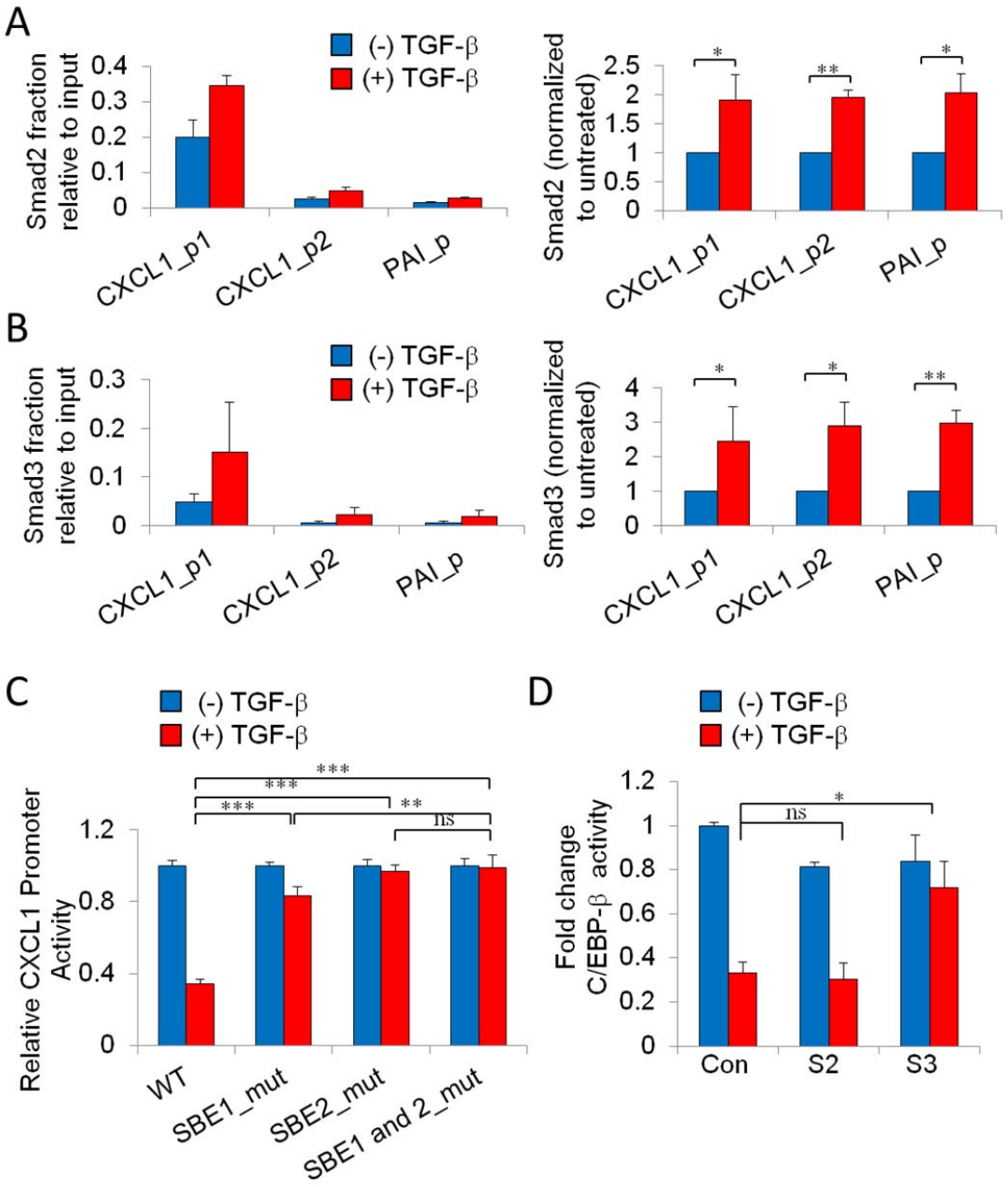
A
Smad2 fraction relative to input
(-) TGF-β
(+) TGF-β
CXCL1_p1
CXCL1_p2
PAI_p
Smad2 (normalized to untreated)
B
Smad3 fraction relative to input
Smad3 (normalized to untreated)
C
Relative CXCL1 Promoter Activity
WT
SBE1_mut
SBE2_mut
SBE1 and 2_mut
ns
D
Fold change C/EBP-β activity
Con
S2
S3

Figure 3.4. Smad3 but not Smad2 suppresses CXCL1 transcription through C/EBP-β dependent mechanisms.

(A-B). 41CAFs were treated with 5 ng/ml of TGF-β for 6 hours, and analyzed for Smad2/3 DNA binding by ChIP assay. DNA was immunoprecipitated using antibodies to *(A).* Smad2 or *(B).* Smad3, or IgG as an isotype control, and amplified by real-time PCR for the CXCL1 promoter region from -271 to -123 using CXCL1_p1 primers, and from -212 to -62 using CXCL1_p2 primers. Smad2/3 binding to PAI_1 promoter was used as a positive control, which was amplified using PAI_p primers. Background from IgG control was subtracted from samples. Left panels show fraction of Smad2 or 3 binding to DNA relative to input control. Right panel shows Smad2 or 3 binding normalized to (-) TGF-β group for each promoter region. *(C).* 41CAFs were transfected with Renilla luciferase plasmids and firefly luciferase reporter plasmids with wild type (WT) CXCL1 promoter region with or without site-directed mutation at SBE1 (SBE1_mut), SBE2 (SBE2_mut) or both (SBE1 and 2_mut). Cells were treated with 5 ng/ml of TGF-β for 24 hours, and assayed for luciferase activity. *(D).* Cells co-expressing C/EBP-β.luc firefly and Renilla luciferase reporter constructs were transfected with control siRNA (Con), siRNAs to Smad2 (S2), Smad3 (S3). Cells were treated with 5 ng/ml of TGF-β for 24 hours, and assayed for luciferase activity. Firefly luciferase values were normalized to Renilla luciferase. Statistical significance was determined by $p<0.05$. not significant (ns), $p>0.05$; *, $p<0.05$; **, $p<0.01$; ***, $p<0.001$. Values are expressed as Mean ± SEM for *(A)* and *(B),* and as Mean ± SD for *(C)* and *(D)* as representative experiments.

luciferase and C/EBP-β firefly luciferase reporter plasmids, were transfected with control siRNAs, or siRNAs to Smad2, Smad3 or both. The cells were treated with TGF-β, and then analyzed for changes in C/EBP-β promoter activity by luciferase assay. 41CAFs expressing control siRNAs showed visible C/EBP-β promoter activity, which was inhibited by TGF-β treatment. Knockdown of Smad3, but not Smad2 increased C/EBP-β promoter activity, compared to control siRNA expressing cells treated with TGF-β (Figure 3.4D). Taken together, these data indicate that both Smad2 and Smad3 bind to the CXCL1 promoter, but Smad3 is required for repression of C/EBP-β, an activator of CXCL1 transcription.

Smad2 and Smad3 proteins negatively regulate CXCL1 expression by inhibiting expression of HGF in mammary CAFs

In addition to decreased expression of TGF-β, mammary CAFs showed increased expression of HGF, compared to normal fibroblasts (Figure 3.5A), consistent with expression patterns of HGF in breast cancer stroma (80, 159). We investigated the possibility that CXCL1 expression was positively regulated by HGF signaling. Transfection of 41CAFs with HGF siRNAs significantly knocked down HGF protein expression, leading to a 62 % decrease in CXCL1 promoter activity, and 26 % reduction in CXCL1 protein expression (Figure 3.5B-D). To further illustrate the functional contribution of HGF in regulating CXCL1 secretion in the context of TGF-β signaling, 41CAFs were treated with increasing doses of HGF in the presence or absence of TGF-β. Secretion of CXCL1 was significantly increased at 20 ng/ml of HGF treatment, and was completely rescued at 40 ng/ml of HGF treatment (Figure 3.5E). Conditional deletion of *Tgfbr2* in mammary fibroblasts increased HGF expression (87, 160). These studies indicated that TGF-β signaling negatively regulated HGF, a positive regulator of CXCL1 expression. To determine this possibility, 41CAFs were treated with TGF-β and

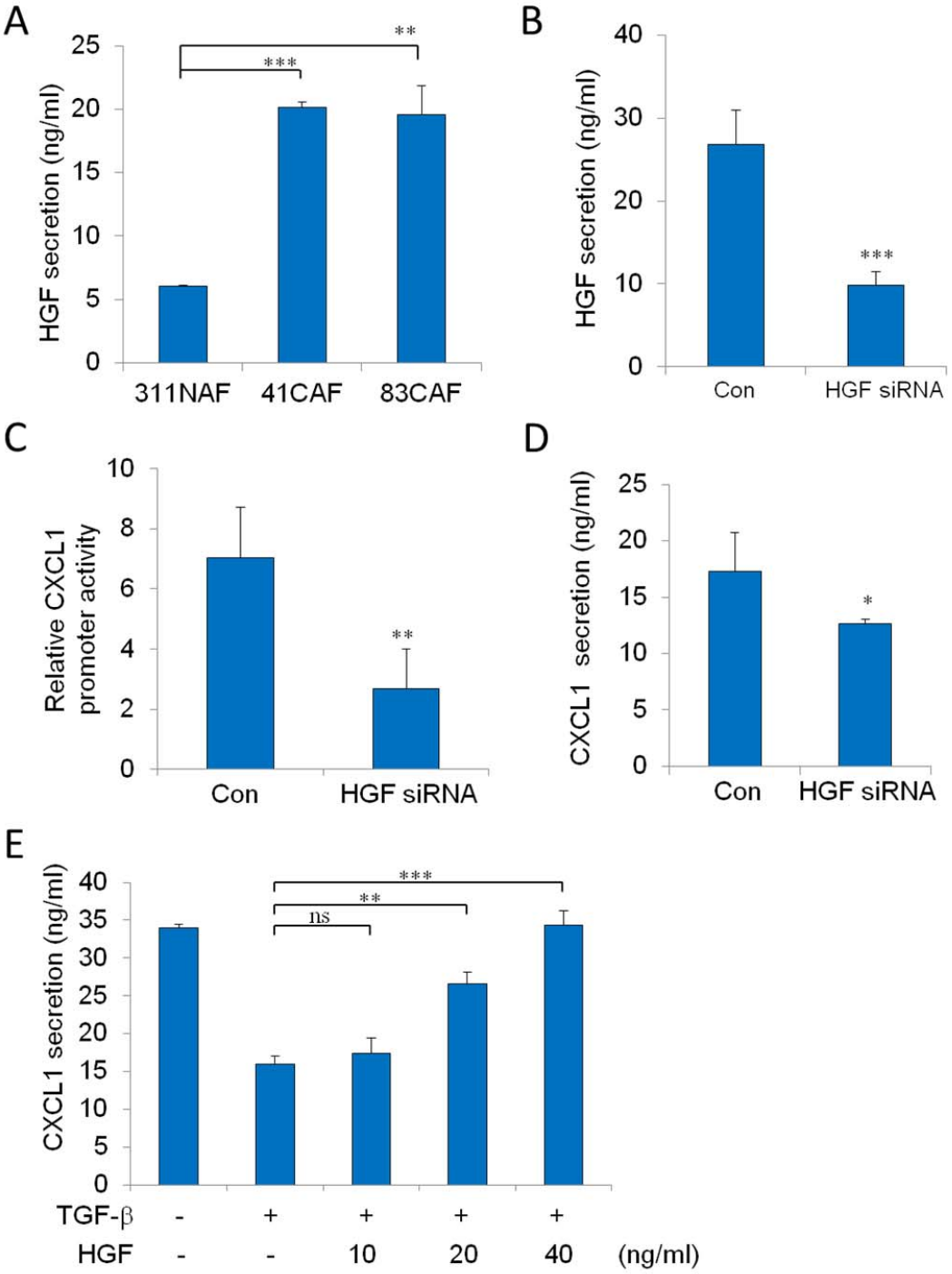
A
HGF secretion (ng/ml)
25
20
15
10
5
0
***
**
311NAF
41CAF
83CAF
B
HGF secretion (ng/ml)
40
30
20
10
0
***
Con
HGF siRNA
C
Relative CXCL1 promoter activity
10
8
6
4
2
0
**
Con
HGF siRNA
D
CXCL1 secretion (ng/ml)
25
20
15
10
5
0
*
Con
HGF siRNA
E
CXCL1 secretion (ng/ml)
40
35
30
25
20
15
10
5
0
***
**
ns
TGF-β - + + + +
HGF - - 10 20 40 (ng/ml)

Figure 3.5. HGF regulates CXCL1 expression in mammary fibroblasts.

(A). Normal mammary fibroblasts (311NAF) or mammary CAF cell lines (83CAF, 41CAF) were analyzed for HGF expression in conditioned media by ELISA. *(B-D).* 41CAFs expressing control siRNA (Con) or siRNAs to HGF were analyzed for HGF expression in conditioned media by ELISA *(B),* transfected with PGL3.luc.CXCL1 and Renilla luciferase plasmids and assayed for luciferase activity, *(C).* or were analyzed for CXCL1 expression in conditioned media by ELISA *(D). (E).* 41CAFs were treated with 5 ng/ml TGF-β with or without increasing concentrations of HGF for 24 hours, and analyzed for CXCL1 expression in conditioned media by ELISA. Firefly luciferase values were normalized to Renilla luciferase. Statistical significance was determined by $p<0.05$. not significant (ns), $p>0.05$; *, $p<0.05$; **, $p<0.01$; ***, $p<0.001$. Values are expressed as Mean ± SD in *(E),* and as Mean ± SEM in *(A-D)*.

examined for changes in HGF expression over time by ELISA. TGF-β treatment did not affect HGF protein expression after 24 hours, but a significant reduction in the level of HGF was observed after 48 hours of TGF-β treatment (Figure 3.6A). We next determined the possibility that Smad2 and Smad3 mediated TGF-β suppression of HGF expression. siRNA knockdown of Smad2 or Smad3 enhanced HGF protein expression in 41CAFs (Figure 3.6B). In summary, these data indicate that TGF-β down-regulates HGF expression through Smad2 and Smad3 dependent mechanisms, in order to suppress CXCL1 expression.

HGF signals to c-Met to positively regulate CXCL1 expression through NF-κB dependent mechanisms

HGF is best known for regulating epithelial cell survival, growth and migration by signaling through c-Met receptor tyrosine kinases (161, 162). Several studies have shown that c-Met is expressed in skin fibroblasts and osteoarthritis (OA) synovial fibroblasts (163, 164). However, HGF signaling in mammary fibroblasts has not been clearly investigated. Our studies indicated that HGF served as a positive regulator of CXCL1 expression in mammary CAFs, we further characterized the mechanisms through which HGF positively regulated CXCL1 expression. We determined whether c-Met receptors were expressed in mammary CAFs, and whether there were any differences in expression, compared to normal mammary fibroblasts. By flow cytometry analysis, the majority of NAFs and CAFs expressed c-Met receptors (Figure 3.7A). By western blot analysis, c-Met receptor expression levels in NAFs and CAFs were lower compared to 4T1 mammary carcinoma cells but were still detectable (Figure 3.7B and Figure 3.8A). To determine whether c-Met receptors were active in mammary CAFs, we assayed for c-Met tyrosine phosphorylation at Tyr1234/1235, auto-phosphorylation sites critical for receptor activation (165). By western blot analysis, 41CAFs showed

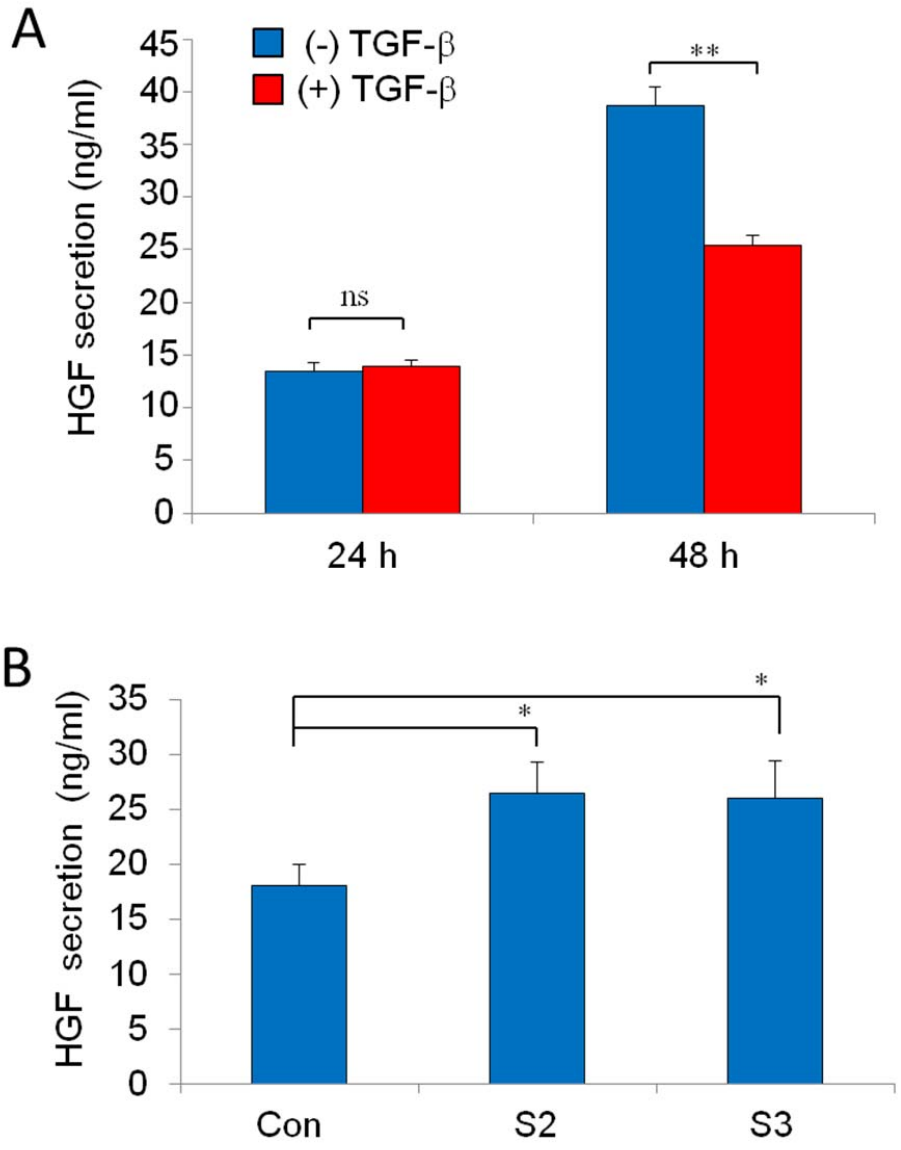
A
(-) TGF-β
(+) TGF-β
HGF secretion (ng/ml)
45
40
35
30
25
20
15
10
5
0
ns
**
24 h
48 h
B
HGF secretion (ng/ml)
35
30
25
20
15
10
5
0
*
*
Con
S2
S3

Figure 3.6. TGF-β inhibits HGF expression through Smad2/3 dependent mechanisms.

(A) 41CAFs were treated with 5ng/ml TGF-β for 24 or 48 hours, and analyzed for CXCL1 expression in conditioned media by ELISA. *(B)* 41CAFs transfected with control siRNA (Con), or siRNAs to Smad2 (S2) or Smad3 (S3), were analyzed for HGF expression in conditioned media by ELISA. Statistical significance was determined by $p<0.05$. not significant (ns), $p>0.05$; *, $p<0.05$; **, $p<0.01$; ***, $p<0.001$. Values are expressed as Mean ± SEM.

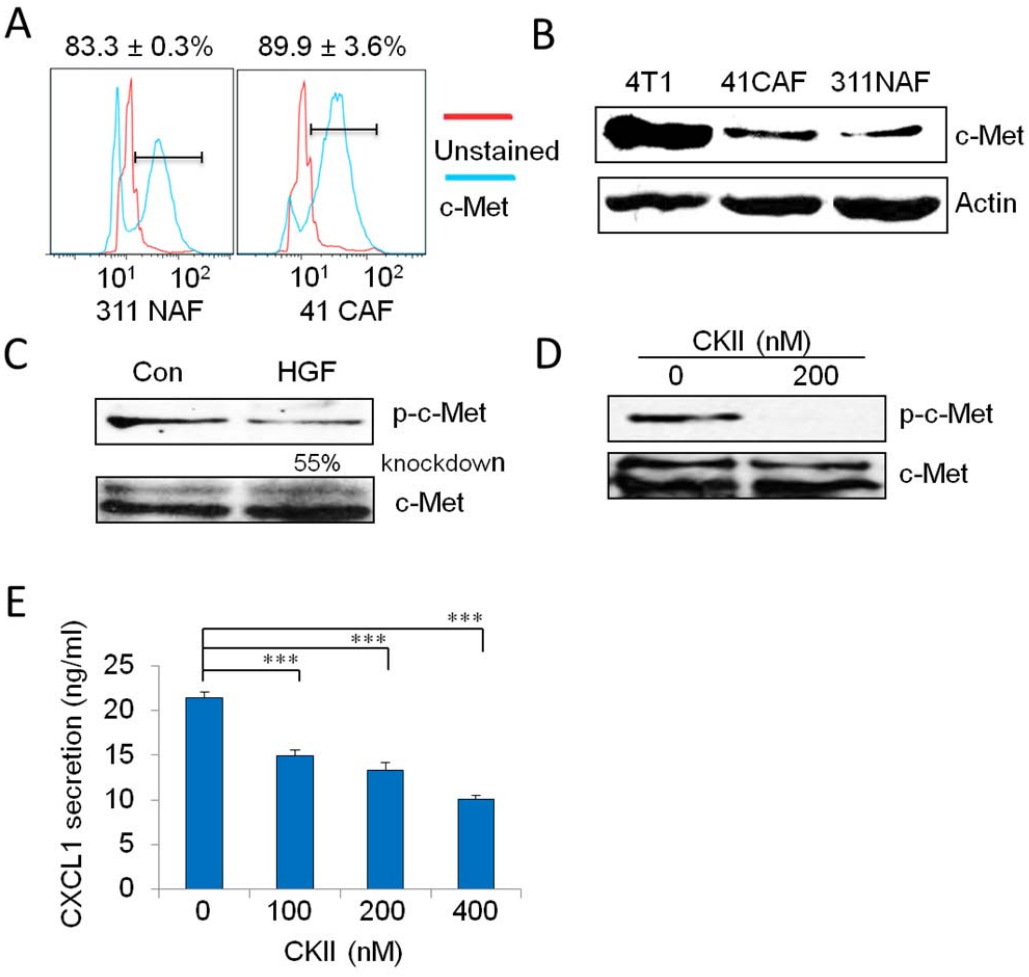
A
83.3 ± 0.3%
89.9 ± 3.6%
Unstained
c-Met
10¹ 10²
311 NAF
10¹ 10²
41 CAF
B
4T1
41CAF
311NAF
c-Met
Actin
C
Con
HGF
p-c-Met
55% knockdown
c-Met
D
CKII (nM)
0
200
p-c-Met
c-Met
E
CXCL1 secretion (ng/ml)
25
20
15
10
5
0
***
***
***
0
100
200
400
CKII (nM)

Figure 3.7. HGF signals to c-Met to regulate CXCL1 expression.

(A-B) 311NAFs and 41CAFs were analyzed for c-Met expression by flow cytometry *(A),* or western blot analysis, with 4T1 mammary carcinoma cells as a positive control *(B). (C)* 41CAFs were transfected with control or HGF siRNAs and analyzed for expression of phosphorylated c-Met by western blot. Expression of phospho-c-Met was normalized to total c-Met by densitometry analysis. *(D)* 41CAFs were treated with c-Met kinase inhibitor type II (CKII) for 1 hour, and analyzed for expression of phosphorylated c-Met (Tyr-1234/1235) and total c-Met by western blot. *(E)* 41CAFs treated with CKII for 48 hours were analyzed for CXCL1 expression by ELISA. Statistical significance was determined by $p<0.05$. not significant (ns), $p>0.05$; *, $p<0.05$; **, $p<0.01$; ***, $p<0.001$. Values are expressed as Mean ± SEM.

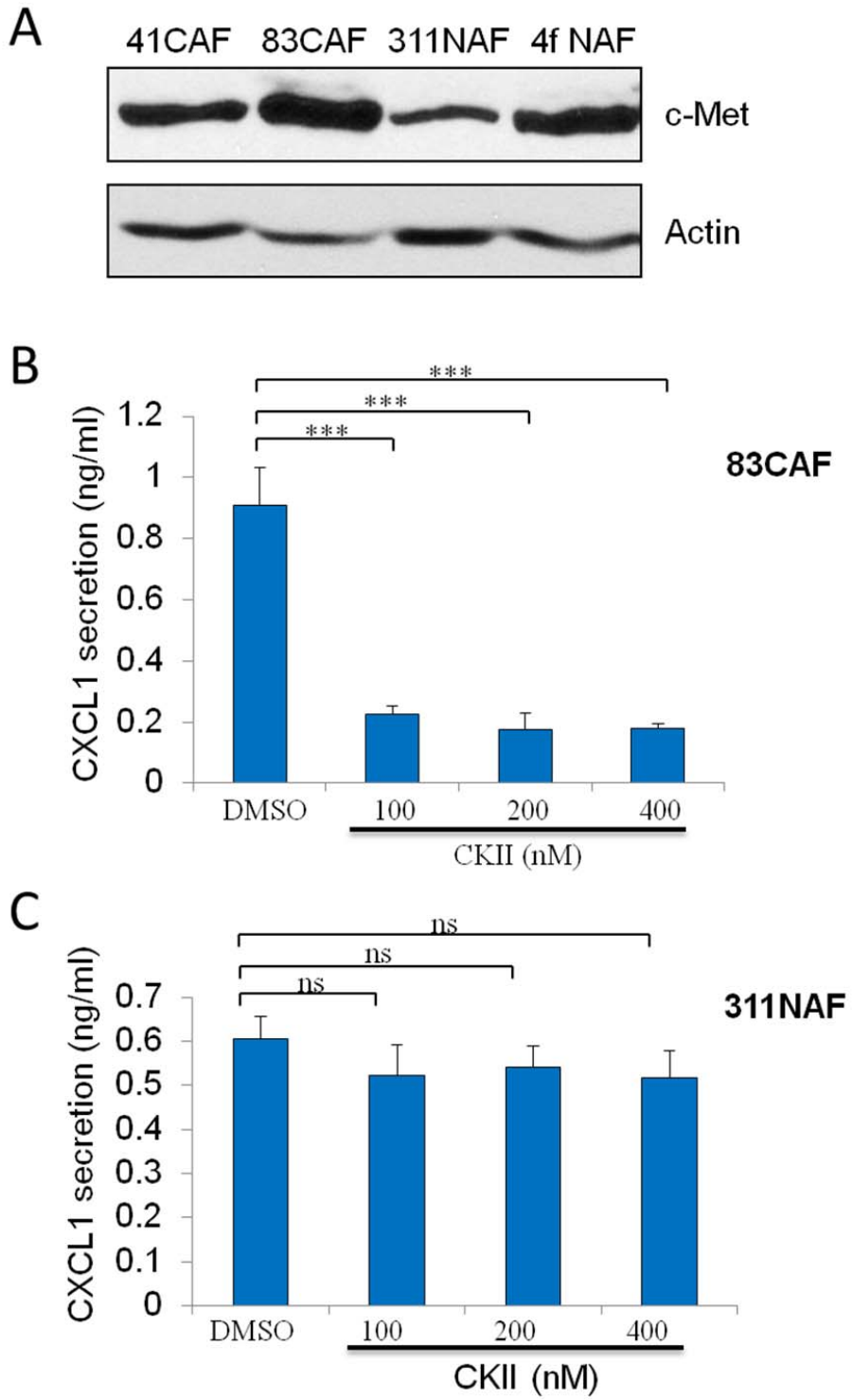
A
41CAF
83CAF
311NAF
4f NAF
c-Met
Actin
B
***
***
***
CXCL1 secretion (ng/ml)
1.2
1
0.8
0.6
0.4
0.2
0
DMSO
100
200
400
CKII (nM)
83CAF
C
ns
ns
ns
CXCL1 secretion (ng/ml)
0.7
0.6
0.5
0.4
0.3
0.2
0.1
0
DMSO
100
200
400
CKII (nM)
311NAF

Figure 3.8. c-Met is expressed in mammary fibroblasts and is required for CXCL1 secretion in carcinoma associated fibroblasts.

(A) 41CAF, 83CAF, 311NAF and 4f NAF were analyzed for c-Met expression by western blot analysis. *(B-C)* 83CAF, 311NAF were treated with CKII for 48 hours, and analyzed for CXCL1 secretion by ELISA. Statistical significance was determined by $p<0.05$. not significant (ns), $p>0.05$; *, $p<0.05$; **, $p<0.01$; ***, $p<0.001$. Values are expressed as Mean ± SEM.

detectable levels of phosphorylated c-Met protein, which was inhibited by siRNA knockdown of HGF (Figure 3.7C). These data indicate that endogenously expressed HGF bound and activated c-Met receptors on mammary CAFs. To determine the functional contribution of c-Met in the regulation of CXCL1 expression, 41CAFs were treated with CKII (also known as PHA665752), a small molecule inhibitor to c-Met, with an IC50 of 200nM (166, 167). CKII treatment of 41CAFs inhibited phosphorylation of c-Met, and significantly reduced CXCL1 protein levels in a dose-dependent manner (Figure 3.7D-E). Similar effect was also observed in another CAF (83CAF) but not in NAF (311NAF) (Figure 3.8), possibly because the expression of HGF in 311NAF is much lower than CAFs (Figure 3.5A). These results indicate that HGF signals to c-Met in mammary CAFs to positively regulate CXCL1 expression. We next examined the downstream mechanisms to understand how CXCL1 expression was positively regulated by HGF/c-Met signaling. Through candidate screening of HGF signaling pathways and known regulators of CXCL1 expression, we identified NF-κB as a possible downstream effector of HGF/c-Met signaling in mammary CAFs. HGF has been shown to regulate activity of NF-κB in various cell types (168, 169), and two NF-κB binding sites have been identified in the CXCL1 promoter (148). We first determined whether NF-κB was regulated by HGF in mammary CAFs. HGF gene expression was silenced in 41CAFs and analyzed for changes in NF-κB activity by luciferase assay. Compared to control siRNA expressing cells, HGF siRNA expressing cells showed a significant reduction in NF-κB activity (Figure 3.9A), indicating endogenous HGF expression regulated NF-κB transcriptional activity in CAFs. 41CAFs were then treated with increasing concentrations of the NF-κB peptide inhibitor, SN50, which inhibits translocation of the NF-κB active complex into the nucleus at an IC50 of 18 μM (170). SN50 treatment of CAFs inhibited NF-κB activity, significantly reducing CXCL1 protein expression in a dose dependent manner (Figure 3.9B). The inhibitory activity of SN50

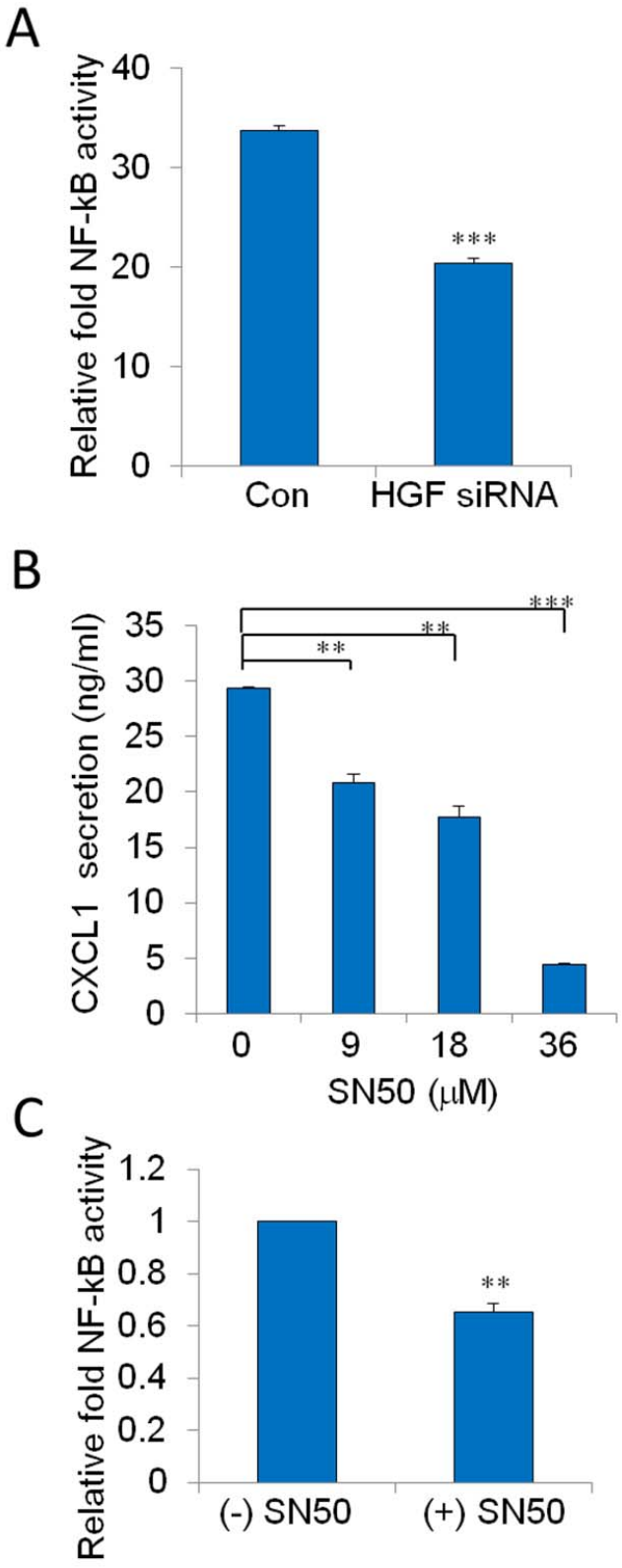
A
Relative fold NF-kB activity
40
30
20
10
0
***
Con
HGF siRNA
B
CXCL1 secretion (ng/ml)
35
30
25
20
15
10
5
0
***
**
**
0
9
18
36
SN50 (μM)
C
Relative fold NF-kB activity
1.2
1
0.8
0.6
0.4
0.2
0
**
(-) SN50
(+) SN50

Figure 3.9. HGF/c-Met signaling regulates CXCL1 expression in mammary fibroblasts through NF-κB dependent mechanisms.

(A) 41CAFs co-expressing pNF-κB.luc firefly and Renilla luciferase reporter plasmids were transfected with control (Con) or HGF siRNAs, and analyzed for NF-κB activity by luciferase assay. *(B)* Cells were treated with increasing concentrations of SN50 for 24 hours, and analyzed for CXCL1 expression in conditioned media by ELISA. *(C)* 41CAFs co-expressing pNF-κB.luc and Renilla luciferase reporter plasmids were treated with 36 μm SN50 for 24 hours, and analyzed for changes in NF-κB activity by luciferase assay. Firefly luciferase values were normalized to Renilla luciferase. Statistical significance was determined by $p<0.05$. not significant (ns), $p>0.05$; *, $p<0.05$; **, $p<0.01$; ***, $p<0.001$. Values are expressed as Mean ± SEM.

was validated through luciferase assay of an NF- κB reporter (Figure 3.9C), characterized in previous studies (171). These data indicate that HGF positively regulates CXCL1 expression in mammary CAFs through an NF-κB dependent manner.

Discussion

CXCL1 is an important regulator of cancer progression and is overexpressed numerous cancer types. Recent studies indicate that fibroblasts are an important source of CXCL1 expression in breast tumors. To understand the mechanisms through which CXCL1 was regulated, we characterized the role of TGF-β and HGF signaling in mammary CAFs. In these studies, we demonstrate that TGF-β negatively regulates and HGF positively regulates CXCL1 expression in mammary CAFs. We propose that TGF-β suppresses CXCL1 expression in mammary fibroblasts partly through Smad2/3 repression of the CXCL1 promoter. TGF-β also inhibits CXCL1 expression by down-regulating expression of HGF. HGF functions as a positive regulator by signaling through c-Met to enhance NF-κB transcriptional activation of CXCL1 (Figure 3.10). Inflammatory cytokines including TNF-α and IL1β positively regulate CXCL1 expression in cancer cells and endothelial cells (71, 172). However, few studies have examined how CXCL1 is negatively regulated in cells. In breast cancer stroma, TGF-β expression was found to be decreased compared to normal breast stroma, inversely correlating with CXCL1 expression (manuscript submitted to BMC Cancer). The present studies show that TGF-β suppresses CXCL1 expression in CAFs. In total, these data suggest that TGF-β suppresses CXCL1 expression in normal breast stroma, and TGF- β expression is down regulated in breast cancer, to enable up-regulation of CXCL1 expression in the stroma. Supporting this hypothesis, we found HGF, a factor overexpressed in CAFs, is negatively regulated by TGF-β signaling. The antagonistic relationship between TGF-β

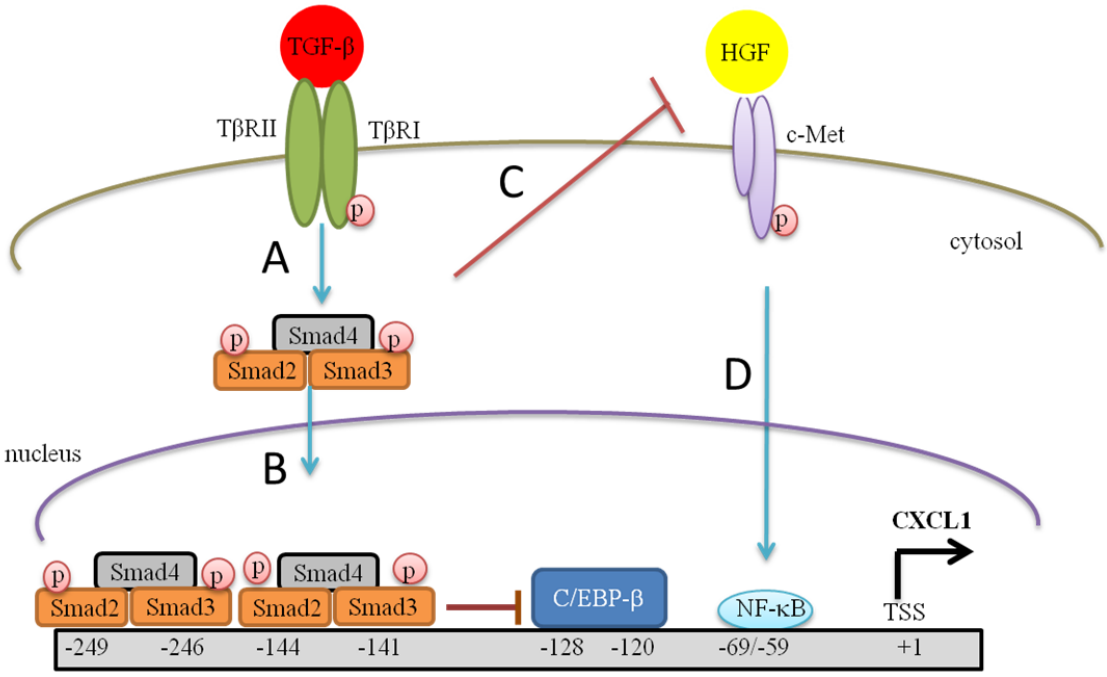
TGF-β
HGF
TβRII
TβRI
c-Met
C
p
cytosol
A
Smad4
Smad2
Smad3
D
nucleus
B
CXCL1
C/EBP-β
NF-κB
TSS
-249
-246
-144
-141
-128
-120
-69/-59
+1

Figure 3.10. Proposed model for TGF-β mediated suppression of CXCL1 in mammary CAFs.

(A) TGF-β signaling leads to phosphorylation of Smad2 and Smad3 proteins, and formation of complexes with Smad4. *(B)* Smad2/3/4 complexes translocate to the nucleus, bind to SBEs located at -249 to -246 and -144 to -141 on the CXCL1 promoter, and repress CXCL1 transcription, partly through suppression of C/EBP-β activity *(C).* Smad2/3 proteins also suppress CXCL1 expression by inhibiting expression of HGF. *(D)* HGF signals through c-Met receptors to activate NF-κB and up-regulate CXCL1 gene expression.

and HGF has been observed during mammary gland development, in which TGF- β serves to regulate ductal branching and morphogenesis and HGF regulates ductal epithelial cell proliferation. TGF-β expression becomes down regulated when HGF becomes up-regulated in normal mammary stroma, strictly controlling mammary gland development (124, 173). In our studies, we show that this antagonistic relationship between TGF-β and HGF may regulate CXCL1 expression in CAFs, through temporal mechanisms. We observed that mammary CAFs treated with TGF-β show a reduction in CXCL1 expression within 24 hours, corresponding to the time period of Smad2/3 activation and binding to the CXCL1 promoter. TGF-β did not suppress HGF expression during this time period. Suppression of CXCL1 levels continued after 24 hours of TGF-β treatment, corresponding to decreased HGF expression levels. These data indicate that the reduction in CXCL1 levels within 24 hours would be due to Smad2 and Smad3 binding to CXCL1 gene promoter, and that TGF-β mediated suppression of HGF signaling contributed to long-term suppression of CXCL1 gene expression in fibroblasts. Taken together, these data indicate that down-regulation of TGF-β and increased HGF signaling in CAFs elevate and sustain CXCL1 expression during cancer progression. Our studies demonstrate important roles for Smad2 and Smad3 in regulating CXCL1 expression in mammary CAFs. Smad2 and Smad3 may function together or in separate complexes with Smad4 to regulate gene expression (145-147). In our studies, we found that Smad2 and Smad3 knockdown enhances CXCL1 mRNA expression in TGF- β treated cells to similar levels. Dual Smad2/3 knockdown did not further affect CXCL1 mRNA levels. Furthermore, ChIP studies showed similar patterns of Smad2 and Smad3 binding to the CXCL1 promoter. These data suggest that Smad2 and Smad3 function in a complex to modulate CXCL1 expression. On the other hand, we noted that Smad3, but not Smad2 was required for repression of C/EBP- β, a transactivator of CXCL1 expression. These data indicate that Smad2 inhibits CXCL1 promoter activity through an

additional mechanism, possibly inhibiting CXCL1 promoter activity through other cooperating factors, independent of Smad3. Interestingly, Smad2 may be expressed as two different splice variants. One splice variant of Smad2 is more prevalent in mammalian cells (174) and contains an insert in the MH1 domain, which is encoded by exon 3 and prevents DNA binding (152, 175). The other variant, commonly referred to as Smad2Δexon3, lacks the insert, and is able to bind DNA to activate gene transcription (175). Both variants are capable of forming complexes with Smad3 and Smad4 (175). It is possible that both Smad2 variants are involved in regulating CXCL1 expression, as the siRNA targeting sequences were not specific to one variant. Smad2/4 complexes interact with a variety of transcription factors, including Sp-1,Fast-1, Mixer and Milk (176, 177). As dual knockdown of Smad2 and Smad3 did not result in an additive or synergistic increase in CXCL1 mRNA levels, compared to Smad2 or Smad3 single knockdown, it is possible that this additional mechanism would indirectly affect Smad2/3 transcriptional repression of the CXCL1 promoter. Investigation of this mechanism would involve characterization of the Smad2 gene variant in mammary CAFs, and pull-down experiments to identify interacting transcription factors, experiments beyond the scope of this report.

In contrast to CXCL1 mRNA levels, we observed that dual knockdown of Smad2 and Smad3 enhanced CXCL1 protein levels compared to individual knockdown of Smad2 or Smad3. These data indicate a mechanism for Smad proteins for inhibiting protein expression, independent of CXCL1 gene transcription. One possible mechanism would involve intracellular CXCL1 protein degradation. Previous studies have shown that TGF-β regulates Smad2-Smurf2 ubiquitin ligase complex to target proteins for degradation by the proteasome (178). Another possibility involves Smad2/3 regulation of proteases that target CXCL1 as a substrate. The metalloproteinase MMP12 cleaves and inactivate C-X-

C chemokines and has been shown to be regulated by TGF-β signaling (179). Combined with CXCL1 transcriptional repression, Smad2/3 proteins could modulate post-translational mechanisms to suppress CXCL1 protein expression in mammary CAFs. In addition to repressing the CXCL1 promoter, we show that Smad2 and Smad3 inhibit CXCL1 expression by down-regulating HGF expression. HGF is known to regulate signaling in epithelial cells during cancer progression. HGF derived from fibroblasts signal to c-Met expressing cancer cells to promote cell growth, survival and invasion (80, 159). These studies are the first to report an important role for HGF/c-Met autocrine signaling in mammary CAFs in regulating gene expression. c-Met expression is lower in fibroblasts compared to 4T1 mammary carcinoma cells, and may be overlooked in immunohistochemistry studies of breast tumor tissues. However, c-Met is expressed in the majority of mammary fibroblasts. While c-Met is expressed at similar levels between NAFs and CAFs, HGF expression is increased in mammary CAFs, and would most likely contribute to CXCL1 overexpression in CAFs. It would be other interest to further explore the role of HGF/c-Met signaling in mammary fibroblasts.

In summary, CAFs are indistinguishable in appearance from normal fibroblasts, but overexpress CXCL1, a chemokine involved in the development of drug resistant tumors. We illustrate important molecular mechanisms modulating CXCL1 expression in mammary CAFs. By understanding how expression of tumor promoting factors is regulated in CAFs, we may better predict how the cancer stroma will influence tumor progression.

Chapter IV: Paracrine versus autocrine CXCL1 signaling in regulating breast cancer cell survival and invasion

Abstract

Stromal cells regulate growth, survival and invasion of different types of cancer, including melanoma, breast cancer and prostate cancer, and mainly through paracrine signaling interactions with epithelial cells. CXCL1 chemokine signals through CXCR2 cell surface receptor to normally regulate recruitment of neutrophils during wound healing and inflammation. In melanoma, ovarian and gastric cancer, autocrine CXCL1/CXCR2 signaling has been shown to promote tumor cell survival, proliferation or invasion depending on tissue of origin. Recently, it has been reported that breast cancer cell-derived CXCL1 recruits myeloid cells, which in turn enhance tumor cell survival and chemo-resistance. However, the role for fibroblast-derived CXCL1 signaling in mammary tumor progression remains poorly understood. Our previous studies indicate that CXCL1 is up-regulated in breast tumor stroma, especially in carcinoma-associated fibroblasts (CAFs). Here we further characterize the expression patterns of CXCL1 and CXCR2 in different subtypes of mouse and human breast cancer cells, as well as in fibroblasts isolated from normal mammary tissues and carcinoma tissues. CXCL1/CXCR2 expression was elevated in basal-like breast cancer cells and CAFs compared to luminal breast cancer cells and normal mammary associated-fibroblasts (NAFs). In addition, we have found that CAF-derived CXCL1 promotes breast cancer cell survival and invasion in a CXCR2-dependent manner. Additionally, knockdown of CXCL1 expression in fibroblasts by siRNA or shRNA, or inhibition of CXCR2 by shRNA or pharmacologic inhibitors significantly block fibroblasts-induced mammary carcinoma cell invasion. By further understanding the functional contribution and molecular mechanisms of paracrine CXCL1/CXCR2 signaling to mammary tumor progression, we may be able to therapeutically target CXCL1 and CXCR2 in invasive breast cancer.

Introduction

Tumor microenvironment is composed of surrounding blood vessels, signaling molecules, extracellular matrix, and multiple cell types including immune cells, fibroblasts. Tumors recruit these components to facilitate their progression and metastasis through bidirectional talk between tumor cells and the microenvironment (20, 21). In contrast to the well-organized homeostasis of the normal cells, tumor microenvironment is deregulated at molecular and cellular levels.

As one of the major components in breast stroma, fibroblasts normally play an important role in maintaining the structural integrity of connective tissues through secretion of extracellular matrix precursors including type I, type III and type V collagen, and fibronectin (23), and get activated during mammary gland development to regulate ductal branching and morphogenesis (25, 26). Fibroblasts are also a major cellular component of the breast tumor microenvironment; yet, the molecular signals that identify cancer associated fibroblasts (CAFs) still remain poorly understood. De-regulated growth and activity of fibroblast is associated with progression and poor patient prognosis of invasive breast cancer, which is characterized by the presence of dense collagenous tumor stroma and accumulation of activated fibroblasts (3,4). Activated fibroblasts exhibit enhanced secretion of extracellular matrix proteins, proteases and growth factors, mediating tissue remodeling in tumor microenvironment. In animal studies, co-grafting of mammary CAFs with mammary carcinoma cells results in increased tumor growth, survival and metastasis (5-7). Conversely, breast tumor outgrowth and cellular invasiveness is inhibited by co-transplantation of normal tissues associated fibroblasts (NAFs) (8,9). While NAFs and CAFs exhibit a uniform cell morphology, molecular profiling studies reveal that CAFs show increased expression of

extracellular matrix proteins, growth factors and cytokines, which may contribute to tumor progression (10-12).

CXCL1 is a member of CXC chemokine family. The biological effects of CXCL1 can be mediated through two class A, rhodopsin-like guanine-protein-coupled receptors (GPCRs): CXCR1 and CXCR2 (53). CXCR1 and CXCR2 has 78% identical amino acid sequences (54, 55), however, due to the differences in the receptor N-terminal sequences, CXCL1 predominantly bind to CXCR2 instead of CXCR1 under physical conditions (56). Accordingly, CXCR2 bind to multiple chemokine ligand including CXCL1, CXCL2, CXCL3, CXCL5, CXCL6, CXCL7 and CXCL8. In breast cancer, increased CXCL1 protein expression has been reported in HER2 positive metastatic breast cancer (66) and was associated with increased tumor growth and pulmonary metastasis of MDA-MB231 breast cancer cells grafted in the mammary fat pads of nude mice (67). Moreover, increased plasma levels of CXCL1 protein are associated with decreased survival of breast cancer patients with metastatic disease (68). Similarly, increased tumoral expression of CXCL1 RNA is associated with metastatic disease, correlating with tumor grade and decreased survival of patients with ER positive breast cancer (10). Recently, it has been reported that tumor cell-derived CXCL1 recruits myeloid cells, which in turn enhance tumor cell survival and chemo-resistance. However, the role for fibroblast-derived CXCL1 signaling in mammary tumor progression has not been fully characterized. Our previous studies indicate that CXCL1 is up-regulated in breast tumor stroma, especially in carcinoma-associated fibroblasts (CAFs), corresponding with poor prognosis of breast cancer patients. Here we further characterize the expression pattern of CXCL1 and CXCR2 in breast cancer cell lines of different subtypes in mouse and human, as well as in normal mammary-associated fibroblasts (NAFs) and CAFs, and

systematically examined the role and molecular mechanisms of paracrine and autocrine CXCL1/CXCR2 signaling in breast cancer progression *in vitro* and *in vivo*.

Materials and Methods

Cell culture

Primary CAFs (41CAF, 83CAF) and 144Epi carcinoma cells were isolated from transgenic mice (FVB) expressing the PyVmT oncogene under the control of Mouse Mammary Tumor Virus Promoter (MMTV) at 12-16 weeks of age. Primary NAFs (311NAF, 4f NAF) were isolated from wild-type C57BL/6 mice at 12-16 weeks of age. Tgfbr2FspKO fibroblasts were isolated from Tgfbr2FspKO mice as described (17). Human CAFs (hCAF 008727, hCAF 02300) were isolated from human breast ductal carcinoma tissues. Human NAFs (hNAF 03280, hNAF 08727) were isolated from normal human breast tissues. All human breast tissues were obtained from Biospecimen Repository Core Facility (BRCF), an IRB approved facility at the University of Kansas Medical Center. Fibroblasts cell lines were generated by spontaneous immortalization of primary mammary fibroblasts and clonal populations of fibroblasts were obtained as described (17). MCF-10A cells were cultured in Dulbecco's modified Eagle medium (DMEM) /F12 containing 5% horse serum/ 100 mg/ml EGF/ 1 mg/ml hydrocortisone/ 1 mg/ml choleratoxin/ 10 mg/ml insulin/ 100 I.U/ml penicillin/ 100 µg/ml streptomycin/ 0.5 µg/ml amphotericin B. All other cells were cultured in complete media, which is DMEM containing 10% fetal bovine serum (FBS)/ MEM nonessential amino acids/ 2 mM L-glutamine/ 100 I.U/ml penicillin/ 100 µg/ml streptomycin/ 0.5 µg/ml amphotericin B.

ELISA

Cells were seeded in 24-well plate at a density of 20,000 cells. To generate conditioned medium, cells were incubated in 500 µl DMEM for indicated time periods,

followed by centrifugation to eliminate cell debris. For *CXCL1 ELISA*, 20 µl conditioned media were diluted in 80 µl DMEM, and analyzed by CXCL1 ELISA kit following manufacturer's instructions (Peprotech, cat. no. 900-K27 for mouse CXCL1; cat. no. 900-K38 for human CXCL1). Reactions were catalyzed using tetramethylbenzidine substrate (Thermo Scientific, cat. no. 34028). Reaction was stopped using 50 µl/well of 2N HCl, read at A_{450nm} using a 1420 multi-label counter (VICTOR3 TM V, PerkinElmer). All samples were analyzed in triplicate. Experiments were repeated at a minimum of triplicate.

Flow cytometry analysis

Cells were cultured in complete medium in 10 cm dishes to 80% of sub-confluence. To detach cells from the plastic, cells were rinsed with PBS twice followed by incubation with 3 mM EDTA at 37℃ for 10-15 min. Cells were washed with 10 ml of complete medium twice, and fixed by neutral formalin buffer (VWR) for 10 min. To remove traces of formalin, cells were washed with PBS twice. For CXCR2 cell surface staining, 500,000 cells were incubated with anti-CXCR2 antibody (cat. no. MAB331-100, R&D Systems) at 1: 100 dilution in PBS on ice for 30 min, washed with PBS twice, and incubated with Alexa Fluor 488 Goat Anti-Mouse IgG secondary antibody (cat. no. A-11029, Life technologies) at 1:1000 dilution in PBS on ice for 30 min. Cells were washed with PBS three times and filtered in PBS prior to analysis. For combined cell surface and intracellular CXCR2 staining, 500,000 cells permeabilized with 0.2% of Tween 20 / PBS at 37℃ for 15 min (180), followed by wash with 0.1% Tween/PBS three times. cells were incubated with anti-CXCR2 antibody (cat. no. MAB331-100, R&D Systems) at 1: 100 dilution in PBS on ice for 30 min, washed with 0.1% Tween / PBS three times, and incubated with Alexa Fluor 488 Goat Anti-Mouse IgG secondary antibody (cat. no. A-11029, Life technologies) at 1:1000 dilution in PBS on ice for 30 min. Cells were washed

with 0.1% Tween/PBS three times and filtered in PBS prior to analysis. Cells were compared with unstained control and secondary antibody-only controls. CXCR2 expression was analyzed on an LSRII flow cytometer (BD Biosciences).

Immunohistochemistry staining

Mouse mammary tumor tissues from in vivo studies were fixed in 10% neutral formalin buffer and embedded in paraffin using the University of Kansas Medical Center Histology Core facilities. Tissue sections (5 μm) were de-waxed and rehydrated in PBS. Sections were subjected to antigen retrieval in 10 mM sodium citrate buffer (pH 6.0) at 100^{o}C for 10 min and washed in PBS. Endogenous peroxidases were quenched in PBS containing 3% H_20_2 and 10% methanol for 30 min. After rinsing in PBS, samples were blocked in PBS containing 5% rabbit serum and incubated with antibodies (1:100) to Ki67 or antibodies (1:100) to cleaved caspase 3 at 4^{o}C overnight. Samples were washed in PBS and incubated with secondary goat biotinylated antibodies (1:500), conjugated with streptavidin peroxidase (cat. no. PK-4000, Vector Labs) and incubated with 3,3'-Diaminobenzidine (DAB) substrate (cat no. K346711, Dako). Sections were counterstained with Harris's hematoxylin for 5 minute, dehydrated and mounted with Cytoseal. The density of Ki67, cleaved caspase 3 positive staining were measured in at least 5 fields at 10x magnification by NIH Image J software. Proliferative (Ki67 positive) and apoptotic indices (cleaved caspase 3) were calculated by determining the relative area of positive stained cells to total number of cells in at least five fields at 10× magnification using Image J software.

siRNA transfection

Negative control siRNAs (cat. no. AM4613, Ambion) and siRNAs targeting two different regions of CXCL1 (cat. no. AM16708, Ambion) were obtained from Santa Cruz

Biotechnology. Transfection of siRNA into the cells was performed according to manufacturer's protocols. Briefly, cells were seeded in a 24-well plate at a density of 20,000 cells and cultured for 24 hours. Cells were rinsed with PBS and Opti-MEM (cat. no. 11058-021, Gibco), and incubated in Opti-MEM with complexes of 12 pmol siRNA and 2.4 µl Lipofectamine 2000 reagent (cat. no. 11668019, Life technologies) for 24 hours. Medium was replaced with Opti-MEM/10%FBS for 24 hours prior to stimulation or starvation.

Retroviral transduction

Phenix cells were transfected with 10 µg of pBabe retroviral construct or pRetrosuper retroviral construct carrying a puromycin selection marker and shRNAs targeting two different regions of CXCR2 (CXCR2/F-6 and CXCR2/G-1), shRNA targeting CXCL1, or GFP gene (Ctrl shRNA) as a specificity control (87). The full hairpin sequence and gene targeting sequences for each shRNA construct are as follows:

CXCR2/F-6 shRNA full hairpin sequence,
TGCTGTTGACAGTGAGCGCGCAGTGTACTTACATATAATATAGTGAAGCCACAGAT
GTATATTATATGTAAGTACACTGCATGCCTACTGCCTCGGA;

CXCR2/F-6 shRNA targeting sequence, 5'-CAGTGTACTTACATATAAT-3';

CXCR2/G-1 shRNA full hairpin sequence,
TGCTGTTGACAGTGAGCGAGGATAACATTTGAAATGTAAATAGTGAAGCCACAGAT
GTATTTACATTTCAAATGTTATCCCTGCCTACTGCCTCGGA;

CXCR2/G-1 shRNA targeting sequence, 5'-GATAACATTTGAAATGTAA-3';

GFP shRNA targeting sequence, 5'-GCTGACGGAGAACAACATC-3'.

Medium containing retrovirus was collected after 48 hours of transfection and used to transduce 144Epi carcinoma cells or 41CAF seeded at 60% subconfluence in 10 cm dishes in the presence of 5 μg/ml Polybrene (cat. no. AL-118, Sigma). 48 hours post infection, cells were placed under puromycin selection (2 μg/ml) (cat. no. P9620, Sigma) in DMEM containing 10% FBS/ MEM nonessential amino acids/ 2 mM L-glutamine/ 100 I.U/ml penicillin/ 100 μg/ml streptomycin/ 0.5 μg/ml amphotericin B. Non-infected 144Epi cells or 41CAF were treated with puromycin as a control.

Invasion assay

8 μm-pore transwell filters (cat. no. 3422, Costar) were pre-coated with DMEM containing 0.5 mg/ml of growth factor reduced matrigel matrix (cat. no. 356230, BD Biosciences) at 37℃ for 1 hour. Carcinoma cells were serum starved and then seeded on transwell upper chambers at a density of 75,000 cells per well with or without recombinant CXCL1 at 37℃ for indicated time periods. For carcinoma cells/fibroblast co-culture invasion assay, fibroblasts were seeded on the underside of matrigel coated transwell filters at a density of 100,000 cells per well for 1 hour, followed by seeding carcinoma cells into transwell upside chambers at a density of 75,000 cells per well 37℃ for indicated time periods. Cells were fixed with 10% neutral formalin buffer (VWR) for 10 minutes and stained with 0.1% crystal violet (cat. no. AC21212-0250, Fisher) for 10 minutes followed by twice of PBS rinse. For the carcinoma cell/fibroblast co-culture invasion assays, carcinoma cells were pre-labeled with fluorochrome dye (cat. no. C2925, Life Technologies). Tumor cells on the upside of the filter were removed by cotton swabs. Carcinoma cells that invaded to the underside of the filter were micrographed under Nikon SMZ-800 stereo microscope with charge coupled device camera; a minimum of four fields per sample were captured at 20 X magnification. Cell

invasion was quantified by measuring the pixel area of crystal violet-stained or fluorochrome dye labeled cells using NIH Image J software (arbitrary units).

Immunofluorescence staining

144Epi PyVmT mammary carcinoma cells were seeded onto sterile cover slips in 24-well plate at a density of 20,000 cells per well for 24 hours. Cells were fixed with 10% neutral formalin buffer (VWR) for 10 min to overnight, followed by wash in methanol at -20℃ for 7 min. After blocking with blocking buffer (PBS containing 3% of FBS) for 1 hour, cells were probed with antibodies (1:100 in blocking buffer) to CXCR2 (cat. no. SC-683, Santa Cruz) at 4℃ overnight. Anti-rabbit Alexa 568 second antibody (1:1000 in blocking buffer) was used to detect specific immunoreaction at room temperature for 2 hours. Antibody specificity was controlled by secondary antibody only and CXCR2 peptide competition (Peptide Control). Cells were counter stained with DAPI (1:500 in PBS) at room temperature for 10 min, and mounted to microscope slides with PBS/glycerol (1:1). Pictures were taken at 10x magnification at multiple fields. CXCR2 expression was quantified by Image J (NIH Software) and compared to Parental control (Par).

Western blot

Cells were rinsed with PBS twice, lysed in RIPA buffer containing 10 mM Tris-HCl, pH 8.0, 0.1 mM EDTA, 0.1% sodium deoxycholate, 0.1% SDS, and 140 mM NaCl, supplemented with a Sigma cocktail of protease and phosphatase inhibitors (cat. no. P8340) and 10 mM of sodium orthovanadate (cat. no. S6508). 80 μg of protein were resolved by 10% SDS-PAGE. The proteins were transferred to nitrocellulose membranes and then probed with antibodies (1:1000) to: phospho-Akt (S-473, cat. no. 4060, Cell Signaling Technology), phospho-ERK1/2 (T-202/Y-204, cat. no. 9101, Cell Signaling Technology), phospho-IKKα/β (S-176/180, cat. no. 2697, Cell Signaling

Technology), Akt (cat. no. 4691S, Cell Signaling Technology), ERK1/2 (cat. no. 9102, Cell Signaling Technology), IKKβ (cat. no. 2678, Cell Signaling Technology). Specific immunoreaction was detected with rabbit secondary antibodies conjugated to horseradish peroxidase and West Pico ECL Western blotting substrate (cat. no. 34080, Thermo SCIENTIFIC).

Statistical analysis

Data are expressed as mean ± S.E. Statistical analysis was performed using two-tailed *t* test or analysis of variance with Bonferroni's post-test of comparisons using GraphPad software. Statistical significance was determined by: not significant (ns); *, $p<0.05$; **, $p<0.01$; ***, $p<0.001$.

Results

Expression patterns of CXCL1 and CXCR2 in breast cancer cells are associated with cell subtypes and tumorigenicity

CXCL1 was up-regulated in various cancer types including melanoma, ovarian, gastric and bladder cancer, associated with invasion and angiogenesis. Overexpression of CXCL1 in breast cancer cells enhance myeloid cell recruitment and facilitate metastatic cancer cell survival and chemo-resistance. However, little is known about CXCL1 expression patterns in breast cancer epithelial cells and surrounding stroma cells. We analyzed CXCL1 protein expression in cultured normal-like MCF-10A human breast epithelial cells, breast cancer cell lines including luminal type MCF-7 cells and basal-like MDA-MB231 cells, and fibroblasts isolated from normal breast tissues (huNAFs) and breast ductal carcinoma tissues (huCAFs). We found that CXCL1 show higher expression in highly invasive basal-like MDA-MB231 cells compared to non-tumorigenic

MCF-10A cells and non-invasive MCF-7 cells (Figure 4.1A). We also observed that huNAFs and huCAFs express equivalent or higher levels of CXCL1 than breast cancer cells, and one of the huCAFs we assayed for exhibited the highest CXCL1 expression level among all cells examined (Figure 4.1A). Accordingly, basal-like 4T1 cells secrete higher levels of CXCL1 than luminal 144Epi cells and other normal-like mammary epithelial cells (Figure 4.1B). Additionally, we found that mammary CAFs show significantly higher expression of CXCL1 than NAFs (Figure 4.1B). Since CXCL1 signals to cell surface receptor CXCR2 to exert its biological effects, we also examined the expression patterns of CXCR2 among human breast epithelial / cancer cells, as well as mouse mammary carcinoma cells, and found that increased extracellular and intracellular expression of CXCR2 is associated with invasiveness of human breast cancer cells but not with mouse mammary carcinoma cells (Figure 4.2). Taken together, the results suggest that, while mouse mammary carcinoma cells exhibited increasing CXCL1 expression corresponding to cell tumorigenicity, human breast cancer cells show increasing CXCR2 expression as well as high CXCL1 expression in invasive basal-like MDA-MB231 cells.

CXCL1 promotes breast cancer cell invasion in CXCR2-dependent manner

CXCL1 has been shown to stimulate tumor cell proliferation and invasion in melanoma, gastric and ovarian cancers(64, 181, 182). MCF-7 is less invasive than MDA-MB231 cells. Hypothesizing that enhanced CXCL1 secretion in breast cancer cells contributes to cell invasion, we examined the effect of added recombinant CXCL1 on MCF-7 cell invasion by transwell invasion assay (Figure 4.3). Compared to untreated cells, CXCL1 significantly enhanced MCF-7 cell invasion by 33% percent at 20 ng/ml, and up to 2.2 fold at 40 ng/ml. At 80 ng/ml, CXCL1 induction of cell invasion was lower than that at 40 ng/ml, but the difference was not significant. Similarly, we compared the

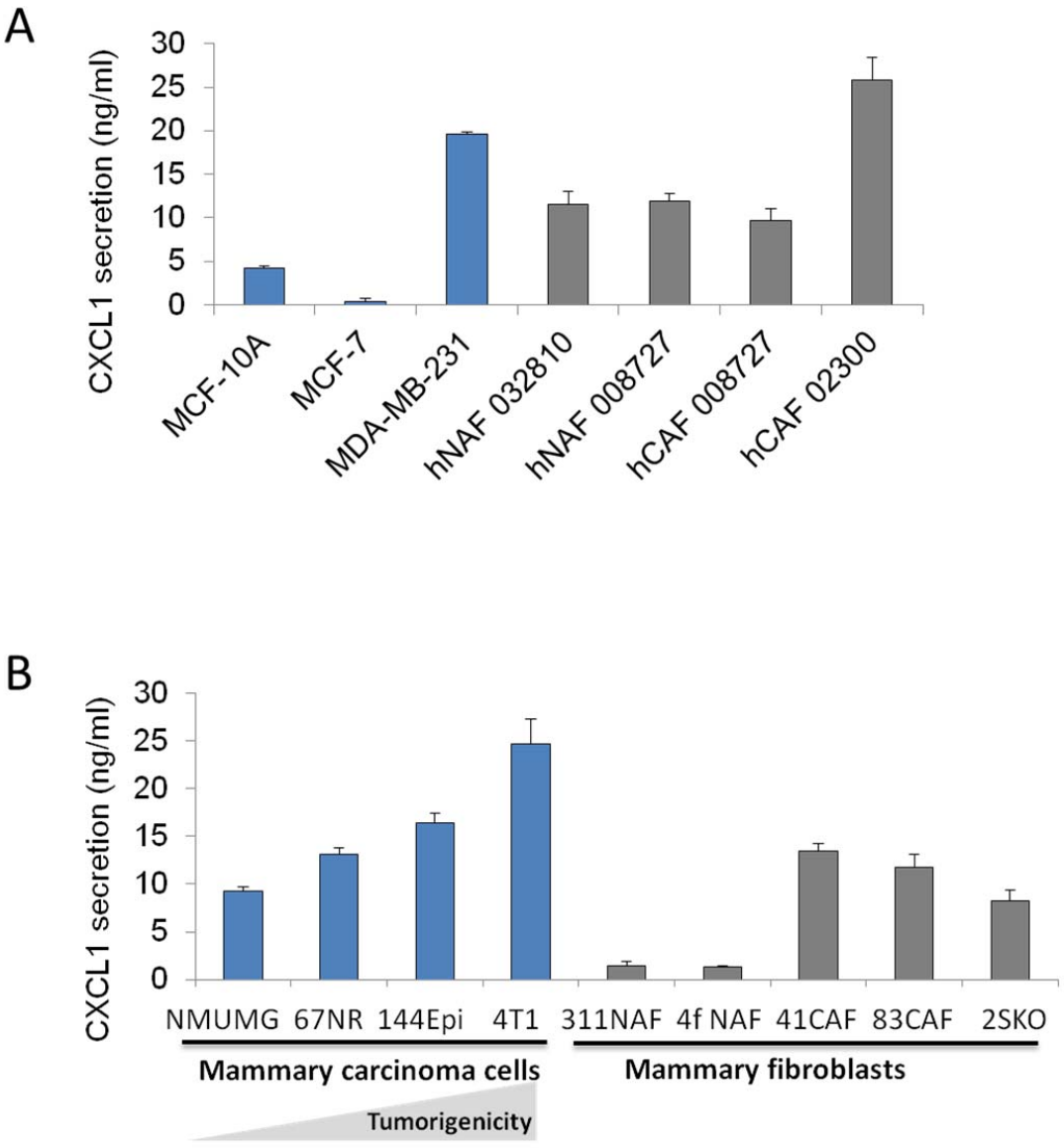
A
CXCL1 secretion (ng/ml)
30
25
20
15
10
5
0
MCF-10A
MCF-7
MDA-MB-231
hNAF 032810
hNAF 008727
hCAF 008727
hCAF 02300
B
CXCL1 secretion (ng/ml)
30
25
20
15
10
5
0
NMUMG
67NR
144Epi
4T1
311NAF
4f NAF
41CAF
83CAF
2SKO
Mammary carcinoma cells
Mammary fibroblasts
Tumorigenicity

Figure 4.1. CXCL1 expression profiling in breast cancer cells and fibroblasts.

(A) Human breast epithelial cells MCF-10A, breast cancer cells MCF-7 and MDA-MB 231, human normal breast tissue associated fibroblasts (huNAF), human breast ductal carcinoma-associated fibroblasts (huCAF) were cultured to sub-confluent state followed by incubation in DMEM for 24 hours. Conditioned media were analyzed for CXCL1 secretion levels by ELISA. *(B)* Mouse mammary carcinoma cells NMuMG, 67NR, 144Epi PyVmT, 4T1, mouse normal mammary tissues associated fibroblasts (NAF), mouse mammary carcinoma associated fibroblasts (CAF), and mammary tumor promoting Tgfbr2 FspKO (2SKO) fibroblasts were cultured to sub-confluent state followed by incubation in DMEM for 24 hours. Conditioned media were analyzed for CXCL1 secretion levels by ELISA. Values are expressed as Mean ± SEM.

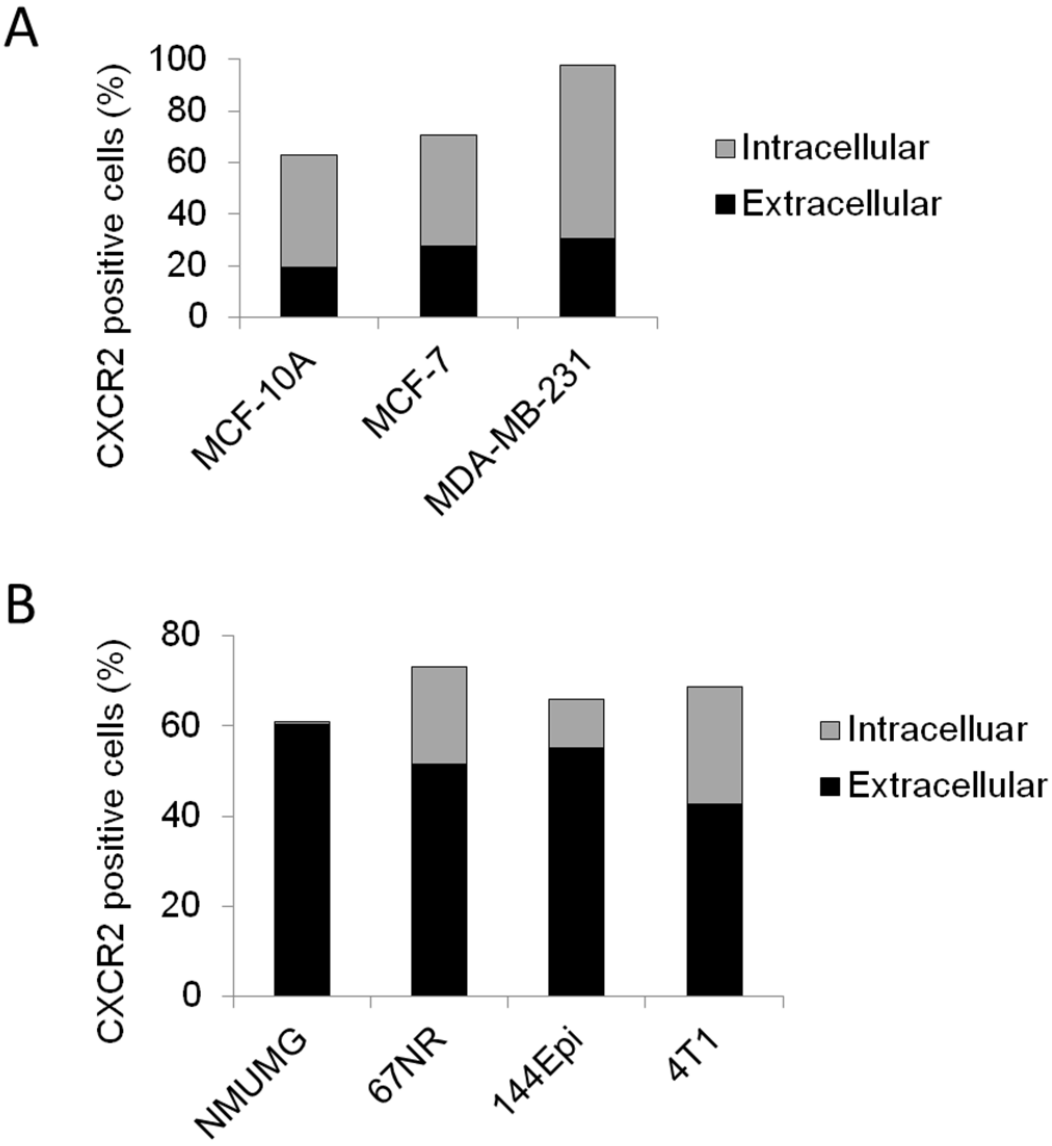
A
CXCR2 positive cells (%)
100
80
60
40
20
0
MCF-10A
MCF-7
MDA-MB-231
Intracellular
Extracellular
B
CXCR2 positive cells (%)
80
60
40
20
0
NMUMG
67NR
144Epi
4T1
Intracelluar
Extracellular

Figure 4.2. CXCR2 expression in breast cancer cells.

(A) Human breast epithelial cells MCF-10A, breast cancer cells MCF-7 and MDA-MB 231 were fixed and stained for CXCR2 expression by flow cytometry analysis. *(B)* Mouse mammary carcinoma cells NMuMG, 67NR, 144Epi PyVmT, 4T1 were fixed and stained for CXCR2 expression by flow cytometry analysis.

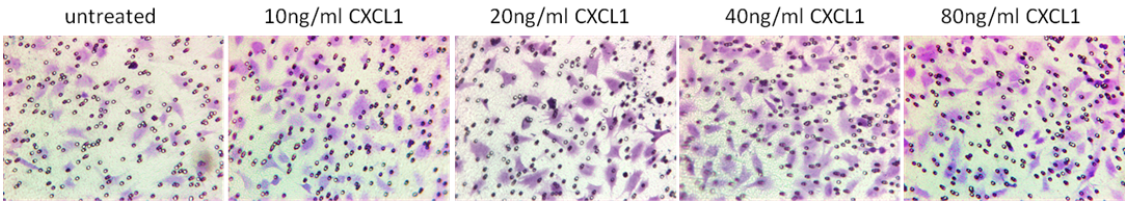
untreated
10ng/ml CXCL1
20ng/ml CXCL1
40ng/ml CXCL1
80ng/ml CXCL1

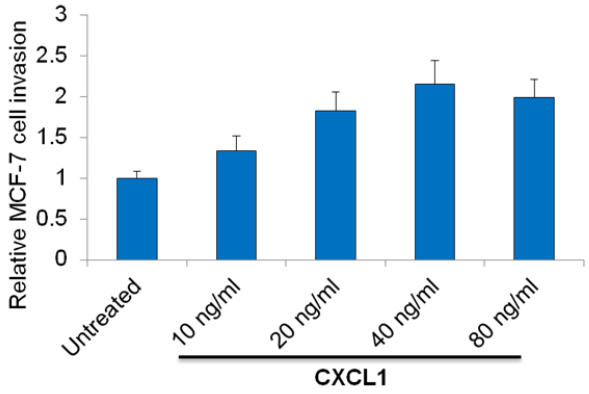
Relative MCF-7 cell invasion
3
2.5
2
1.5
1
0.5
0
Untreated
10 ng/ml
20 ng/ml
40 ng/ml
80 ng/ml
CXCL1

Figure 4.3. CXCL1 promotes human breast cancer cell invasion in a dose-dependent manner.

MCF-7 cells were cultured in the upper chambers of the matrigel coated transwell inserts in the absence or presence of indicated dosages of CXCL1 in both upper and lower chambers for 24hours. After formalin fixation, cells in the upper chambers were swabbed off, and the cells invaded to the lower surfaces of the inserts were stained with crystal violet. Pictures were taken under microscope at multiple fields. Cell invasion was quantified using Image J, and normalized to untreated cells. Statistical significance was determined by $p<0.05$. not significant (ns), $p>0.05$; *, $p<0.05$; **, $p<0.01$; ***, $p<0.001$. Values are expressed as Mean ± SEM.

cell invasion ability of two mouse mammary carcinoma cell lines 144Epi and 4T1, and investigated the effect of adding recombinant CXCL1 on cell invasion (Figure 4.4). Consistent with published in vivo studies that 4T1 cell is more metastatic than 144Epi-PyVmT cells when grafted in mice, we observed significantly higher levels of cell invasion of 4T1 than 144Epi-PyVmT cells *in vitro* as determined by transwell invasion assays. CXCL1 promoted 144Epi-PyVmT cell invasion in a dose dependent manner on all dosages used. On the other hand, although increased cell invasion was observed in CXCL1 treated 4T1 cells, extra CXCL1 at dosages higher than 20 ng/ml did not further enhance cell invasion. These data indicate that CXCL1 plays an important role in inducing cell invasion in both human and mouse breast cancer cells in dose-dependent manner.

Autocrine CXCL1 signaling is required for invasion capability in highly invasive breast cancer cells

Studies have shown direct correlation of ectopic CXCL1 expression and invasive potential of gastric and bladder cancer cells. Our studies indicate that expression of CXCL1 is positively correlated with tumorigenicity of mouse mammary carcinomas cells (Figure 4.1*B*). To further examine the role of autocrine CXCL1 signaling on tumor cell invasion, we transiently knocked down expression of CXCL1 by siRNA and measured cell invasion ability in 4T1 cells, which have relatively high constitutive CXCL1 expression. CXCL1 secretion was significantly inhibited by 50-70% with siRNA compared with control cells (Figure 4.5). We found that 4T1 cells show increasing cell invasion from 24 hours to 48 hours, which was markedly reduced upon deletion of CXCL1, and the reduction of cell invasion was proportional to that of CXCL1 secretion levels (Figure 4.5). Similar experiments were performed in 144Epi PyVmT cells, which secrete lower levels of CXCL1 than 4T1 cells. However, cell invasion of 144Epi PyVmT

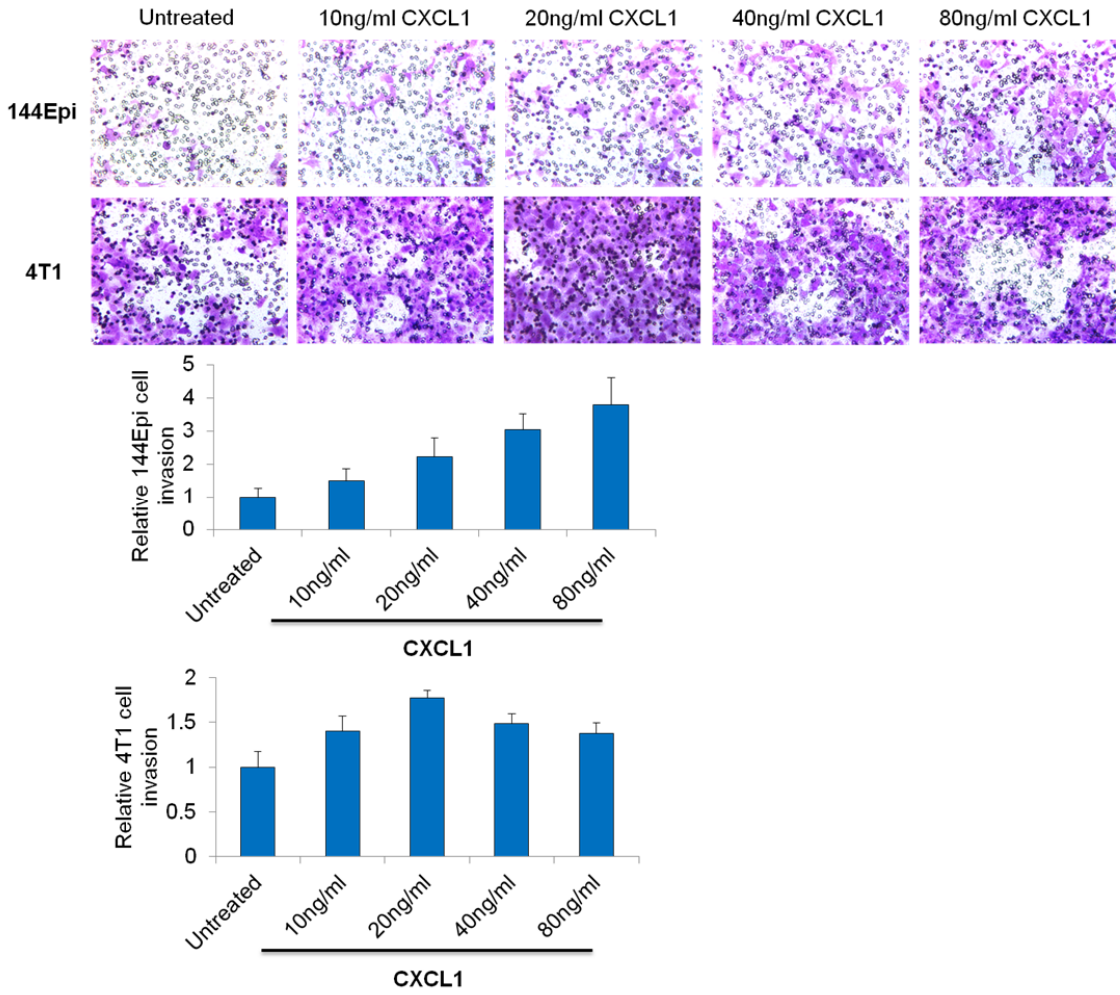
Untreated
10ng/ml CXCL1
20ng/ml CXCL1
40ng/ml CXCL1
80ng/ml CXCL1
144Epi
4T1
Relative 144Epi cell invasion
5
4
3
2
1
0
Untreated
10ng/ml
20ng/ml
40ng/ml
80ng/ml
CXCL1
Relative 4T1 cell invasion
2
1.5
1
0.5
0
Untreated
10ng/ml
20ng/ml
40ng/ml
80ng/ml
CXCL1

Figure 4.4. CXCL1 promotes mouse mammary carcinoma cell invasion in a dose-dependent manner.

144Epi or 4T1 mouse mammary carcinoma cells were cultured in the upper chambers of the matrigel coated transwell inserts in the absence or presence of indicated dosages of CXCL1 in both upper and lower chambers for 24hours. After formalin fixation, cells in the upper chambers were swabbed off, and the cells invaded to the lower surfaces of the inserts were stained with crystal violet. Pictures were taken under microscope at multiple fields. Cell invasion was quantified using Image J, and normalized to untreated cells. Statistical significance was determined by $p<0.05$. not significant (ns), $p>0.05$; *, $p<0.05$; **, $p<0.01$; ***, $p<0.001$. Values are expressed as Mean ± SD from a representative experiment.

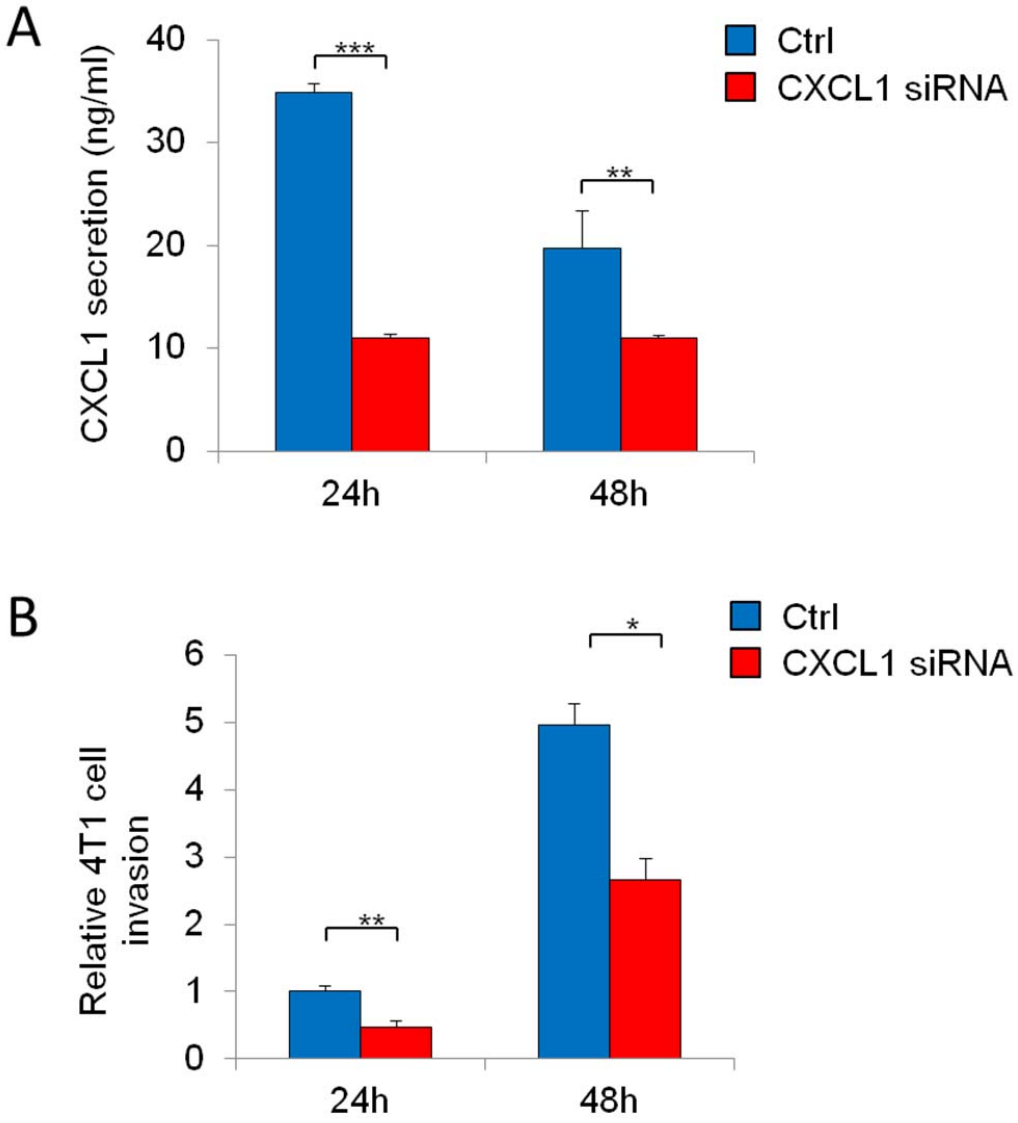
A
CXCL1 secretion (ng/ml)
40
30
20
10
0
***
**
24h
48h
Ctrl
CXCL1 siRNA
B
Relative 4T1 cell invasion
6
5
4
3
2
1
0
**
*
24h
48h
Ctrl
CXCL1 siRNA

Figure 4.5. Autocrine CXCL1 signaling is required formouse 4T1 mammary carcinoma cell invasion.

(A) mouse mammary carcinoma cells were transfected with control siRNA (Ctrl) or siRNA to CXCL1 (CXCL1 siRNA), and cultured in the upper chambers of the matrigel coated transwell for 24 and 48 hours. Conditioned media were analyzed for CXCL1 secretion by ELISA. *(B)* After formalin fixation, cells in the upper chambers were swabbed off, and the cells invaded to the lower surfaces of the inserts were stained with crystal violet. Pictures were taken under microscope at multiple fields. Cell invasion was quantified using Image J, and normalized to control siRNA transfected cell invasion at 24 hours. Statistical significance was determined by $p<0.05$. *, $p<0.05$; **, $p<0.01$; ***, $p<0.001$. Values are expressed as Mean ± SEM.

cells is much lower than that of 4T1 cells at 24 hours and 48 hours, and no significant reduction was observed upon CXCL1 depletion (data not shown). Taken together, these data indicate that autocrine CXCL1 plays an essential role in cell invasion in 4T1 mammary carcinoma cells with relatively high CXCL1 expression, but does not have significant effect in 144Epi PyVmT cells with relatively low CXCL1 expression.

Paracrine CXCL1 from carcinoma-associated fibroblasts promotes breast cancer cell invasion

Our studies indicate that carcinoma-associated fibroblasts (CAFs) ectopically secrete higher levels of CXCL1 than normal fibroblasts, and thus are another main source of CXCL1 in the tumor microenvironment. We next assessed the potential role for CAFs and CAF-derived CXCL1 in inducing mammary carcinoma cell invasion using a transwell cell invasion model, in which carcinoma cells were co-cultured with fibroblasts with a border of matrigel layer in between mimicking the basement membrane in tumor microenvironment. In order to specifically identify invaded carcinoma cells, they were pre-labeled with fluorochrome dye (CMFDA), which can sustain its fluorescent signal for at least 7 to 10 days. We found that 41CAF with high CXCL1 secretion significantly promote 144Epi PyVmT and 4T1 mammary carcinoma cell at 12 and 24 hours (Figure 4.6). Interestingly, in serum free condition, cell invasion capability of 144Epi PyVmT and 4T1 cells were remarkably diminished compared with that in low serum condition (Figure 4.6 and Figure 4.4). CXCL1 is expressed in both tumor cells and fibroblasts. In order to determine and compare the functional contribution of fibroblast- and tumor cell-derived CXCL1 to tumor cell invasion, we transiently inhibited CXCL1 expression by siRNA in each cell types or both, and co-cultured them in the transwell for 24 hours. CXCL1 secretion levels of siRNA transfected cells were determined by ELISA (Figure 4.7). 70% to 75% knockdown of CXCL1 was achieved in 41CAF, 144Epi PyVmT and 4T1 cells. In

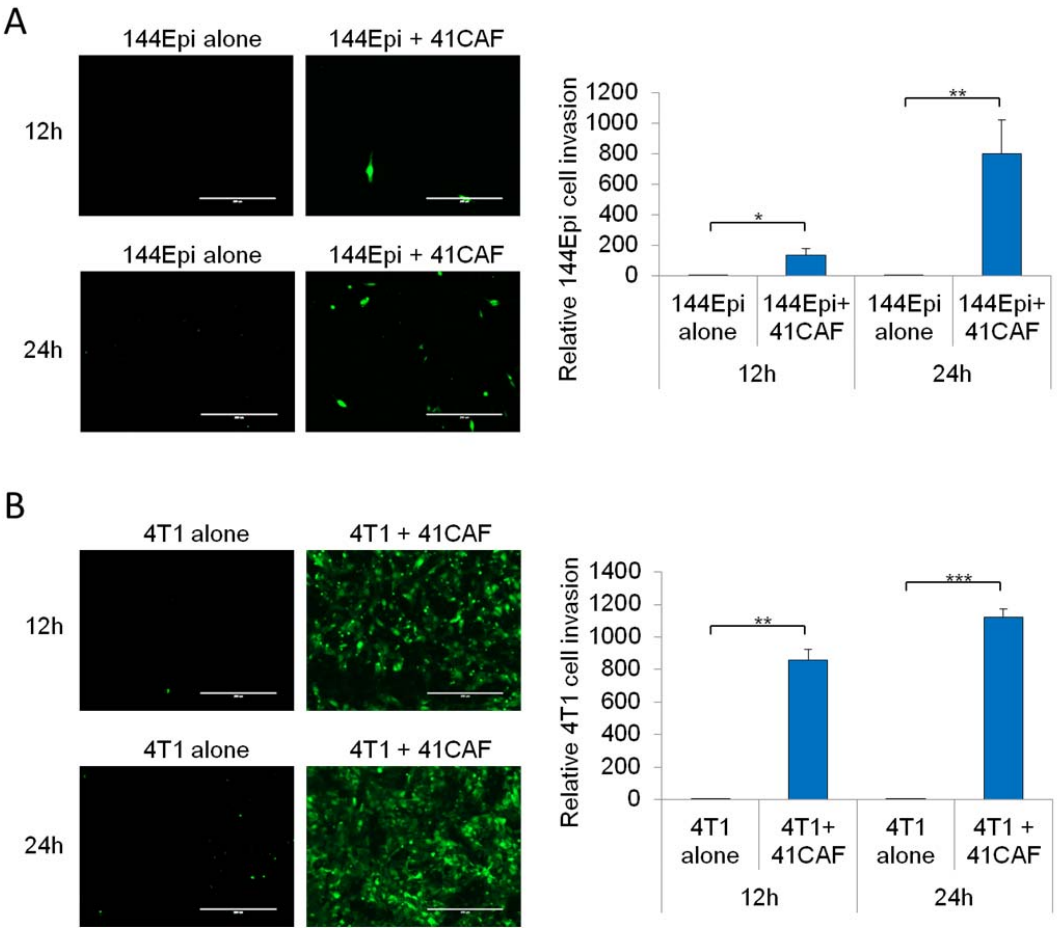
A
144Epi alone
144Epi + 41CAF
12h
24h
144Epi alone
144Epi + 41CAF
Relative 144Epi cell invasion
1200
1000
800
600
400
200
0
*
**
144Epi alone
144Epi+ 41CAF
144Epi alone
144Epi+ 41CAF
12h
24h
B
4T1 alone
4T1 + 41CAF
12h
24h
4T1 alone
4T1 + 41CAF
Relative 4T1 cell invasion
1400
1200
1000
800
600
400
200
0
**
***
4T1 alone
4T1+ 41CAF
4T1 alone
4T1 + 41CAF
12h
24h

Figure 4.6. Mammary CAFs promote 144Epi and 4T1 carcinoma cell invasion.

144Epi or 4T1 mouse mammary carcinoma cells were pre-labeled by fluorochrome dye (CMFDA), and cultured in the upper chambers of the matrigel coated transwell inserts in the absence or presence of mammary carcinoma-associated fibroblasts (41CAF) cultured on the lower surface of transwell inserts for 12 and 24 hours. After formalin fixation, cells in the upper chambers were swabbed off, and the cells invaded to the lower surfaces of the inserts were visualized under fluorescence microscope. Pictures were taken at multiple fields. Cell invasion was quantified using Image J, and normalized to control siRNA transfected cell invasion at 24 hours. Statistical significance was determined by $p<0.05$. *, $p<0.05$; **, $p<0.01$; ***, $p<0.001$. Values are expressed as Mean ± SEM.

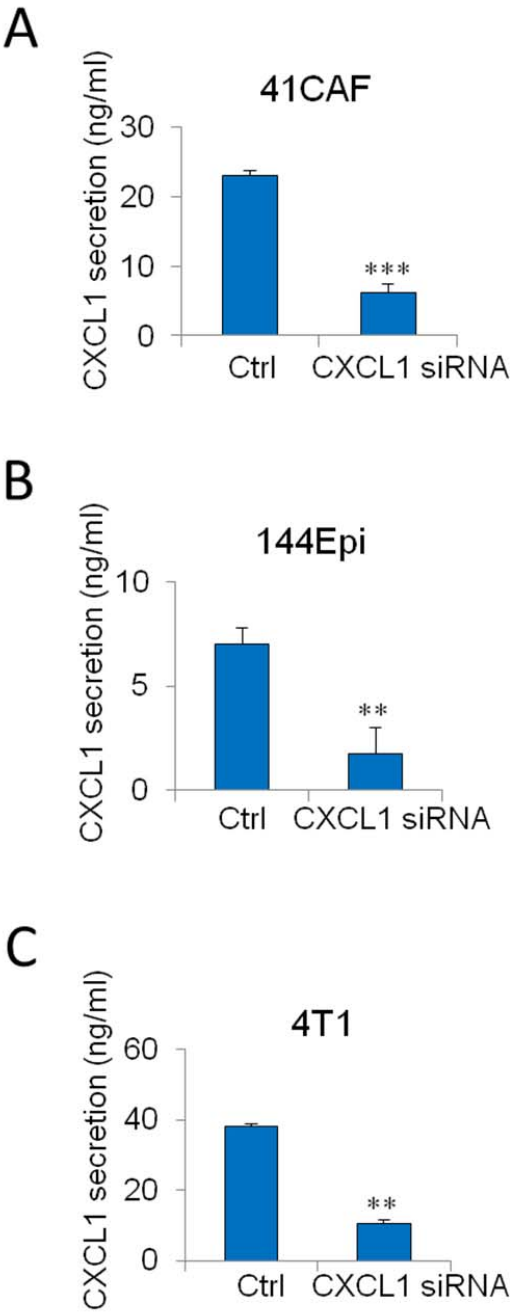
A
41CAF
CXCL1 secretion (ng/ml)
30
20
10
0
***
Ctrl
CXCL1 siRNA
B
144Epi
CXCL1 secretion (ng/ml)
10
5
0
**
Ctrl
CXCL1 siRNA
C
4T1
CXCL1 secretion (ng/ml)
60
40
20
0
**
Ctrl
CXCL1 siRNA

Figure 4.7. Confirmation of CXCL1 siRNA knockdown in individually cultured 41CAF, 144Epi and 4T1 cells.

Mammary carcinoma-associated fibroblasts (41CAF) and fluorochrome dye pre-labeled 144Epi, 4T1 mouse mammary carcinoma cells were transfected with control siRNA (Ctrl) or siRNA to CXCL1 (CXCL1 siRNA). Cells were seeded in matrigel coated 24 well plates for 24 hours. Condition media was collected and analyzed for CXCL1 secretion levels by ELISA. Statistical significance was determined by $p<0.05$. **, $p<0.01$; ***, $p<0.001$. Values are expressed as Mean ± SEM.

addition, we determined CXCL1 secretion levels in tumor cells cultured with 41CAFs in transwells using the same method. Interestingly, inhibition of CXCL1 expression in 144Epi or 4T1 cells alone had no significant effect on the overall CXCL1 expression levels in the co-culture microenvironment (Figure 4.8). In addition, CXCL1 knockdown in 41CAFs significantly reduced overall amount of CXCL1 with 144Epi cells but not with 4T1 cells. Also, we noticed that with CXCL1 knockdown in 41CAFs, additive effects of CXCL1 inhibition were achieved in 41CAFs co-cultured with CXCL1 siRNA transfected 4T1 cells but not with 144Epi cells (Figure 4.8).

As for cell invasion, blockade of autocrine CXCL1 signaling in 144Epi PyVmT cell or 4T1 cells had no significant effect on tumor cell invasion, correlating with unaffected overall CXCL1 expression levels in the co-culture microenvironments (Figure 4.9). Nevertheless, blockade of paracrine CXCL1 signaling by siRNA transfection of 41CAFs significantly reduced tumor cell invasion in both 144Epi: 41CAF and 4T1: 41CAF cells. siRNA inhibition of both autocrine and paracrine CXCL1 signaling further suppressed 144Epi cell invasion, yet has no further inhibitory effect on 4T1 cell invasion (Figure 4.9).

Paracrine CXCL1 signaling induced breast cancer cell invasion was dependent on CXCR2 expression in tumor cells

CXCL1 signals to its cell surface receptor CXCR2 to regulate cell invasion in gastric and bladder cancer. Here we examined the role for CXCR2 in paracrine CXCL1 signaling induced breast cancer cell invasion. We generated two 144Epi PyVmT mouse mammary carcinoma cell lines with decreased expression of CXCR2 by infecting the parental 144Epi cells (Par) with retroviruses expressing shRNAs targeting CXCR2 gene at different exon regions (named as F-6, G-1 respectively). CXCR2 expression levels was determined by immunofluorescence staining and flowcytometry analysis (Figure

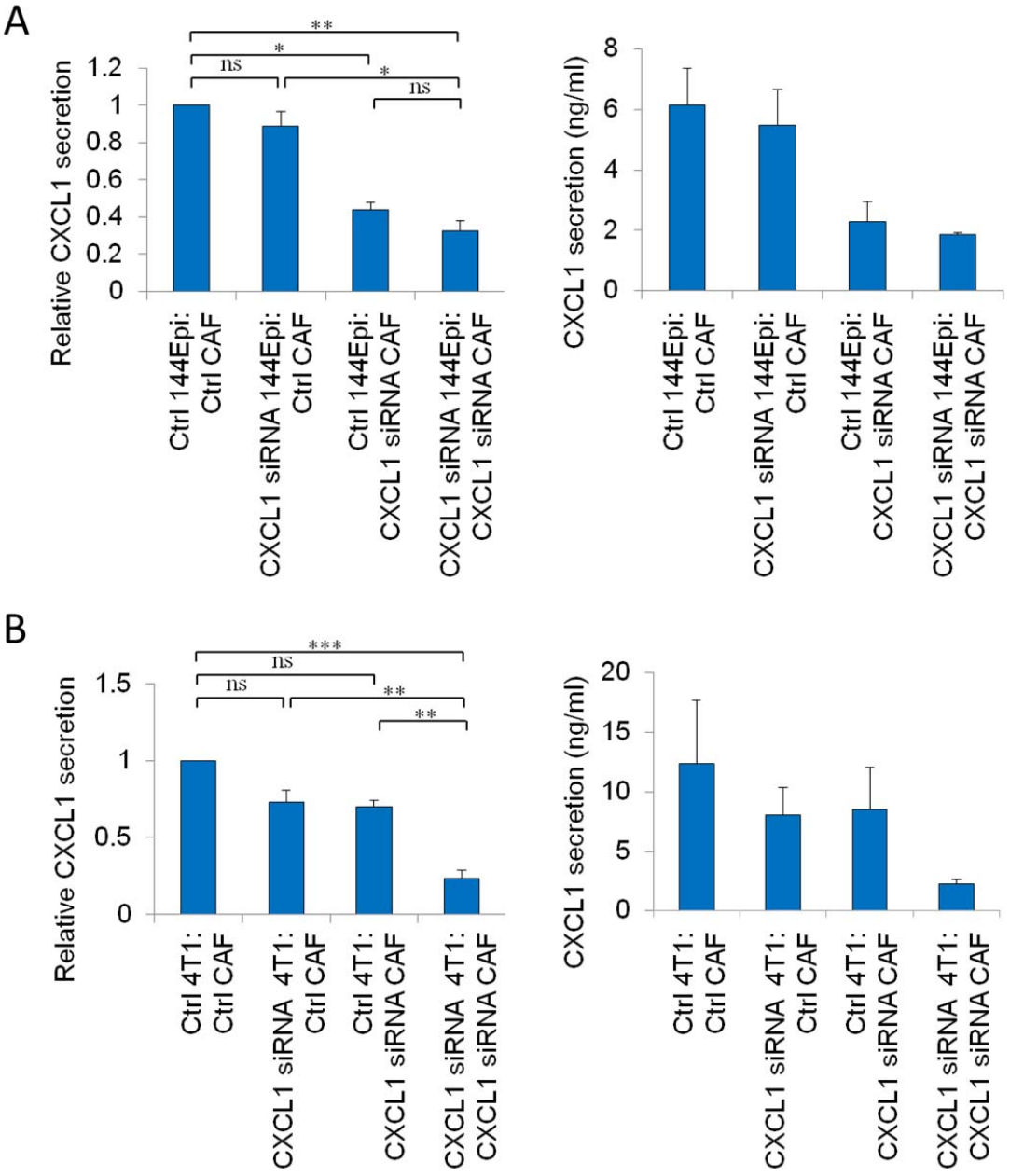
A
Relative CXCL1 secretion
1.2
1
0.8
0.6
0.4
0.2
0
**
*
ns
*
ns
Ctrl 144Epi: Ctrl CAF
CXCL1 siRNA 144Epi: Ctrl CAF
Ctrl 144Epi: CXCL1 siRNA CAF
CXCL1 siRNA 144Epi: CXCL1 siRNA CAF
CXCL1 secretion (ng/ml)
8
6
4
2
0
Ctrl 144Epi: Ctrl CAF
CXCL1 siRNA 144Epi: Ctrl CAF
Ctrl 144Epi: CXCL1 siRNA CAF
CXCL1 siRNA 144Epi: CXCL1 siRNA CAF
B
Relative CXCL1 secretion
1.5
1
0.5
0
***
ns
ns
**
**
Ctrl 4T1: Ctrl CAF
CXCL1 siRNA 4T1: Ctrl CAF
Ctrl 4T1: CXCL1 siRNA CAF
CXCL1 siRNA 4T1: CXCL1 siRNA CAF
CXCL1 secretion (ng/ml)
20
15
10
5
0
Ctrl 4T1: Ctrl CAF
CXCL1 siRNA 4T1: Ctrl CAF
Ctrl 4T1: CXCL1 siRNA CAF
CXCL1 siRNA 4T1: CXCL1 siRNA CAF

Figure 4.8. siRNA knockdown of CXCL1 expression in co-cultured 41CAFs and 144Epi or 4T1 carcinoma cells.

Fluorochrome dye (CMFDA) pre-labeled 144Epi, 4T1 mouse mammary carcinoma cells and mammary carcinoma-associated fibroblasts (41CAF) were transfected with control siRNA (Ctrl) or siRNA to CXCL1 (CXCL1 siRNA). 144Epi *(A)* or 4T1 *(B)* cells were cultured in the upper chambers of the matrigel coated transwell inserts in the presence of mammary CAFs cultured on the lower surface of transwell inserts for 24 hours. Mixed conditioned media from both upper and lower chambers were collected and analyzed for CXCL1 secretion levels by ELISA. CXCL1 secretion levels were normalized to control siRNA transfected tumor cells co-cultured with control siRNA transfected CAFs as shown on the left. Un-normalized CXCL1 secretion levels from three independent experiments were shown on the right. Statistical significance was determined by $p<0.05$. not significant (ns), $p>0.05$; *, $p<0.05$; **, $p<0.01$; ***, $p<0.001$. Values are expressed as Mean ± SEM.

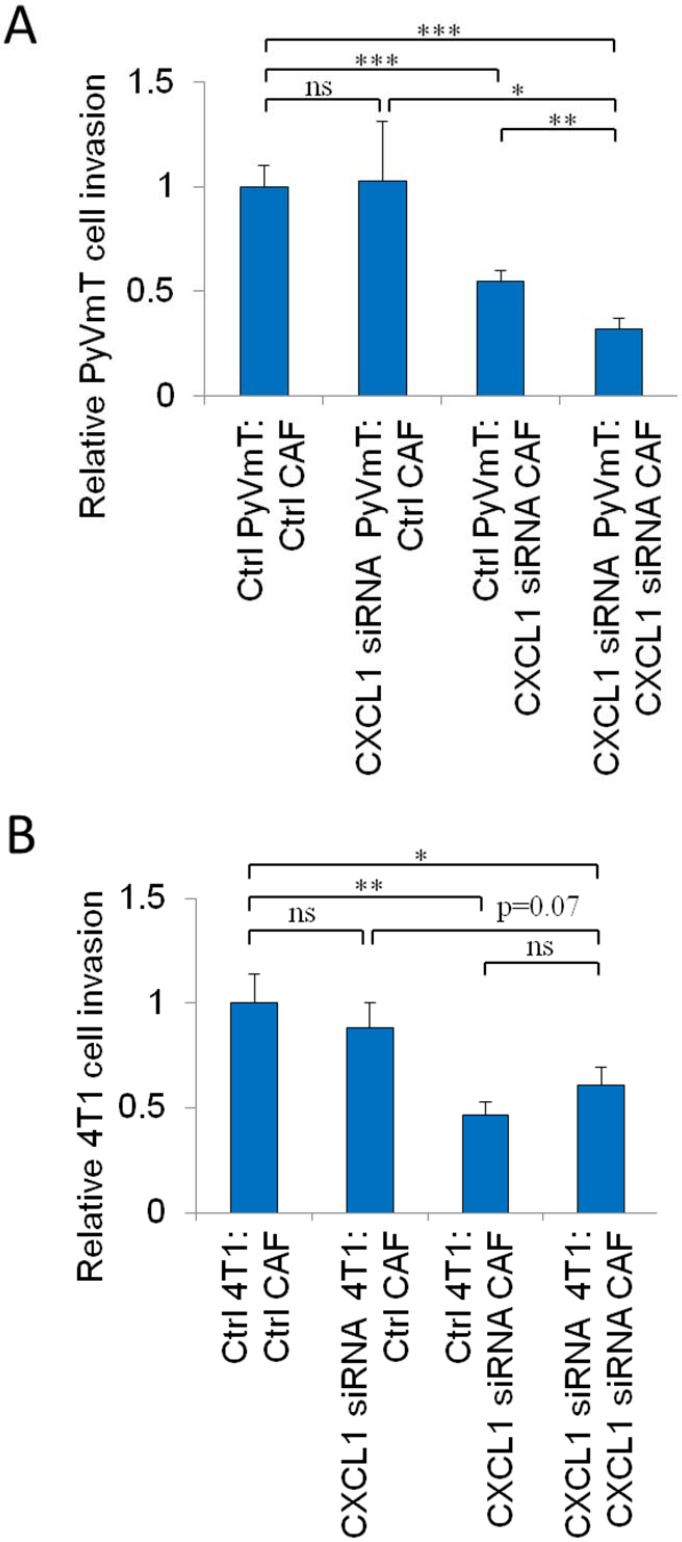
A
Relative PyVmT cell invasion
1.5
1
0.5
0
***
***
ns
*
**
Ctrl PyVmT: Ctrl CAF
CXCL1 siRNA PyVmT: Ctrl CAF
Ctrl PyVmT: CXCL1 siRNA CAF
CXCL1 siRNA PyVmT: CXCL1 siRNA CAF
B
Relative 4T1 cell invasion
1.5
1
0.5
0
*
**
ns
p=0.07
ns
Ctrl 4T1: Ctrl CAF
CXCL1 siRNA 4T1: Ctrl CAF
Ctrl 4T1: CXCL1 siRNA CAF
CXCL1 siRNA 4T1: CXCL1 siRNA CAF

Figure 4.9. Fibroblast-derived paracrine CXCL1signling promotes 144Epi and 4T1 carcinoma cell invasion.

Fluorochrome dye (CMFDA) pre-labeled 144Epi, 4T1 mouse mammary carcinoma cells and mammary carcinoma-associated fibroblasts (41CAF) were transfected with control siRNA (Ctrl) or siRNA to CXCL1 (CXCL1 siRNA). 144Epi *(A)* or 4T1 *(B)* cells were cultured in the upper chambers of the matrigel coated transwell inserts in the presence of mammary CAFs cultured on the lower surface of transwell inserts for 24 hours. After formalin fixation, cells in the upper chambers were swabbed off, and the cells invaded to the lower surfaces of the inserts were visualized under fluorescence microscope. Pictures were taken at multiple fields. Cell invasion was quantified using Image J, and normalized to control siRNA transfected tumor cells co-cultured with control siRNA transfected CAFs. Statistical significance was determined by $p<0.05$. not significant (ns), $p>0.05$; *, $p<0.05$; **, $p<0.01$; ***, $p<0.001$. Values are expressed as Mean ± SEM.

4.10*A* and data not shown). The results indicate that we have achieved 60% to 85% knockdown of CXCR2 expression in the two generated cell lines: 144Epi CXCR2/F-6 and 144Epi CXCR2/G-1 compared with parental 144Epi cells or control shRNA expressing cells. Similarly, we have generated 41CAF cell line with decreased expression of CXCL1 (CXCL1-shRNA CAF), which was confirmed by ELISA (Figure 4.10B). To examine the effect of CXCR2 inhibition on tumor cell invasion induced by autocrine and fibroblast-derived paracrine CXCL1 signaling, tumor cell invasion was determined on 144Epi carcinoma cells (Par, CXCR2/F-6, CXCR2/G-1) cultured alone, with control parental CAF or CXCL1-shRNA CAF at 24 hours (Figure 4.11). We found that tumor cell invasion is quite low when 144Epi tumor cells were cultured alone, and no significant differences were observed among parental cells (Par) and the two CXCR2 knockdown cells (CXCR2/F-6, CXCR2/G-1). Parental 41CAF with high CXCL1 secretion levels remarkably induced 144Epi cell invasion. Although only partially, knockdown of CXCR2 by shRNAs significantly reduced 144Epi cell invasion. Consistent with siRNA knockdown studies (Figure 4.9A), knockdown of CXCL1 expression in 41CAF show significantly lower capability of inducing 144Epi cell invasion compared to parental 41CAF, and tumor cell CXCR2 knockdown did not lead to any significant difference in cell invasion from parental cells (Figure 4.11).

CXCL1 stimulates breast cancer cell invasion via activation of Akt and NF-KB signaling pathways

Previous studies indicate that CXCL1 induce cancer cell invasion, through binding to its cell surface receptor CXCR2, which is a G protein coupled receptor (GPCR) favoring coupling to Gαi protein subunit (183). In addition, studies in other types of cancers including prostate, ovarian and stomach cancer have shown that through activating ERK1/2 MAPK, PI3K/Akt, NF-κB signaling pathways, CXCL1/CXCR2 signaling regulates

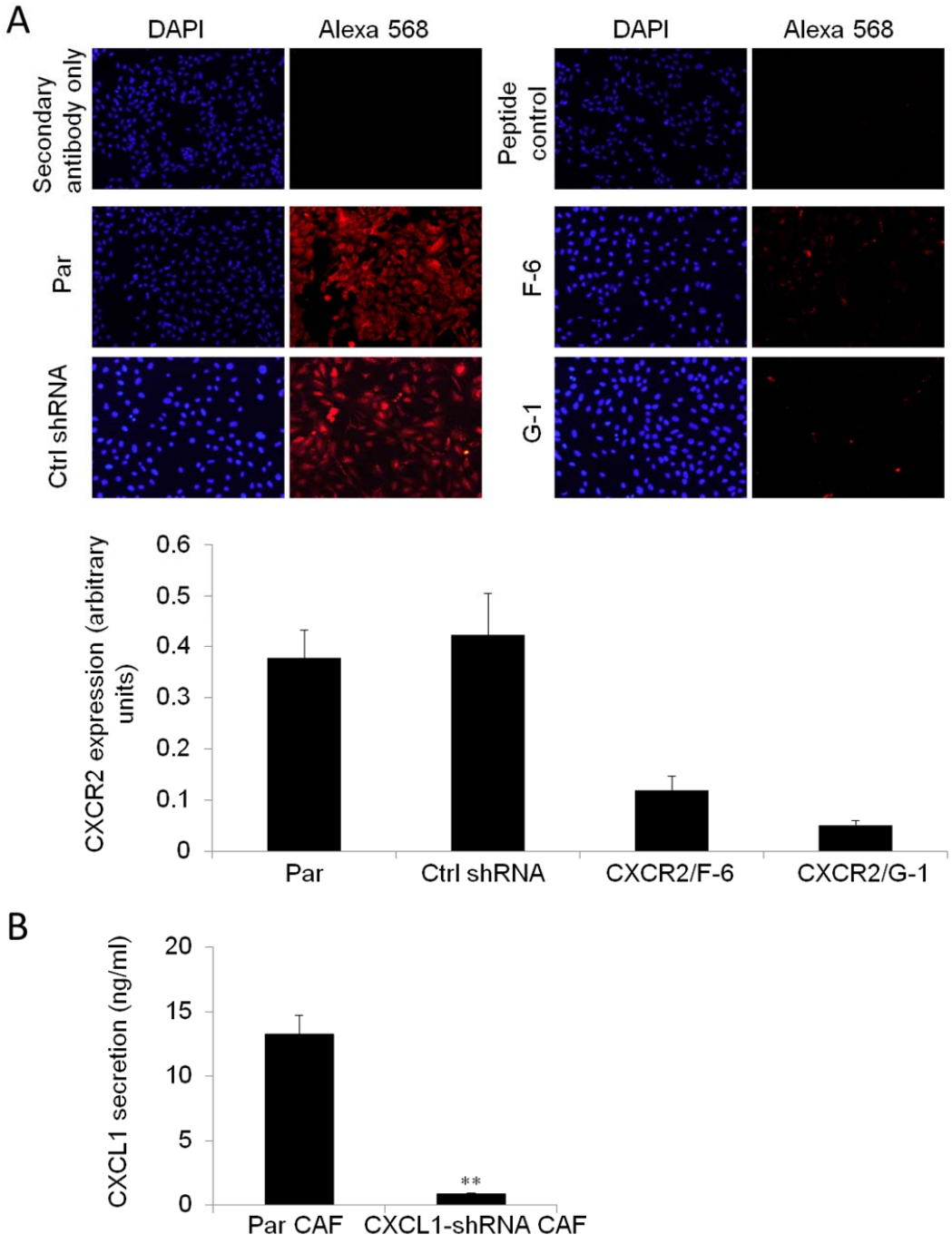
A
DAPI
Alexa 568
DAPI
Alexa 568
Secondary antibody only
Peptide control
Par
F-6
Ctrl shRNA
G-1
CXCR2 expression (arbitrary units)
0.6
0.5
0.4
0.3
0.2
0.1
0
Par
Ctrl shRNA
CXCR2/F-6
CXCR2/G-1
B
CXCL1 secretion (ng/ml)
20
15
10
5
0
**
Par CAF
CXCL1-shRNA CAF

Figure 4.10. Stable knockdown of CXCR2 in 144EPI mammary carcinoma cells and CXCL1 in mouse mammary CAFs.

(A) CXCR2 shRNAs (F-6, G-1) or control shRNAs (Ctrl shRNA) were stably expressed in 144Epi mammary carcinoma cells, and analyzed for expression of CXCR2 by immunofluorescence staining. Cells were visualized by rabbit secondary antibodies to Alexa-568. Antibody specificity was controlled by secondary antibody only and CXCR2 peptide competition (Peptide Control). CXCR2 expression was quantified by Image J. Cells were compared to Parental control (Par). *(B)* Mouse mammary carcinoma-associated fibroblasts (41CAF) were infected with retroviruses expressing CXCL1 shRNA followed by neomycin selection. Conditioned media from parental and CXCL1 shRNA expressing CAFs were collected and assayed for CXCL1 secretion by ELISA. Statistical significance was determined by $p<0.05$. **, $p<0.01$. Values are expressed as Mean ± SEM.

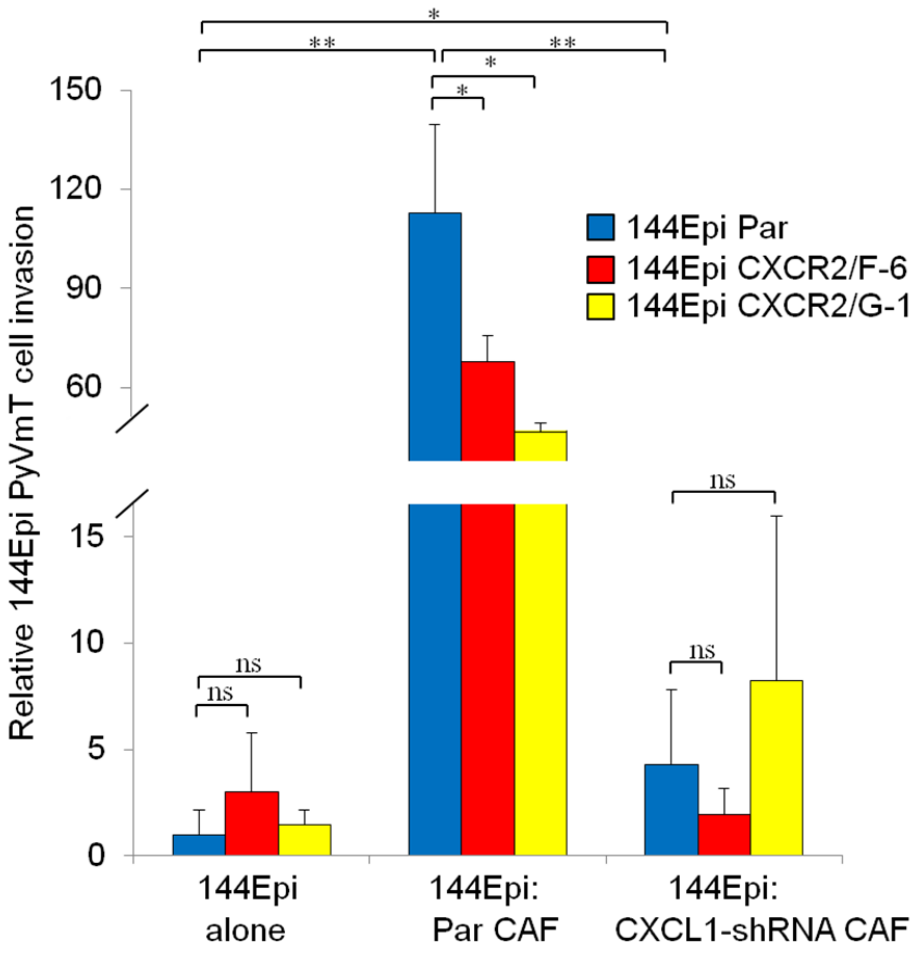
Relative 144Epi PyVmT cell invasion
150
120
90
60
15
10
5
0
*
**
**
*
*
ns
ns
ns
ns
144Epi Par
144Epi CXCR2/F-6
144Epi CXCR2/G-1
144Epi alone
144Epi: Par CAF
144Epi: CXCL1-shRNA CAF

Figure 4.11. Paracrine CXCL1 signaling from carcinoma-associated fibroblasts induce carcinoma cell invasion in a CXCR2-dependent manner.

Parental 144Epi mouse mammary carcinoma cells (144Epi Par), CXCR2-shRNA expressing 144Epi cells (144Epi CXCR2/F-6, G-1) were pre-labeled by fluorochrome dye (CMFDA), and cultured in the upper chambers of the matrigel coated transwell inserts in the absence or presence of parental mammary carcinoma-associated fibroblasts (41CAF Par) or CXCL1-shRNA expressing 41CAFs (CXCL1-shRNA CAF) cultured on the lower surface of transwell inserts for 24 hours. After formalin fixation, cells in the upper chambers were swabbed off, and the cells invaded to the lower surfaces of the inserts were visualized under fluorescence microscope. Pictures were taken at multiple fields. Cell invasion was quantified using Image J, and normalized to 144Epi Par alone cell invasion. Statistical significance was determined by $p<0.05$. not significant (ns), $p>0.05$; *, $p<0.05$; **, $p<0.01$; ***, $p<0.001$. Values are expressed as Mean ± SEM.

cell proliferation, survival, invasion and angiogenesis (184-188). However, the molecular mechanisms through which CXCL1 regulate breast cancer cell survival and invasion remains to be fully clarified.

To clarify the molecular mechanism, we treated MCF-7 breast cancer cells with recombinant CXCL1 at a dosage which powerfully induce cell invasion and examined changes of candidate signaling pathways (ERK1/2, Akt, NF-κB) by western blots. NF-κB is sequestered in the cytosol by its inhibitor IκB (inhibitor of NF-κB) proteins, and activation of Iκκ by phosphorylation is required for phosphorylation of IκB, which leads to IκB degradation and release of NF-κB for nuclear translocation and activation of gene transcription. The results indicate that CXCL1 continuously stimulates phosphorylation of Akt and Iκκα/β as early as 20 seconds post treatment, but has no significant effect on levels of phosphorylated ERK1/2 (Figure 4.12A). We did similar profiling for these signaling pathways in 144Epi mouse mammary carcinoma cells, and so far we have observed that CXCL1 stimulates phosphorylation of Iκκα/β in 144Epi cells, but the response is much slower than that in MCF-7 cells (Figure 4.12B). It was shown that Akt promotes HT1080 fibrosarcoma cell invasion through activating NF-κB transcriptional activity thus enhancing expression of metalloproteinase-9 (MMP-9) (189). Other studies also indicate that Akt is activated by phosphatidylinositol 3-kinases (PI3K) and may interact with NF-κB to promote breast cancer cell survival and invasion, and that Akt activates NF-κB via regulating Iκκ (Inhibitor of NF-κB kinase) activity, resulting in transcription of pro-survival genes (190). On the other hand, Akt can regulate cell survival independently through phosphorylating BAD (which is a pro-apoptotic protein of the Bcl-2 family) on Ser136, which makes BAD dissociate from the Bcl-2/Bcl-X complex to promote cell survival (191). We speculate that Akt and NF-κB either work independently or coordinate with each other in these biological processes, which will be

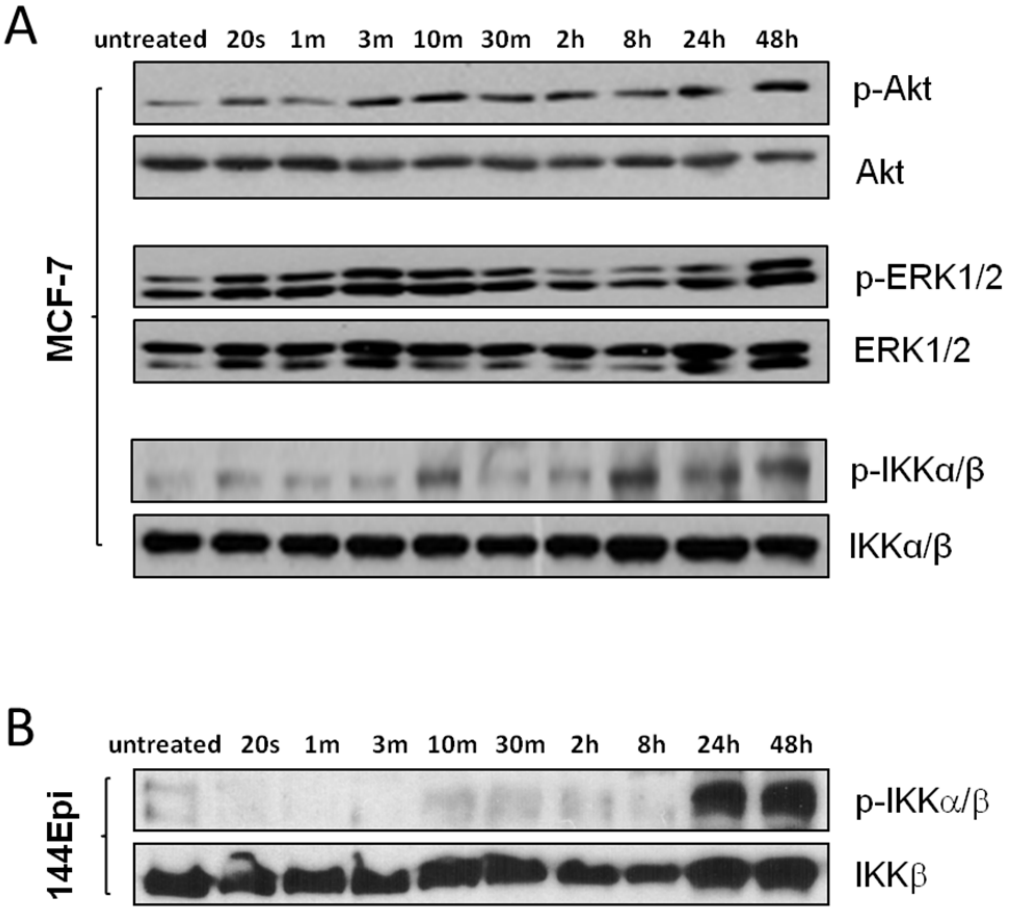
A
untreated 20s 1m 3m 10m 30m 2h 8h 24h 48h
p-Akt
Akt
p-ERK1/2
ERK1/2
p-IKKα/β
IKKα/β
MCF-7
B
untreated 20s 1m 3m 10m 30m 2h 8h 24h 48h
p-IKKα/β
IKKβ
144Epi

Figure 4.12. CXCL1 activates NF-κB signaling pathways in MCF-7 and 144Epi cells and activate Akt signaling pathway in MCF-7 cells.

Cultured MCF-7 human breast cancer cells *(A)* or 144Epi mouse mammary carcinoma cells *(B)* were starved in serum free media overnight, then treated with recombinant CXCL1 (40ng/ml) for indicated time periods (s, second; m, minute; h, hour). Whole cell lysates were collected and analyzed for phosphorylation status of Akt (S473), ERK1/2 (T202/Y204) and/or Ikkα/β (S176/180) by western blots. The whole amount of Akt, Ikkα/β and ERK1/2 were immunoblotted as loading control. Presented are representative blots from three independent experiments.

determined in future studies using pharmacologic inhibitors to PI3K/Akt signaling and or Ikkα/β /IκB /NF-κB signaling.

Carcinoma-associated fibroblasts promote tumor growth, local invasion and tumor cell survival corresponding to enhanced secretion of CXCL1

Previous studies indicate that stable knockdown of TGF-β type II receptor by cre-loxP blocked TGF-β signaling in mammary fibroblasts (2SKO fibroblasts) and enhanced expression of CXCL1 and HGF at both transcriptional and translational levels compared with control floxed fibroblasts and (Figure 2.9A-B) and (160). In addition, we have shown that 41CAF isolated from PyVmT transgenic mammary tumor bearing mice show elevated CXCL1 and HGF secretion alone with decreased TGF-β signaling compared to normal fibroblast (311NAF). Furthermore, both 2SKO and 41CAF promotes 4T1 mammary tumor cell invasion in vitro (Figure 4.8B) and (160). These data indicate that 2SKO fibroblasts share many of the characteristics with 41CAFs, thus a great model to study the role of paracrine CXCL1 signaling in mammary tumor progression in the context of TGF-beta signaling. To determine the effect of fibroblast-derived CXCL1 on tumor growth, we grafted 144Epi mouse mammary carcinoma cells alone, with 2SKO or 311NAF fibroblasts into C57/BL6 mice (Figure 4.13). Specifically, we isolated collagen from C57/BL6 mice, which allows us to use the more physiological relevant C57/BL6 mouse mode instead of nude mice model. The results indicate that 2SKO fibroblasts enhanced tumor growth by 2.2 fold at 60 days compared to 144Epi cell grafted alone or with 311NAFs (Table 4.1). Additionally, tumor tissues were immunostained with Ki67 and cleaved caspase 3 markers to analyze for changes of tumor cell proliferation and cell apoptosis. The results indicate that when co-grafted with 2SKO fibroblasts, knockdown of CXCR2 in 144Epi tumor cells resulted in decreased cell proliferation and increased cell apoptosis compared to parental 144Epi tumor cells (Figure 4.14).

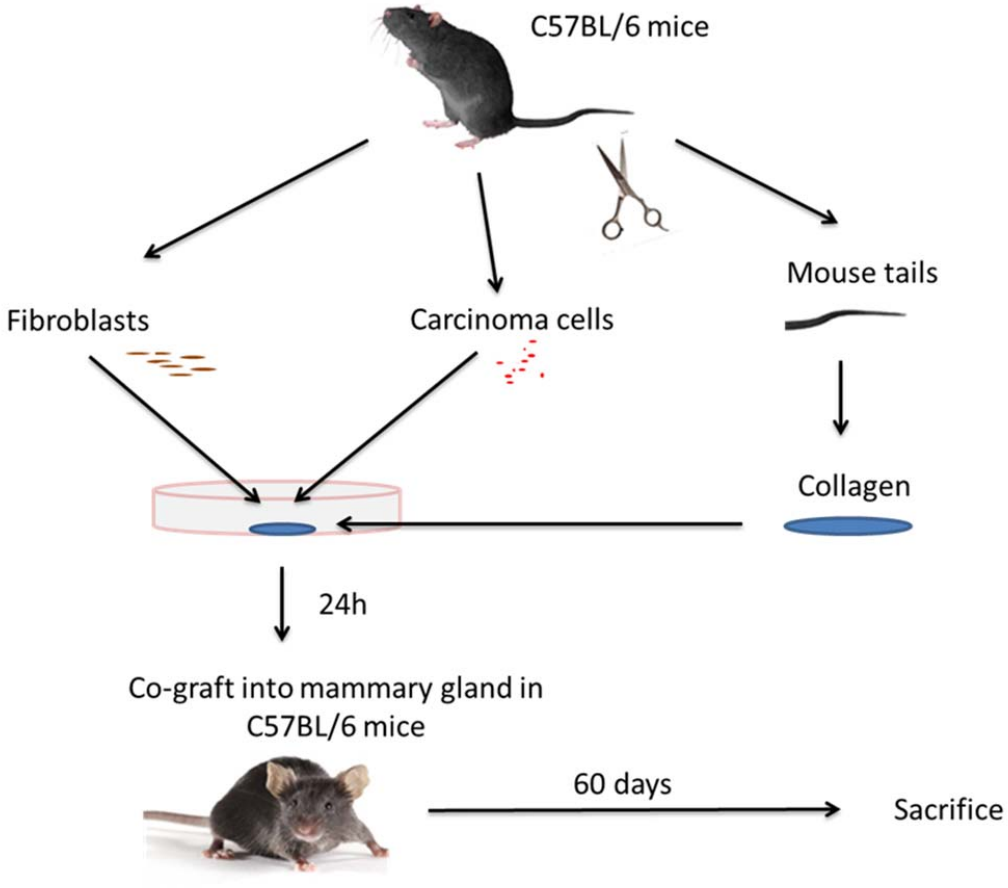

Co-transplantatio of fibroblasts and tumor cells

Fibroblasts	Tumor cells
--	144Epi Par
311NAF	144Epi Ctrl
$Tgfbr2^{FspKO}$ (2SKO)	144Epi CXCR2/F-6
	144Epi CXCR2/G-1

Figure 4.13. Orthotopic transplantation mouse model.

144Epi mammary carcinoma cells were isolated from C57/BL6 PyVmT transgenic mice and spontaneously immortalized. 311NAF were isolated from mammary gland of wild type C57/BL6 mice. Collagen was isolated from C57/BL6 mouse tail tenders. 144Epi carcinoma cells (Par, parental cell; Ctrl, control shRNA expressing cell; CXCR2/F-6 or CXCR2/G-1, CXCR2 shRNA expressing cell) were cultured alone or with indicated mammary fibroblasts in mouse tail collagen overnight (see table for experimental design) to allow cell-cell contact, and grafted into the inguinal mammary gland of C57/BL6 mice. Tumor growth and *in vivo* cell proliferation and survival were measured at day 60.

Table 4.1. 2SKO fibroblasts promote 144Epi tumor growth in C57/BL6 mice.

Cell Grafting	Tumor Mass (g)	n
144Epi alone	0.429 ± 0.133	10
144Epi : 311NAF	0.445 ± 0.112	13
144Epi : 2SKO	0.948 ± 0.269	9

A

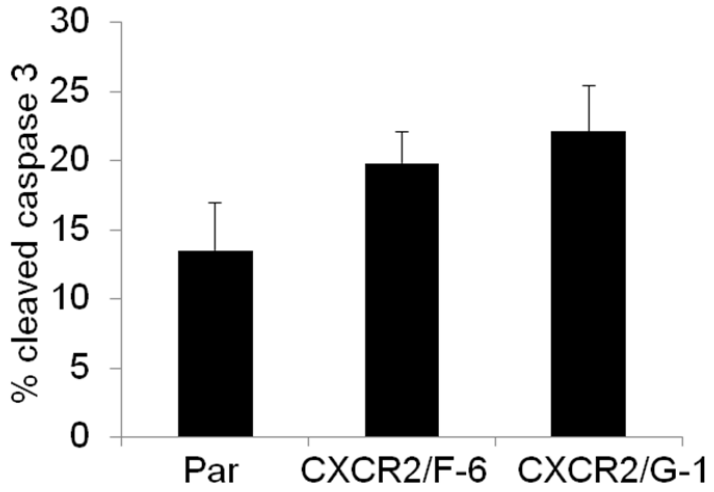
% cleaved caspase 3
30
25
20
15
10
5
0
Par
CXCR2/F-6
CXCR2/G-1

B

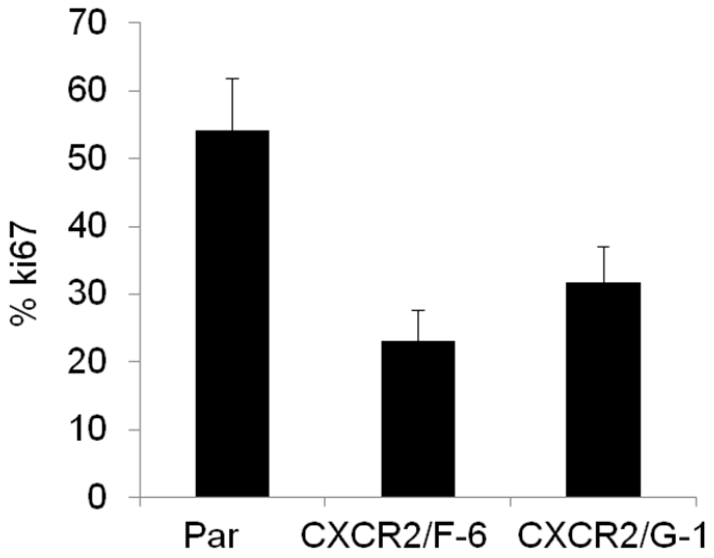
% ki67
70
60
50
40
30
20
10
0
Par
CXCR2/F-6
CXCR2/G-1

Figure 4.14. CXCR2 knockdown in mammary carcinoma cells reduces in vivo tumor cell proliferation and survival enhanced by Tgfbr2FspKO fibroblasts.

CXCR2 shRNAs (F-6, G-1) were stably expressed in 144Epi mammary carcinoma cells, co-grafted with Tgfbr2FspKO (2SKO) fibroblasts and analyzed for changes in tumor cell proliferation and survival by immunostaining for Ki67 and cleaved caspase 3 on tumor tissues at 60 days (N=8/group).

Discussion

Fibroblasts are one of the most important components in tumor microenvironment, and carcinoma-associated fibroblasts have been shown to promote tumor progression in a variety of cancers. Our previous studies demonstrated that TGF-β signaling deficient mammary fibroblasts (2SKO) promote tumor progression with enhanced expression of CXCL1 at mRNA levels, and that TGF-β signaling negatively regulates expression of CXCL1 at transcription and protein levels in mammary fibroblasts. To understand the mechanisms through which carcinoma-associated fibroblasts promote mammary tumor progression in the context of TGF-β signaling, we characterized the role of autocrine and fibroblast-derived paracrine CXCL1 signaling in breast cancer progression *in vitro* and *in vivo*.

In these studies, we demonstrate that CXCL1 exhibits higher expression in cytokeratin 14 (CK14) positive basal-like 4T1 mammary carcinoma cells than the cytokeratin 18 (CK18) positive luminal 144Epi mammary carcinoma cells. In addition, we found that CXCR2 show higher expression both on cell surface and intracellular on basal-like MDA-MB231 human breast cancer cells than luminal MCF-7 cells and normal-like MCF-10A breast epithelial cells. These observations suggest that the expression of CXCL1/CXCR2 signaling components were significantly up-regulated in both human and mouse basal-like breast cancer cells in different manners, associated with enhanced invasiveness and tumorgenicity. Furthermore, we show that CXCL1 stimulate breast cancer cell invasion corresponding to activation of similar signaling pathways such as NF-κB pathways in both human and mouse breast cancer cells. These studies suggest that understanding the role of aberrant CXCL1/CXCR2 signaling in mammary carcinoma may help develop novel therapeutic strategies targeting CXCL1/CXCR2 signaling.

Treatment with different amounts (up to 80 ng/ml) of recombinant CXCL1 had no significant effect on MCF-7 breast cancer cell proliferation but remarkably promoted cell survival in a dose-dependent manner under serum free conditions (Figure 4.15). Similar results on cell survival were achieved in 144Epi PyVmT mouse mammary carcinoma cell (Figure 4.16). These results are consistent with published studies, in which CL66 and 4T1 mouse mammary carcinoma cells treated with CXCR2 inhibitors showed no significant differences in cell proliferation *in vitro* (192). It was shown that shRNA knockdown of CXCR2 expression in 4T1 mouse mammary carcinoma cells significantly lowered number of cells invading through Matrigel (192). In our studies, inhibition of CXCL1 secretion by siRNA transfection significantly reduced 4T1 cell invasion. Interestingly, we did not observe significant changes of cell invasion in luminal 144Epi PyVmT cells when either CXCL1 or CXCR2 was knocked down (data not shown). These data indicate that autocrine CXCL1/CXCR2 signaling is restrictedly essential for basal-like mammary carcinoma cell invasion.

CXCL1 expression was significantly elevated in invasive ductal carcinoma stroma and in mammary carcinoma associated fibroblasts. Using multiple approaches, we analyzed the functional contribution of enhanced CXCL1 expression in 41CAF cell line on mammary carcinoma cell invasion. Blockade of paracrine CXCL1 signaling in 41CAFs significantly reduced cell invasion in both 144Epi and 4T1 cells. However, while inhibition of both autocrine and paracrine CXCL1 signaling further suppressed 144Epi luminal mammary carcinoma cell invasion, further inhibitory effect on cell invasion was not observed in 4T1 basal-like mammary carcinoma cells (Figure 4.9). Considering the relative expression levels of CXCL1 in these carcinoma cells and CAFs, we may conclude that luminal carcinoma cells secrete lower levels of CXCL1 than basal-like carcinoma cells thus are more responsive to paracrine CXCL1 signaling from CAFs.

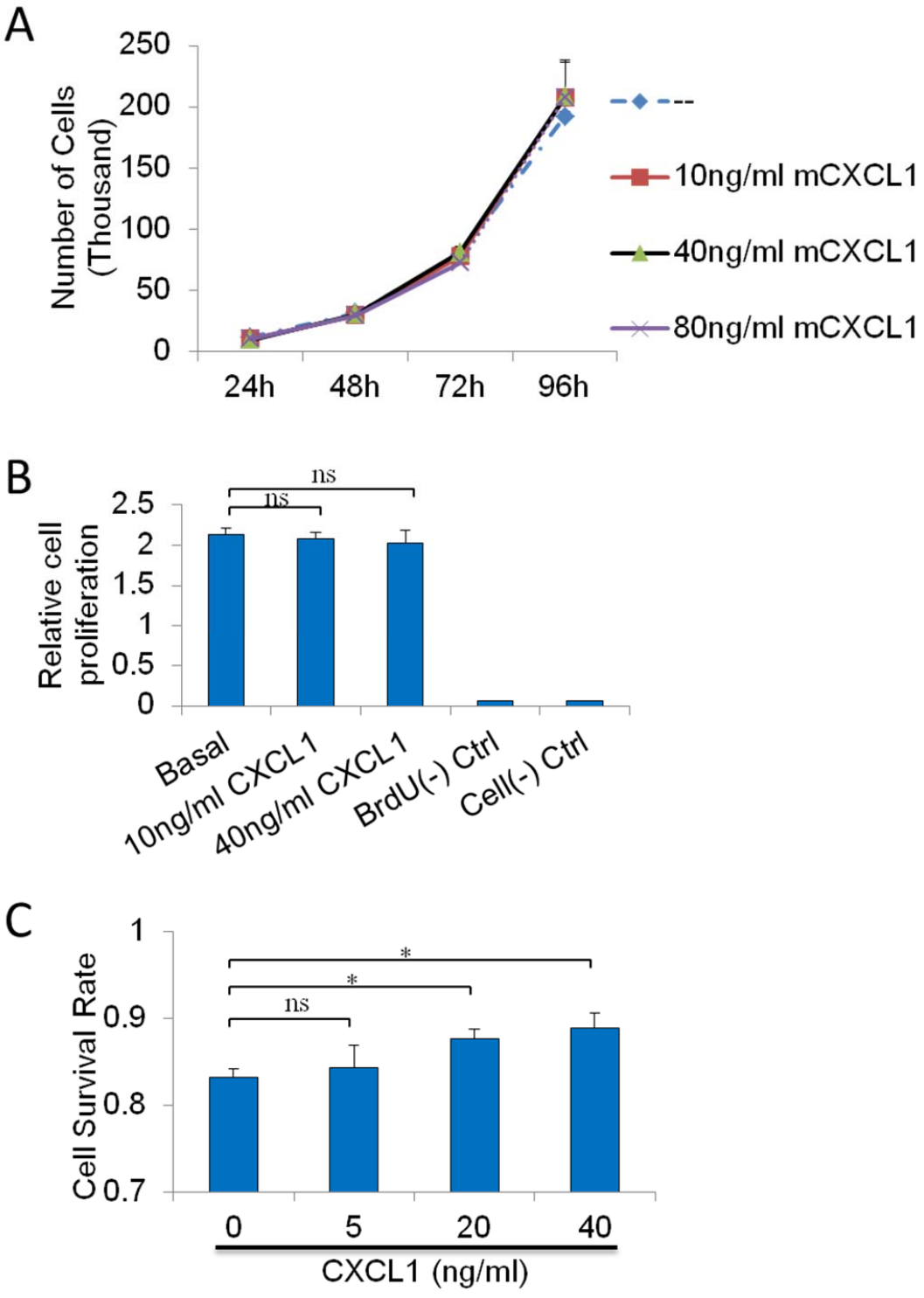
A
Number of Cells (Thousand)
250
200
150
100
50
0
24h
48h
72h
96h
--
10ng/ml mCXCL1
40ng/ml mCXCL1
80ng/ml mCXCL1
B
Relative cell proliferation
2.5
2
1.5
1
0.5
0
ns
ns
Basal
10ng/ml CXCL1
40ng/ml CXCL1
BrdU(-) Ctrl
Cell(-) Ctrl
C
Cell Survival Rate
1
0.9
0.8
0.7
*
*
ns
0
5
20
40
CXCL1 (ng/ml)

Figure 4.15. CXCL1 promotes MCF-7 breast cancer cell survival but has no significant effect on cell proliferation.

(A) MCF-7 cells were seeded in 24 well plate in cell growth media (DMEM+10%FBS) for indicated time periods and manually counted. (*B*) MCF-7 cells were assayed for changes in cell proliferation by BrdU incorporation assay for 24 hours. (*C*) MCF-7 cells were seeded in 24 well plate in DMEM for 48 hours and stained with trypan blue. Pictures were taken at multiple fields. Viable and dead cells were manually counted. Statistical significance was determined by $p<0.05$. not significant (ns), $p>0.05$; *, $p<0.05$. Values are expressed as Mean ± SEM.

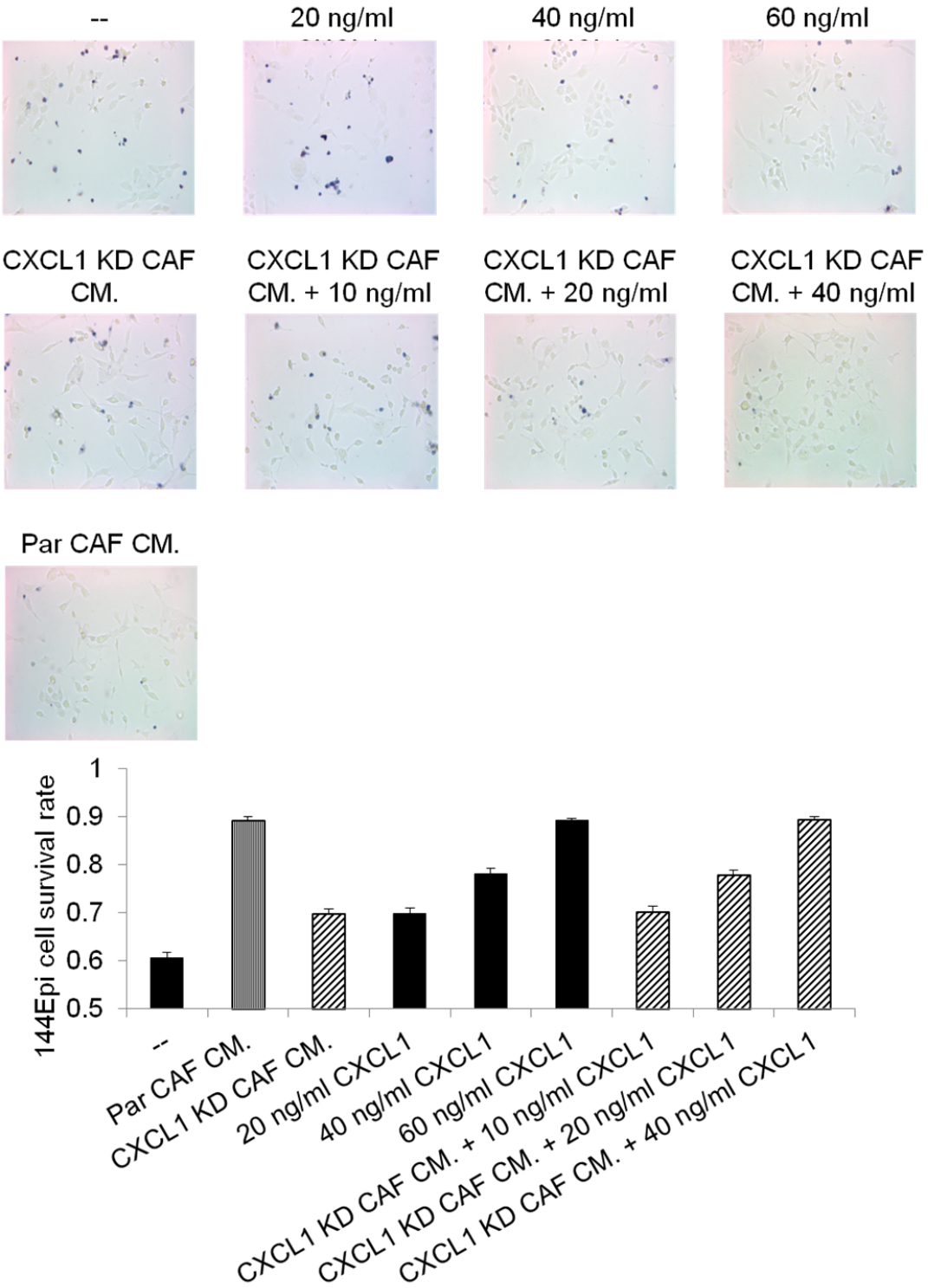
--
20 ng/ml
40 ng/ml
60 ng/ml
CXCL1 KD CAF CM.
CXCL1 KD CAF CM. + 10 ng/ml
CXCL1 KD CAF CM. + 20 ng/ml
CXCL1 KD CAF CM. + 40 ng/ml
Par CAF CM.
144Epi cell survival rate
1
0.9
0.8
0.7
0.6
0.5
--
Par CAF CM.
CXCL1 KD CAF CM.
20 ng/ml CXCL1
40 ng/ml CXCL1
60 ng/ml CXCL1
CXCL1 KD CAF CM. + 10 ng/ml CXCL1
CXCL1 KD CAF CM. + 20 ng/ml CXCL1
CXCL1 KD CAF CM. + 40 ng/ml CXCL1

Figure 4.16. CAF derived CXCL1 promotes mammary carcinoma cell survival in a dose-dependent manner.

144Epi PyVmT cells were seeded in 6-well plate in DMEM with or without CAF conditioned media or recombinant CXCL1 as indicated. At 48 hours, cells were stained with trypan blue. Pictures were taken at multiple fields. Viable and dead cells were manually counted. Values are expressed as Mean ± SD from a representative experiment.

Tumor metastasis is a complex multi-step process involving invasion, intravasation, extravasation, distant growth and neo-vasculature development. Recent published studies indicated that inhibition of CXCR2 expression significantly inhibited lung metastasis in BALB/c mice orthotopically injected with Cl66 mouse mammary carcinoma cells at 12 weeks (192). In our studies, we have not identified any changes of lung metastasis upon blocking CXCL1 secretion from 2SKO fibroblast or diminishing CXCR2 expression in 144Epi mammary carcinoma cells. A trivial explanation for this could be that fibroblast-derived CXCL1/CXCR2 signaling plays different role *in vivo* compared to *in vitro*, in which it significantly promotes tumor cell invasion. However, this is improbable for two reasons. Firstly, formation of metastatic foci was quantified in lung tissues from grafted mice at day 60, however, the number of metastatic nodules were so low (0 to 3 for most of the groups) that we were not able to obtain conclusive results from it. Since 144Epi PyVmT cells does not have high metastatic potential compared with other metastatic mammary carcinoma cell lines such as 4T1, and that nude mouse model develop tumor and metastasis quicker than C57/BL6 mouse model, it is conceivable that better understanding of the role for paracrine CXCL1 signaling on mammary tumor metastasis could be gained using nude mice model, in which 4T1 cells are co-grafted with high CXCL1 expressing Tgfbr2 FspKO (2SKO) fibroblasts with appropriate controls. Secondly, even though there are no significant changes of lung metastasis in vivo as the current data indicate, it is possible that CXCL1/CXCR2 signaling plays a more important role in local cell invasion, therefore, we are not likely to observe significant changes of distant (lung) metastasis within the period of time (60 days). To address this hypothesis, future studies may involve examining the effect of blocking paracrine CXCL1/CXCR2 signaling between mammary fibroblast and carcinoma cells on tumor cell local invasion, which can be determined by H/E staining on primary tumors and marginal mammary gland tissues.

Chapter V: Future Directions and Concluding Remarks

It has been shown that patients who are diagnosed with localized breast cancers have more than 94% chance of survival, underlining the importance of early detection. Two of the most commonly used screening methods for breast cancer is physical examination of the breasts by healthcare provider and mammography, which offers an approximate likelihood whether a lump is cancer or not. Other options include microscopic analysis of tissue sample (or biopsy), special imaging by ultrasound or MRI. After accurate diagnosis of breast cancer, it is important to clarify the histopathology, grade, stage and receptor status of breast cancer. This will be based on immunohistochemistry staining for specific prognostic markers, and possibly PET or CT scans. In addition, various types of high-throughput DNA, RNA or protein testing including DNA microarrays, next generation sequencing (NGS) are occasionally used to further classify breast cancer subtypes. Although the accuracy of these methods have been largely improved in the last few decades, there are still some weaknesses. For instance, PET or CT scans have procedures exposing patient to substantial amount of potentially dangerous ionizing radiation, and thus may outweigh the possible benefits especially in breast cancer cases with low risk for metastasis (193). DNA microarrays, NGS take longer time to get the results and are still costly compared with other traditional prognostic approaches, and the different biological significance of gene expression between DNA/RNA levels and protein levels further weakens the clinical application for accurate prognosis. The present dissertation reveal that elevated CXCL1 expression in breast tumor stroma is associated with invasive ductal carcinoma, correlates with high recurrence and poor survival outcome, and is independent of currently applied prognostic markers. Therefore, breast cancer stroma CXCL1 expression determined by immunohistochemistry staining may have great potential to be adopted in breast cancer prognosis.

Previous studies focused on the role of autocrine CXCL1 signaling in tumor epithelial cells. CXCL1/CXCR2 signaling have been well studied in melanoma tumorigenesis, and more studies have revealed its important role in the progression of other invasive cancers such as gastric cancer, prostate cancer and ovarian cancer. In addition, CXCL1/CXCR2 signaling in breast cancer has recently been revealed to link metastasis and chemo-resistance, in which cancer cells overexpressing CXCL1 and 2 are primed for survival in metastatic sites, where CXCL1/2 attract myeloid cells into tumor and produce chemokines such as S100A8/9 to enhance cancer cell survival (71). Although chemotherapeutic reagents kill rapid proliferating cancer cells, they triggers TNF-α expression from stromal cells, which act on tumor cells via NF-κB to enhance CXCL1/2 secretion and amplify the cell survival loop. Blockade of CXCR2 potently breaks this cycle as a chemotherapy against chemo-resistance (71). In this dissertation, we demonstrated that in breast cancer microenvironment, fibroblast is a large source of secreted CXCL1, especially in poorly differentiated high grade breast cancer stroma, and that carcinoma-associated mammary fibroblasts exhibited enhanced CXCL1 expression compared with normal mammary fibroblasts, which is necessary and sufficient to induce breast tumor cell invasion. Our studies provide new insights into current understanding of breast cancer microenvironment and demonstrate a novel mechanism of breast epithelial cell: fibroblast interactions.

Targeted therapy in combination with other therapies for breast cancer has been studied for decades, and has been proved to be effective in certain cancer subtypes. For example, Tamoxifen, an antagonist of estrogen receptor, has been commonly used for treatment for women who have been diagnosed with advanced positive estrogen receptor (ER+) breast cancer for a few decades. Although Tamoxifen may lead to some general side effects such as hot flashes, weight gain, vaginal dryness, depression, and

some rarely occurrence of increased risk of blood clots in leg and lungs, overgrowth of lining of the uterus, it has been approved to be highly effective in lowering the risk of breast cancer recurrence and prevention of breast cancer. Tamoxifen binds to estrogen receptor on the surface of breast cancer cells to block the proliferative effects of estrogen has on breast cancer cells. Additionally, for HER2 positive breast tumors, treatment of Trastuzumab (Herceptin) have been proved to be clinically effective.

Although some combination of surgery, radiation therapy and chemotherapy have been widely applied to basal-like / triple negative breast cancer (TNBC), targeted therapies for basal–like tumors has not been approved so far, partially due to the limited understanding of molecular mechanisms and targeted genes related to basal-like breast tumor pathologenesis. However, a few promising strategies targeting EGF receptor (EGFR), αB-crystallin and cyclin E have been identified (194). For example, EGFR and its downstream signaling pathways have been shown to regulate epithelial-mesenchymal transition (EMT), cell migration and invasion. In addition, half of cases of triple-negative (TNBC) breast cancer and inflammatory breast cancer (IBC) overexpress EGFR, making EGFR-targeted therapy a promising strategy to pursue (195). Another example is the use of cisplatin in breast cancer treatment. In particular forms of TNBC, p63 and p73 were overexpressed. Studies have shown that cisplatin, a plantinum-containing anti-cancer drug, can break up the binding of p63 and p73 to induce DNA crosslinking, which leads to failure of DNA repair and ultimately triggers apoptosis of cancer cells. Although cisplatin is effective in many types of cancer, especially in testicular cancer (cure rate improved from 10% to 85%), it has some serious deficiencies for breast cancer treatment. The majority of breast cancer patients treated with cisplatin eventually relapse with cisplatin-resistant disease. Some mechanisms including changes in drug uptake and efflux have been proposed, yet more specifically studies found that

expression patterns of p63 and p73 in breast cancer patients may dictate the effectiveness of cisplatin treatment.

In this dissertation, we have characterized a correlation between CXCR2 expression patterns and breast cancer cell subtypes. We found that higher CXCR2 expression is associated with basal-like / TNBC breast cancer cells other than luminal or normal breast epithelial cells. In addition, we have found that while no significant difference in CXCR2 expression patterns among mouse mammary carcinoma cell lines were observed, enhanced CXCL1 expression is correlated with highly invasive basal-like 4T1 cells other than luminal and normal like epithelial cells, and that CXCL1 is also up-regulated in mouse mammary CAFs compared with NAFs. Moreover, our studies have indicated that while autocrine CXCL1 signaling is required for tumor cell invasion in high CXCL1 expressing mammary carcinoma cells, paracrine CXCL1 signaling from CAFs more potently induce mammary carcinoma cell invasion in a CXCR2-dependent manner. Taken together, our studies provide sufficient evidences that autocrine and paracrine CXCL1 signaling was enhanced in basal-like breast cancer cells, and promotes breast cancer cell invasion and tumor growth. Therefore, targeting breast cancer epithelial cells: fibroblasts interactions by blocking CXCL1/CXCR2 signaling may be of great therapeutic potential.

The success of Her2/neu antibody Trastuzumab for treatment of HER2+ metastatic breast cancer and of the ABL inhibitor imatinib for the treatment of BCR-ABL translocation bearing chronic myelogenous leukemia has validated the essential role and great potential as “druggable” target of protein kinase family (196). In 1998, the first CXCR2 non-peptide inhibitor SB22502 was identified to inhibit CXCL1/CXCL8 dependent neutrophil chemotaxis *in vivo* (197). Till now, many CXCR2 inhibitors are tested in animal models and clinical trials and promising results were obtained in lung

diseases such as asthma and COPD (72). Additionally, a team at Memorial Sloan-Kettering Cancer Center has shown that CXCR2 antagonists sensitized tumors to chemotherapy in mice with metastatic breast cancer, and additional preclinical studies are underway with the intention of moving the antagonists into clinical trials for breast cancer.

HGF is a well-known mesenchymal cell-derived paracrine cellular growth factor that targets and acts primarily on epithelial cells and endothelial cells through c-Met to regulate cell survival, growth and motility (48,49). The prevalence of HGF/c-Met pathway activation in human malignancies has driven a rapid growth in drug discovery programs targeting HGF/c-Met signaling. Till 2014, more than twenty different therapeutic agents have entered human clinical trials, including HGF monoclonal antibodies, c-Met monoclonal antibodies, and small molecule c-Met kinase inhibitors (196). A few studies have shown c-Met expression in skin and osteoarthritis (OA) synovial fibroblasts (50,51), yet HGF signaling in mammary fibroblasts has not been clearly investigated. In this dissertation, we have examined the expression of c-Met in mammary fibroblasts, and characterized the functional role of autocrine HGF signaling in regulating CXCL1 expression in fibroblast. Although studies have shown promising results of HGF/c-Met inhibition in combination with other targeted therapies, challenges still exists in developing c-Met inhibitors into useful drugs. For example, more studies are needed to determine the clinical efficacy of c-Met targeting as a single agent. And more importantly, lack of responsiveness to these therapeutic reagents have been observed in subsets of patients, which indicates the necessity for further understanding the pathologic mechanisms of HGF/c-Met signaling in cancers. In this dissertation, we have demonstrated a novel potential mechanism that enhanced HGF/c-Met signaling in mammary carcinoma-associated fibroblasts help maintain high levels of CXCL1

expression, which promotes breast cancer cell invasion and tumor progression, and that c-Met/HGF signaling is negatively regulated by TGF-β signaling in a Smad2/3-dependent manner. Taken together, these results suggest that HGF/c-Met signaling is a potential therapeutic target to control CXCL1 expression in fibroblast and thus to block CXCL1-mediated fibroblast: tumor cell interactions.

Constitutive NF-κB activation is an emerging hallmark in a variety types of cancers including melanoma, colon, pancreatic, ovarian and breast cancers. Studies in melanoma and other inflammatory diseases such as arthritis suggested that activated NF-κB contributes to enhanced expression of chemokines including CXCL1 in melanoma cells, neutrophils and cancer epithelial cells. And here we identified that CXCL1 can in turn signals to breast tumor cells to activate NF-κB activity. Taken together, these studies may suggest another interesting tumor-promoting signaling loop in terms of promoting tumor cell survival and invasion, and that examining the effect of NF-κB signaling inhibition by pharmacologic inhibitors in breast cancer progression in the context of fibroblast: tumor cell interactions will be beneficial to the development of novel target therapies for breast cancer.

In all, using multiple *in vitro* and *in vivo* models, we have summarized results demonstrating the capacity of CXCL1, which is overexpressed in breast cancer stroma especially in fibroblasts, to induce breast cancer epithelial cell survival and invasion, and modulate tumor progression. More generally, we provide insights into the field that TGF-β/Smad2,3 signaling pathways may play an anti-tumorigenic role in breast cancer through inhibition of CXCL1 secretion in mammary fibroblasts, and discussed the potential of blocking paracrine CXCL1/CXCR2 signaling pathways as a targeted therapy for treatment of basal-like breast cancer. Although blockade of the paracrine CXCL1/CXCR2 has shown promising tumor retarding effects in C57/BL6 transplantation

mouse model, more effective and feasible models with which to evaluate the potential therapeutic effect on tumor local invasion and metastasis remain to be tested.

Chapter VI: References

1. Siegel R, Ma J, Zou Z, Jemal A. Cancer statistics, 2014. CA: a cancer journal for clinicians. 2014;64(1):9-29. Epub 2014/01/09. doi: 10.3322/caac.21208. PubMed PMID: 24399786.

2. Desantis C, Ma J, Bryan L, Jemal A. Breast cancer statistics, 2013. CA: a cancer journal for clinicians. 2013. doi: 10.3322/caac.21203. PubMed PMID: 24114568.

3. Siegel R, Naishadham D, Jemal A. Cancer statistics, 2013. CA: a cancer journal for clinicians. 2013;63(1):11-30. Epub 2013/01/22. doi: 10.3322/caac.21166. PubMed PMID: 23335087.

4. De Laurentiis M, Cianniello D, Caputo R, Stanzione B, Arpino G, Cinieri S, et al. Treatment of triple negative breast cancer (TNBC): current options and future perspectives. Cancer treatment reviews. 2010;36 Suppl 3:S80-6. Epub 2010/12/07. doi: 10.1016/S0305-7372(10)70025-6. PubMed PMID: 21129616.

5. Rodler E, Korde L, Gralow J. Current treatment options in triple negative breast cancer. Breast disease. 2010;32(1-2):99-122. Epub 2011/07/23. doi: 10.3233/BD-2010-0304. PubMed PMID: 21778572.

6. Whiffen A, El-Tamer M, Taback B, Feldman S, Joseph KA. Predictors of breast cancer development in women with atypical ductal hyperplasia and atypical lobular hyperplasia. Annals of surgical oncology. 2011;18(2):463-7. Epub 2010/09/30. doi: 10.1245/s10434-010-1340-5. PubMed PMID: 20878246.

7. Ma XJ, Salunga R, Tuggle JT, Gaudet J, Enright E, McQuary P, et al. Gene expression profiles of human breast cancer progression. Proceedings of the National Academy of Sciences of the United States of America. 2003;100(10):5974-9. Epub 2003/04/26. doi: 10.1073/pnas.0931261100. PubMed PMID: 12714683; PubMed Central PMCID: PMC156311.

8. Masood S. Prognostic/predictive factors in breast cancer. Clinics in laboratory medicine. 2005;25(4):809-25, viii. Epub 2005/11/26. doi: 10.1016/j.cll.2005.08.012. PubMed PMID: 16308094.

9. Taneja P, Maglic D, Kai F, Zhu S, Kendig RD, Fry EA, et al. Classical and Novel Prognostic Markers for Breast Cancer and their Clinical Significance. Clinical Medicine Insights Oncology. 2010;4:15-34. Epub 2010/06/23. PubMed PMID: 20567632; PubMed Central PMCID: PMC2883240.

10. Bieche I, Chavey C, Andrieu C, Busson M, Vacher S, Le Corre L, et al. CXC chemokines located in the 4q21 region are up-regulated in breast cancer. Endocrine-related cancer. 2007;14(4):1039-52. Epub 2007/11/30. doi: 10.1677/erc.1.01301. PubMed PMID: 18045955.

11. Fujimoto H, Sangai T, Ishii G, Ikehara A, Nagashima T, Miyazaki M, et al. Stromal MCP-1 in mammary tumors induces tumor-associated macrophage infiltration

and contributes to tumor progression. Int J Cancer. 2009;125(6):1276-84. doi: 10.1002/ijc.24378. PubMed PMID: 19479998.

12. Bombonati A, Sgroi DC. The molecular pathology of breast cancer progression. The Journal of pathology. 2011;223(2):307-17. Epub 2010/12/03. doi: 10.1002/path.2808. PubMed PMID: 21125683; PubMed Central PMCID: PMC3069504.

13. Harkins B, Geyer CE, Jr. Overcoming treatment challenges in advanced breast cancer. Semin Oncol Nurs. 2007;23(4 Suppl 2):S10-6. Epub 2008/01/26. doi: S0749-2081(07)00090-3 [pii]

10.1016/j.soncn.2007.10.003. PubMed PMID: 18054677.

14. Amar S, Roy V, Perez EA. Treatment of metastatic breast cancer: looking towards the future. Breast Cancer Res Treat. 2009;114(3):413-22. Epub 2008/05/10. doi: 10.1007/s10549-008-0032-3. PubMed PMID: 18465221.

15. Romond EH, Perez EA, Bryant J, Suman VJ, Geyer CE, Jr., Davidson NE, et al. Trastuzumab plus adjuvant chemotherapy for operable HER2-positive breast cancer. The New England journal of medicine. 2005;353(16):1673-84. Epub 2005/10/21. doi: 10.1056/NEJMoa052122. PubMed PMID: 16236738.

16. Hasebe T, Tsuda H, Tsubono Y, Imoto S, Mukai K. Fibrotic focus in invasive ductal carcinoma of the breast: a histopathological prognostic parameter for tumor recurrence and tumor death within three years after the initial operation. Jpn J Cancer Res. 1997;88(6):590-9. Epub 1997/06/01. doi: S0910505097826324 [pii]. PubMed PMID: 9263537.

17. Finak G, Bertos N, Pepin F, Sadekova S, Souleimanova M, Zhao H, et al. Stromal gene expression predicts clinical outcome in breast cancer. Nature medicine. 2008;14(5):518-27. Epub 2008/04/29. doi: 10.1038/nm1764. PubMed PMID: 18438415.

18. Yamashita J, Ogawa M, Yamashita S, Nomura K, Kuramoto M, Saishoji T, et al. Immunoreactive hepatocyte growth factor is a strong and independent predictor of recurrence and survival in human breast cancer. Cancer Res. 1994;54(7):1630-3. PubMed PMID: 8137271.

19. Ahn S, Cho J, Sung J, Lee JE, Nam SJ, Kim KM, et al. The prognostic significance of tumor-associated stroma in invasive breast carcinoma. Tumour Biol. 2012;33(5):1573-80. doi: 10.1007/s13277-012-0411-6. PubMed PMID: 22581521.

20. Joyce JA, Pollard JW. Microenvironmental regulation of metastasis. Nature reviews Cancer. 2009;9(4):239-52. Epub 2009/03/13. doi: 10.1038/nrc2618. PubMed PMID: 19279573; PubMed Central PMCID: PMC3251309.

21. Quail DF, Joyce JA. Microenvironmental regulation of tumor progression and metastasis. Nature medicine. 2013;19(11):1423-37. Epub 2013/11/10. doi: 10.1038/nm.3394. PubMed PMID: 24202395; PubMed Central PMCID: PMC3954707.

22. Rodier F, Campisi J. Four faces of cellular senescence. The Journal of cell biology. 2011;192(4):547-56. Epub 2011/02/16. doi: 10.1083/jcb.201009094. PubMed PMID: 21321098; PubMed Central PMCID: PMC3044123.

23. Kalluri R, Zeisberg M. Fibroblasts in cancer. Nature reviews Cancer. 2006;6(5):392-401. Epub 2006/03/31. doi: 10.1038/nrc1877. PubMed PMID: 16572188.

24. Simian M, Hirai Y, Navre M, Werb Z, Lochter A, Bissell MJ. The interplay of matrix metalloproteinases, morphogens and growth factors is necessary for branching of mammary epithelial cells. Development. 2001;128(16):3117-31. Epub 2001/11/02. PubMed PMID: 11688561; PubMed Central PMCID: PMC2785713.

25. Wiseman BS, Werb Z. Stromal effects on mammary gland development and breast cancer. Science. 2002;296:1046-9.

26. Polyak K, Kalluri R. The role of the microenvironment in mammary gland development and cancer. Cold Spring Harb Perspect Biol. 2010;2(11):a003244. Epub 2010/07/02. doi: 10.1101/cshperspect.a003244. PubMed PMID: 20591988.

27. Polanska UM, Orimo A. Carcinoma-associated fibroblasts: non-neoplastic tumour-promoting mesenchymal cells. Journal of cellular physiology. 2013;228(8):1651-7. Epub 2013/03/06. doi: 10.1002/jcp.24347. PubMed PMID: 23460038.

28. Ostman A, Augsten M. Cancer-associated fibroblasts and tumor growth--bystanders turning into key players. Current opinion in genetics & development. 2009;19(1):67-73. doi: 10.1016/j.gde.2009.01.003. PubMed PMID: 19211240.

29. Hasebe T, Mukai K, Tsuda H, Ochiai A. New prognostic histological parameter of invasive ductal carcinoma of the breast: clinicopathological significance of fibrotic focus. Pathol Int. 2000;50(4):263-72. PubMed PMID: 10849311.

30. Anastassiades OT, Pryce DM. Fibrosis as in indication of time in infiltrating breast cancer and its importance in prognosis. Br J Cancer. 1974;29(3):232-9. PubMed PMID: 4364382; PubMed Central PMCID: PMC2009096.

31. Mezi S, Aloise G, Marzullo A, Marchei P, Di Benedetto A, Modica A, et al. [Prognostic significance of desmoplasia in breast carcinoma. A preliminary clinical study]. Il Giornale di chirurgia. 1997;18(5):263-8. PubMed PMID: 9312252.

32. Goss P, Parsons PG. The effect of hyperthermia and melphalan on survival of human fibroblast strains and melanoma cell lines. Cancer research. 1977;37(1):152-6. Epub 1977/01/01. PubMed PMID: 830403.

33. Lotti F, Jarrar AM, Pai RK, Hitomi M, Lathia J, Mace A, et al. Chemotherapy activates cancer-associated fibroblasts to maintain colorectal cancer-initiating cells by IL-17A. J Exp Med. 2013;210(13):2851-72. doi: 10.1084/jem.20131195. PubMed PMID: 24323355; PubMed Central PMCID: PMC3865474.

34. Sun Y, Campisi J, Higano C, Beer TM, Porter P, Coleman I, et al. Treatment-induced damage to the tumor microenvironment promotes prostate cancer therapy resistance through WNT16B. Nat Med. 2012;18(9):1359-68. doi: 10.1038/nm.2890. PubMed PMID: 22863786; PubMed Central PMCID: PMC3677971.

35. Loeffler M, Kruger JA, Niethammer AG, Reisfeld RA. Targeting tumor-associated fibroblasts improves cancer chemotherapy by increasing intratumoral drug uptake. J Clin Invest. 2006;116(7):1955-62. doi: 10.1172/JCI26532. PubMed PMID: 16794736; PubMed Central PMCID: PMC1481657.

36. Brennen WN, Rosen DM, Wang H, Isaacs JT, Denmeade SR. Targeting carcinoma-associated fibroblasts within the tumor stroma with a fibroblast activation protein-activated prodrug. J Natl Cancer Inst. 2012;104(17):1320-34. doi: 10.1093/jnci/djs336. PubMed PMID: 22911669; PubMed Central PMCID: PMC3529592.

37. Narra K, Mullins SR, Lee HO, Strzemkowski-Brun B, Magalong K, Christiansen VJ, et al. Phase II trial of single agent Val-boroPro (Talabostat) inhibiting Fibroblast Activation Protein in patients with metastatic colorectal cancer. Cancer Biol Ther. 2007;6(11):1691-9. PubMed PMID: 18032930.

38. Hofheinz RD, al-Batran SE, Hartmann F, Hartung G, Jager D, Renner C, et al. Stromal antigen targeting by a humanised monoclonal antibody: an early phase II trial of sibrotuzumab in patients with metastatic colorectal cancer. Onkologie. 2003;26(1):44-8. Epub 2003/03/08. doi: 10.1159/000069863

ONK26044 [pii]. PubMed PMID: 12624517.

39. Vered M, Dayan D, Yahalom R, Dobriyan A, Barshack I, Bello IO, et al. Cancer-associated fibroblasts and epithelial-mesenchymal transition in metastatic oral tongue squamous cell carcinoma. International journal of cancer Journal international du cancer. 2010;127(6):1356-62. Epub 2010/03/27. doi: 10.1002/ijc.25358. PubMed PMID: 20340130.

40. Sakai N, Tager AM. Fibrosis of two: Epithelial cell-fibroblast interactions in pulmonary fibrosis. Biochimica et biophysica acta. 2013;1832(7):911-21. Epub 2013/03/19. doi: 10.1016/j.bbadis.2013.03.001. PubMed PMID: 23499992; PubMed Central PMCID: PMC4041487.

41. Parrinello S, Coppe JP, Krtolica A, Campisi J. Stromal-epithelial interactions in aging and cancer: senescent fibroblasts alter epithelial cell differentiation. Journal of cell science. 2005;118(Pt 3):485-96. Epub 2005/01/20. doi: 10.1242/jcs.01635. PubMed PMID: 15657080.

42. Rinehart CA, Torti VR. Aging and cancer: the role of stromal interactions with epithelial cells. Molecular carcinogenesis. 1997;18(4):187-92. Epub 1997/04/01. PubMed PMID: 9142212.

43. DePinho RA. The age of cancer. Nature. 2000;408(6809):248-54. Epub 2000/11/23. doi: 10.1038/35041694. PubMed PMID: 11089982.

44. Olumi AF, Grossfeld GD, Hayward SW, Carroll PR, Tlsty TD, Cunha GR. Carcinoma-associated fibroblasts direct tumor progression of initiated human prostatic epithelium. Cancer research. 1999;59(19):5002-11. Epub 1999/10/16. PubMed PMID: 10519415.

45. Liao CP, Adisetiyo H, Liang M, Roy-Burman P. Cancer-associated fibroblasts enhance the gland-forming capability of prostate cancer stem cells. Cancer research. 2010;70(18):7294-303. Epub 2010/09/03. doi: 10.1158/0008-5472.CAN-09-3982. PubMed PMID: 20807814; PubMed Central PMCID: PMC2940948.

46. {Balkwill B, F. R. The chemokine system and cancer. The Journal of pathology. 2012;226(2):148-57. doi: 10.1002/path.3029. PubMed PMID: 21989643.

47. White GE, Iqbal AJ, Greaves DR. CC chemokine receptors and chronic inflammation--therapeutic opportunities and pharmacological challenges. Pharmacol Rev. 2013;65(1):47-89. doi: 10.1124/pr.111.005074. PubMed PMID: 23300131.

48. Greaves NS, Ashcroft KJ, Baguneid M, Bayat A. Current understanding of molecular and cellular mechanisms in fibroplasia and angiogenesis during acute wound healing. J Dermatol Sci. 2013;72(3):206-17. doi: 10.1016/j.jdermsci.2013.07.008. PubMed PMID: 23958517.

49. Strieter RM, Polverini PJ, Kunkel SL, Arenberg DA, Burdick MD, Kasper J, et al. The functional role of the ELR motif in CXC chemokine-mediated angiogenesis. The Journal of biological chemistry. 1995;270(45):27348-57. Epub 1995/11/10. PubMed PMID: 7592998.

50. Strieter RM, Belperio JA, Burdick MD, Keane MP. CXC chemokines in angiogenesis relevant to chronic fibroproliferation. Current drug targets Inflammation and allergy. 2005;4(1):23-6. PubMed PMID: 15720231.

51. Stillie R, Farooq SM, Gordon JR, Stadnyk AW. The functional significance behind expressing two IL-8 receptor types on PMN. J Leukoc Biol. 2009;86(3):529-43. doi: 10.1189/jlb.0208125. PubMed PMID: 19564575.

52. Haskill S, Peace A, Morris J, Sporn SA, Anisowicz A, Lee SW, et al. Identification of three related human GRO genes encoding cytokine functions. Proceedings of the National Academy of Sciences of the United States of America. 1990;87(19):7732-6. Epub 1990/10/01. PubMed PMID: 2217207; PubMed Central PMCID: PMC54822.

53. Holmes WE, Lee J, Kuang WJ, Rice GC, Wood WI. Structure and functional expression of a human interleukin-8 receptor. Science. 1991;253(5025):1278-80. Epub 1991/09/13. PubMed PMID: 1840701.

54. Reutershan J. CXCR2--the receptor to hit? Drug news & perspectives. 2006;19(10):615-23. Epub 2007/02/15. doi: 10.1358/dnp.2006.19.10.1068009. PubMed PMID: 17299604.

55. Nasser MW, Raghuwanshi SK, Malloy KM, Gangavarapu P, Shim JY, Rajarathnam K, et al. CXCR1 and CXCR2 activation and regulation. Role of aspartate 199 of the second extracellular loop of CXCR2 in CXCL8-mediated rapid receptor internalization. The Journal of biological chemistry. 2007;282(9):6906-15. Epub 2007/01/06. doi: 10.1074/jbc.M610289200. PubMed PMID: 17204468.

56. Rajagopalan L, Rajarathnam K. Ligand selectivity and affinity of chemokine receptor CXCR1. Role of N-terminal domain. The Journal of biological chemistry. 2004;279(29):30000-8. Epub 2004/05/11. doi: 10.1074/jbc.M313883200. PubMed PMID: 15133028.

57. Richmond A, Yang J, Su Y. The good and the bad of chemokines/chemokine receptors in melanoma. Pigment cell & melanoma research. 2009;22(2):175-86. Epub 2009/02/19. doi: 10.1111/j.1755-148X.2009.00554.x. PubMed PMID: 19222802; PubMed Central PMCID: PMC2848967.

58. Milliken D, Scotton C, Raju S, Balkwill F, Wilson J. Analysis of chemokines and chemokine receptor expression in ovarian cancer ascites. Clinical cancer research : an official journal of the American Association for Cancer Research. 2002;8(4):1108-14. Epub 2002/04/12. PubMed PMID: 11948121.

59. Blum DL, Koyama T, M'Koma AE, Iturregui JM, Martinez-Ferrer M, Uwamariya C, et al. Chemokine markers predict biochemical recurrence of prostate cancer following prostatectomy. Clinical cancer research : an official journal of the American Association for Cancer Research. 2008;14(23):7790-7. Epub 2008/12/03. doi: 10.1158/1078-0432.CCR-08-1716. PubMed PMID: 19047106; PubMed Central PMCID: PMC3050736.

60. Kuo PL, Huang MS, Hung JY, Chou SH, Chiang SY, Huang YF, et al. Synergistic effect of lung tumor-associated dendritic cell-derived HB-EGF and CXCL5 on cancer progression. Int J Cancer. 2013. doi: 10.1002/ijc.28673. PubMed PMID: 24346967.

61. Zhou SL, Dai Z, Zhou ZJ, Chen Q, Wang Z, Xiao YS, et al. CXCL5 contributes to tumor metastasis and recurrence of intrahepatic cholangiocarcinoma by recruiting infiltrative intratumoral neutrophils. Carcinogenesis. 2014. doi: 10.1093/carcin/bgt397. PubMed PMID: 24293410.

62. Balkwill F. Cancer and the chemokine network. Nature reviews Cancer. 2004;4(7):540-50. Epub 2004/07/02. doi: 10.1038/nrc1388. PubMed PMID: 15229479.

63. Kakinuma T, Hwang ST. Chemokines, chemokine receptors, and cancer metastasis. Journal of leukocyte biology. 2006;79(4):639-51. Epub 2006/02/16. doi: 10.1189/jlb.1105633. PubMed PMID: 16478915.

64. Dhawan P, Richmond A. Role of CXCL1 in tumorigenesis of melanoma. Journal of leukocyte biology. 2002;72(1):9-18. Epub 2002/07/09. PubMed PMID: 12101257; PubMed Central PMCID: PMC2668262.

65. Payne AS, Cornelius LA. The role of chemokines in melanoma tumor growth and metastasis. J Invest Dermatol. 2002;118(6):915-22. PubMed PMID: 12060384.

66. Vazquez-Martin A, Colomer R, Menendez JA. Protein array technology to detect HER2 (erbB-2)-induced 'cytokine signature' in breast cancer. Eur J Cancer. 2007;43(7):1117-24. Epub 2007/03/24. doi: 10.1016/j.ejca.2007.01.037. PubMed PMID: 17379503.

67. Li J, Sidell N. Growth-related oncogene produced in human breast cancer cells and regulated by Syk protein-tyrosine kinase. Int J Cancer. 2005;117(1):14-20. PubMed PMID: 15880583.

68. Divella R, Daniele A, Savino E, Palma F, Bellizzi A, Giotta F, et al. Circulating levels of transforming growth factor-betaeta (TGF-beta) and chemokine (C-X-C motif) ligand-1 (CXCL1) as predictors of distant seeding of circulating tumor cells in patients with metastatic breast cancer. Anticancer Res. 2013;33(4):1491-7. PubMed PMID: 23564790.

69. Karnoub AE, Dash AB, Vo AP, Sullivan A, Brooks MW, Bell GW, et al. Mesenchymal stem cells within tumour stroma promote breast cancer metastasis. Nature. 2007;449(7162):557-63. Epub 2007/10/05. doi: 10.1038/nature06188. PubMed PMID: 17914389.

70. Orimo A, Gupta PB, Sgroi DC, Arenzana-Seisdedos F, Delaunay T, Naeem R, et al. Stromal fibroblasts present in invasive human breast carcinomas promote tumor growth and angiogenesis through elevated SDF-1/CXCL12 secretion. Cell. 2005;121(3):335-48. Epub 2005/05/11. doi: 10.1016/j.cell.2005.02.034. PubMed PMID: 15882617.

71. Acharyya S, Oskarsson T, Vanharanta S, Malladi S, Kim J, Morris PG, et al. A CXCL1 paracrine network links cancer chemoresistance and metastasis. Cell. 2012;150(1):165-78. Epub 2012/07/10. doi: 10.1016/j.cell.2012.04.042. PubMed PMID: 22770218; PubMed Central PMCID: PMC3528019.

72. Stadtmann A, Zarbock A. CXCR2: From Bench to Bedside. Frontiers in immunology. 2012;3:263. Epub 2012/09/01. doi: 10.3389/fimmu.2012.00263. PubMed PMID: 22936934; PubMed Central PMCID: PMC3426767.

73. Sunahara RK, Dessauer CW, Gilman AG. Complexity and diversity of mammalian adenylyl cyclases. Annual review of pharmacology and toxicology. 1996;36:461-80. Epub 1996/01/01. doi: 10.1146/annurev.pa.36.040196.002333. PubMed PMID: 8725398.

74. Varnai P, Rother KI, Balla T. Phosphatidylinositol 3-kinase-dependent membrane association of the Bruton's tyrosine kinase pleckstrin homology domain visualized in single living cells. The Journal of biological chemistry. 1999;274(16):10983-9. Epub 1999/04/10. PubMed PMID: 10196179.

75. Servant G, Weiner OD, Herzmark P, Balla T, Sedat JW, Bourne HR. Polarization of chemoattractant receptor signaling during neutrophil chemotaxis. Science. 2000;287(5455):1037-40. Epub 2000/02/11. PubMed PMID: 10669415; PubMed Central PMCID: PMC2822871.

76. Glogauer M, Marchal CC, Zhu F, Worku A, Clausen BE, Foerster I, et al. Rac1 deletion in mouse neutrophils has selective effects on neutrophil functions. J Immunol. 2003;170(11):5652-7. Epub 2003/05/22. PubMed PMID: 12759446.

77. Gu Y, Filippi MD, Cancelas JA, Siefring JE, Williams EP, Jasti AC, et al. Hematopoietic cell regulation by Rac1 and Rac2 guanosine triphosphatases. Science. 2003;302(5644):445-9. Epub 2003/10/18. doi: 10.1126/science.1088485. PubMed PMID: 14564009.

78. Massague J, Seoane J, Wotton D. Smad transcription factors. Genes & development. 2005;19(23):2783-810. Epub 2005/12/03. doi: 10.1101/gad.1350705. PubMed PMID: 16322555.

79. Derynck R, Akhurst RJ, Balmain A. TGF-beta signaling in tumor suppression and cancer progression. Nature genetics. 2001;29(2):117-29. Epub 2001/10/05. doi: 10.1038/ng1001-117. PubMed PMID: 11586292.

80. Jedeszko C, Victor BC, Podgorski I, Sloane BF. Fibroblast hepatocyte growth factor promotes invasion of human mammary ductal carcinoma in situ. Cancer research. 2009;69(23):9148-55. Epub 2009/11/19. doi: 10.1158/0008-5472.CAN-09-1043. PubMed PMID: 19920187; PubMed Central PMCID: PMC2789178.

81. Valluru M, Staton CA, Reed MW, Brown NJ. Transforming Growth Factor-beta and Endoglin Signaling Orchestrate Wound Healing. Frontiers in physiology. 2011;2:89. Epub 2011/12/14. doi: 10.3389/fphys.2011.00089. PubMed PMID: 22164144; PubMed Central PMCID: PMC3230065.

82. Shinde AV, Frangogiannis NG. Fibroblasts in myocardial infarction: a role in inflammation and repair. Journal of molecular and cellular cardiology. 2014;70:74-82. Epub 2013/12/11. doi: 10.1016/j.yjmcc.2013.11.015. PubMed PMID: 24321195; PubMed Central PMCID: PMC3995820.

83. Kuperwasser C, Chavarria T, Wu M, Magrane G, Gray JW, Carey L, et al. Reconstruction of functionally normal and malignant human breast tissues in mice. Proceedings of the National Academy of Sciences of the United States of America. 2004;101(14):4966-71. Epub 2004/03/31. doi: 10.1073/pnas.0401064101. PubMed PMID: 15051869; PubMed Central PMCID: PMC387357.

84. Tuxhorn JA, McAlhany SJ, Yang F, Dang TD, Rowley DR. Inhibition of transforming growth factor-beta activity decreases angiogenesis in a human prostate cancer-reactive stroma xenograft model. Cancer research. 2002;62(21):6021-5. Epub 2002/11/05. PubMed PMID: 12414622.

85. Tuxhorn JA, Ayala GE, Smith MJ, Smith VC, Dang TD, Rowley DR. Reactive stroma in human prostate cancer: induction of myofibroblast phenotype and extracellular matrix remodeling. Clinical cancer research : an official journal of the American Association for Cancer Research. 2002;8(9):2912-23. Epub 2002/09/17. PubMed PMID: 12231536.

86. Fang WB, Jokar I, Chytil A, Moses HL, Abel T, Cheng N. Loss of one Tgfbr2 allele in fibroblasts promotes metastasis in MMTV: polyoma middle T transgenic and transplant mouse models of mammary tumor progression. Clinical & experimental metastasis. 2011;28(4):351-66. Epub 2011/03/05. doi: 10.1007/s10585-011-9373-0. PubMed PMID: 21374085; PubMed Central PMCID: PMC3373018.

87. Cheng N, Chytil A, Shyr Y, Joly A, Moses HL. Enhanced hepatocyte growth factor signaling by type II transforming growth factor-beta receptor knockout fibroblasts promotes mammary tumorigenesis. Cancer research. 2007;67(10):4869-77. Epub 2007/05/15. doi: 10.1158/0008-5472.CAN-06-3381. PubMed PMID: 17495323.

88. Cheng N, Bhowmick NA, Chytil A, Gorksa AE, Brown KA, Muraoka R, et al. Loss of TGF-beta type II receptor in fibroblasts promotes mammary carcinoma growth and invasion through upregulation of TGF-alpha-, MSP- and HGF-mediated signaling networks. Oncogene. 2005;24(32):5053-68. Epub 2005/04/28. doi: 10.1038/sj.onc.1208685. PubMed PMID: 15856015; PubMed Central PMCID: PMC3074577.

89. Gao MQ, Kim BG, Kang S, Choi YP, Yoon JH, Cho NH. Human breast cancer-associated fibroblasts enhance cancer cell proliferation through increased TGF-alpha cleavage by ADAM17. Cancer letters. 2013;336(1):240-6. Epub 2013/05/21. doi: 10.1016/j.canlet.2013.05.011. PubMed PMID: 23684931.

90. Liao D, Luo Y, Markowitz D, Xiang R, Reisfeld RA. Cancer associated fibroblasts promote tumor growth and metastasis by modulating the tumor immune microenvironment in a 4T1 murine breast cancer model. PloS one. 2009;4(11):e7965. Epub 2009/12/04. doi: 10.1371/journal.pone.0007965. PubMed PMID: 19956757; PubMed Central PMCID: PMC2775953.

91. Hu M, Yao J, Carroll DK, Weremowicz S, Chen H, Carrasco D, et al. Regulation of in situ to invasive breast carcinoma transition. Cancer Cell. 2008;13(5):394-406. Epub 2008/05/06. doi: S1535-6108(08)00091-3 [pii]

10.1016/j.ccr.2008.03.007. PubMed PMID: 18455123.

92. Sadlonova A, Mukherjee S, Bowe DB, Gault SR, Dumas NA, Van Tine BA, et al. Human breast fibroblasts inhibit growth of the MCF10AT xenograft model of proliferative breast disease. The American journal of pathology. 2007;170(3):1064-76. Epub 2007/02/27. doi: 10.2353/ajpath.2007.060031. PubMed PMID: 17322389; PubMed Central PMCID: PMC1864888.

93. Chen J, Li H, SundarRaj N, Wang JH. Alpha-smooth muscle actin expression enhances cell traction force. Cell Motil Cytoskeleton. 2007;64(4):248-57. Epub 2006/12/22. doi: 10.1002/cm.20178. PubMed PMID: 17183543.

94. Ronnov-Jessen L, Petersen O. Induction of alpha-smooth muscle actin by transforming factor-beta 1 in quiescent human breast gland fibroblasts. Implication for myofibroblast generation in breast neoplasia. Lab Invest. 1993;68(6):696-707.

95. Sugimoto H, Mundel TM, Kieran MW, Kalluri R. Identification of fibroblast heterogeneity in the tumor microenvironment. Cancer biology & therapy. 2006;5(12):1640-6. Epub 2006/11/16. PubMed PMID: 17106243.

96. Karagiannis GS, Saraon P, Jarvi KA, Diamandis EP. Proteomic signatures of angiogenesis in androgen-independent prostate cancer. Prostate. 2014;74(3):260-72. doi: 10.1002/pros.22747. PubMed PMID: 24166580.

97. Linder N, Konsti J, Turkki R, Rahtu E, Lundin M, Nordling S, et al. Identification of tumor epithelium and stroma in tissue microarrays using texture analysis. Diagnostic pathology. 2012;7:22. Epub 2012/03/06. doi: 10.1186/1746-1596-7-22. PubMed PMID: 22385523; PubMed Central PMCID: PMC3315400.

98. Lehr HA, van der Loos CM, Teeling P, Gown AM. Complete chromogen separation and analysis in double immunohistochemical stains using Photoshop-based image analysis. The journal of histochemistry and cytochemistry : official journal of the Histochemistry Society. 1999;47(1):119-26. Epub 1998/12/19. PubMed PMID: 9857219.

99. Finak G, Sadekova S, Pepin F, Hallett M, Meterissian S, Halwani F, et al. Gene expression signatures of morphologically normal breast tissue identify basal-like tumors. Breast Cancer Res. 2006;8(5):R58. doi: 10.1186/bcr1608. PubMed PMID: 17054791; PubMed Central PMCID: PMC1779486.

100. Guy C, Cardiff R, Muller W. Induction of mammary tumors by expression a polyomavirus middle T oncogene: a transgenic mouse model for metastatic disease. Mol Cell Biol. 1992;12:954-61.

101. Erbas B, Provenzano E, Armes J, Gertig D. The natural history of ductal carcinoma in situ of the breast: a review. Breast cancer research and treatment. 2006;97(2):135-44. Epub 2005/12/02. doi: 10.1007/s10549-005-9101-z. PubMed PMID: 16319971.

102. Yerushalmi R, Hayes MM, Gelmon KA. Breast carcinoma--rare types: review of the literature. Ann Oncol. 2009;20(11):1763-70. doi: 10.1093/annonc/mdp245. PubMed PMID: 19602565.

103. Leonard GD, Swain SM. Ductal carcinoma in situ, complexities and challenges. J Natl Cancer Inst. 2004;96(12):906-20. Epub 2004/06/17. PubMed PMID: 15199110.

104. Gallagher PG, Bao Y, Prorock A, Zigrino P, Nischt R, Politi V, et al. Gene expression profiling reveals cross-talk between melanoma and fibroblasts: implications for host-tumor interactions in metastasis. Cancer research. 2005;

65(10):4134-46. Epub 2005/05/19. doi: 10.1158/0008-5472.CAN-04-0415. PubMed PMID: 15899804.

105. Pickup M, Novitskiy S, Moses HL. The roles of TGFbeta in the tumour microenvironment. Nature reviews Cancer. 2013;13(11):788-99. Epub 2013/10/18. doi: 10.1038/nrc3603. PubMed PMID: 24132110; PubMed Central PMCID: PMC4025940.

106. Moore-Smith L, Pasche B. TGFBR1 signaling and breast cancer. J Mammary Gland Biol Neoplasia. 2011;16(2):89-95. Epub 2011/04/05. doi: 10.1007/s10911-011-9216-2. PubMed PMID: 21461994.

107. Gorska AE, Jensen RA, Shyr Y, Aakre ME, Bhowmick NA, Moses HL. Transgenic mice expressing a dominant-negative mutant type II transforming growth factor-beta receptor exhibit impaired mammary development and enhanced mammary tumor formation. Am J Pathol. 2003;163(4):1539-49. PubMed PMID: 14507660.

108. Paraiso KH, Smalley KS. Fibroblast-mediated drug resistance in cancer. Biochem Pharmacol. 2013;85(8):1033-41. doi: 10.1016/j.bcp.2013.01.018. PubMed PMID: 23376122.

109. Lu P, Vogel C, Wang R, Yao X, Marcotte EM. Absolute protein expression profiling estimates the relative contributions of transcriptional and translational regulation. Nature biotechnology. 2007;25(1):117-24. doi: 10.1038/nbt1270. PubMed PMID: 17187058.

110. Shankavaram UT, Reinhold WC, Nishizuka S, Major S, Morita D, Chary KK, et al. Transcript and protein expression profiles of the NCI-60 cancer cell panel: an integromic microarray study. Mol Cancer Ther. 2007;6(3):820-32. doi: 10.1158/1535-7163.MCT-06-0650. PubMed PMID: 17339364.

111. Gry M, Rimini R, Stromberg S, Asplund A, Ponten F, Uhlen M, et al. Correlations between RNA and protein expression profiles in 23 human cell lines. BMC genomics. 2009;10:365. doi: 10.1186/1471-2164-10-365. PubMed PMID: 19660143; PubMed Central PMCID: PMC2728742.

112. Amiri KI, Richmond A. Fine tuning the transcriptional regulation of the CXCL1 chemokine. Progress in nucleic acid research and molecular biology. 2003;74:1-36. PubMed PMID: 14510072; PubMed Central PMCID: PMC3140403.

113. Bachmeier BE, Mohrenz IV, Mirisola V, Schleicher E, Romeo F, Hohneke C, et al. Curcumin downregulates the inflammatory cytokines CXCL1 and -2 in breast cancer cells via NFkappaB. Carcinogenesis. 2008;29(4):779-89. Epub 2007/11/15. doi: 10.1093/carcin/bgm248. PubMed PMID: 17999991.

114. Gubin MM, Calaluce R, Davis JW, Magee JD, Strouse CS, Shaw DP, et al. Overexpression of the RNA binding protein HuR impairs tumor growth in triple negative breast cancer associated with deficient angiogenesis. Cell Cycle. 2010;9(16):3337-46. doi: 10.4161/cc.9.16.12711. PubMed PMID: 20724828; PubMed Central PMCID: PMC3041167.

115. Fonseca-Sanchez MA, Perez-Plasencia C, Fernandez-Retana J, Arechaga-Ocampo E, Marchat LA, Rodriguez-Cuevas S, et al. microRNA-18b is upregulated in breast cancer and modulates genes involved in cell migration. Oncology reports. 2013;30(5):2399-410. doi: 10.3892/or.2013.2691. PubMed PMID: 23970382.

116. Fan X, Chen X, Deng W, Zhong G, Cai Q, Lin T. Up-regulated microRNA-143 in cancer stem cells differentiation promotes prostate cancer cells metastasis by modulating FNDC3B expression. BMC Cancer. 2013;13:61. doi: 10.1186/1471-2407-13-61. PubMed PMID: 23383988; PubMed Central PMCID: PMC3585861.

117. Fan J, Ishmael FT, Fang X, Myers A, Cheadle C, Huang SK, et al. Chemokine transcripts as targets of the RNA-binding protein HuR in human airway epithelium. J Immunol. 2011;186(4):2482-94. doi: 10.4049/jimmunol.0903634. PubMed PMID: 21220697; PubMed Central PMCID: PMC3872785.

118. Yoo JK, Jung HY, Kim CH, Son WS, Kim JK. miR-7641 modulates the expression of CXCL1 during endothelial differentiation derived from human embryonic stem cells. Archives of pharmacal research. 2013;36(3):353-8. doi: 10.1007/s12272-013-0067-9. PubMed PMID: 23444042.

119. Pecot CV, Rupaimoole R, Yang D, Akbani R, Ivan C, Lu C, et al. Tumour angiogenesis regulation by the miR-200 family. Nature communications. 2013;4:2427. doi: 10.1038/ncomms3427. PubMed PMID: 24018975; PubMed Central PMCID: PMC3904438.

120. Poluri KM, Joseph PR, Sawant KV, Rajarathnam K. Molecular basis of glycosaminoglycan heparin binding to the chemokine CXCL1 dimer. J Biol Chem. 2013;288(35):25143-53. doi: 10.1074/jbc.M113.492579. PubMed PMID: 23864653; PubMed Central PMCID: PMC3757178.

121. Barlow J, Yandell D, Weaver D, Casey T, Plaut K. Higher stromal expression of transforming growth factor-beta type II receptors is associated with poorer prognosis breast tumors. Breast Cancer Res Treat. 2003;79(2):149-59. PubMed PMID: 12825850.

122. Meulmeester E, Ten Dijke P. The dynamic roles of TGF-beta in cancer. The Journal of pathology. 2011;223(2):205-18. Epub 2010/10/20. doi: 10.1002/path.2785. PubMed PMID: 20957627.

123. Pardali K, Moustakas A. Actions of TGF-beta as tumor suppressor and pro-metastatic factor in human cancer. Biochim Biophys Acta. 2007;1775(1):21-62. PubMed PMID: 16904831.

124. Moses H, Barcellos-Hoff MH. TGF-beta biology in mammary development and breast cancer. Cold Spring Harbor perspectives in biology. 2011;3(1):a003277. Epub 2010/09/03. doi: 10.1101/cshperspect.a003277. PubMed PMID: 20810549; PubMed Central PMCID: PMC3003461.

125. Mu L, Katsaros D, Lu L, Preti M, Durando A, Arisio R, et al. TGF-beta1 genotype and phenotype in breast cancer and their associations with IGFs and patient survival. Br J Cancer. 2008;99(8):1357-63. doi: 10.1038/sj.bjc.6604689. PubMed PMID: 18827819; PubMed Central PMCID: PMC2570529.

126. Mizukami Y, Nonomura A, Yamada T, Kurumaya H, Hayashi M, Koyasaki N, et al. Immunohistochemical demonstration of growth factors, TGF-alpha, TGF-beta, IGF-I and neu oncogene product in benign and malignant human breast tissues. Anticancer Res. 1990;10(5A):1115-26. Epub 1990/09/01. PubMed PMID: 1978632.

127. Figueroa JD, Flanders KC, Garcia-Closas M, Anderson WF, Yang XR, Matsuno RK, et al. Expression of TGF-beta signaling factors in invasive breast cancers: relationships with age at diagnosis and tumor characteristics. Breast Cancer Res Treat. 2010;121(3):727-35. doi: 10.1007/s10549-009-0590-z. PubMed PMID: 19937272.

128. de Kruijf EM, Dekker TJ, Hawinkels LJ, Putter H, Smit VT, Kroep JR, et al. The prognostic role of TGF-beta signaling pathway in breast cancer patients. Ann Oncol. 2013;24(2):384-90. doi: 10.1093/annonc/mds333. PubMed PMID: 23022998.

129. Desruisseau S, Palmari J, Giusti C, Romain S, Martin PM, Berthois Y. Determination of TGFbeta1 protein level in human primary breast cancers and its relationship with survival. Br J Cancer. 2006;94(2):239-46. doi: 10.1038/sj.bjc.6602920. PubMed PMID: 16404434; PubMed Central PMCID: PMC2361106.

130. Bascom CC, Wolfshohl JR, Coffey RJ, Jr., Madisen L, Webb NR, Purchio AR, et al. Complex regulation of transforming growth factor beta 1, beta 2, and beta 3 mRNA expression in mouse fibroblasts and keratinocytes by transforming growth factors beta 1 and beta 2. Mol Cell Biol. 1989;9(12):5508-15. PubMed PMID: 2586525; PubMed Central PMCID: PMC363721.

131. Kim SJ, Angel P, Lafyatis R, Hattori K, Kim KY, Sporn MB, et al. Autoinduction of transforming growth factor beta 1 is mediated by the AP-1 complex. Mol Cell Biol. 1990;10(4):1492-7. PubMed PMID: 2108318; PubMed Central PMCID: PMC362252.

132. Micke P, Ostman A. Exploring the tumour environment: cancer-associated fibroblasts as targets in cancer therapy. Expert Opin Ther Targets. 2005;9(6):1217-33. doi: 10.1517/14728222.9.6.1217. PubMed PMID: 16300472.

133. Berking C, Takemoto R, Schaider H, Showe L, Satyamoorthy K, Robbins P, et al. Transforming growth factor-beta1 increases survival of human melanoma through stroma remodeling. Cancer Res. 2001;61(22):8306-16. PubMed PMID: 11719464.

134. Kretzschmar M, Doody J, Timokhina I, Massague J. A mechanism of repression of TGFbeta/ Smad signaling by oncogenic Ras. Genes Dev. 1999;13(7):804-16. PubMed PMID: 10197981; PubMed Central PMCID: PMC316599.

135. Matsumura N, Huang Z, Mori S, Baba T, Fujii S, Konishi I, et al. Epigenetic suppression of the TGF-beta pathway revealed by transcriptome profiling in ovarian cancer. Genome research. 2011;21(1):74-82. doi: 10.1101/gr.108803.110. PubMed PMID: 21156726; PubMed Central PMCID: PMC3012928.

136. Hinshelwood RA, Huschtscha LI, Melki J, Stirzaker C, Abdipranoto A, Vissel B, et al. Concordant epigenetic silencing of transforming growth factor-beta signaling pathway genes occurs early in breast carcinogenesis. Cancer research. 2007;67(24):11517-27. Epub 2007/12/20. doi: 10.1158/0008-5472.CAN-07-1284. PubMed PMID: 18089780.

137. Allinen M, Beroukhim R, Cai L, Brennan C, Lahti-Domenici J, Huang H, et al. Molecular characterization of the tumor microenvironment in breast cancer. Cancer cell. 2004;6(1):17-32. Epub 2004/07/21. doi: 10.1016/j.ccr.2004.06.010. PubMed PMID: 15261139.

138. Frings O, Augsten M, Tobin NP, Carlson J, Paulsson J, Pena C, et al. Prognostic significance in breast cancer of a gene signature capturing stromal PDGF signaling. The American journal of pathology. 2013;182(6):2037-47. Epub 2013/04/16. doi: 10.1016/j.ajpath.2013.02.018. PubMed PMID: 23583284.

139. Zaja-Milatovic S, Richmond A. CXC chemokines and their receptors: a case for a significant biological role in cutaneous wound healing. Histology and histopathology. 2008;23(11):1399-407. Epub 2008/09/12. PubMed PMID: 18785122; PubMed Central PMCID: PMC3140405.

140. Kobayashi Y. The role of chemokines in neutrophil biology. Frontiers in bioscience : a journal and virtual library. 2008;13:2400-7. Epub 2007/11/06. PubMed PMID: 17981721.

141. Luan J, Shattuck-Brandt R, Haghnegahdar H, Owen JD, Strieter R, Burdick M, et al. Mechanism and biological significance of constitutive expression of MGSA/GRO

chemokines in malignant melanoma tumor progression. Journal of leukocyte biology. 1997;62(5):588-97. Epub 1997/11/19. PubMed PMID: 9365113.

142. Miyake M, Lawton A, Goodison S, Urquidi V, Rosser CJ. Chemokine (C-X-C motif) ligand 1 (CXCL1) protein expression is increased in high-grade prostate cancer. Pathology, research and practice. 2014;210(2):74-8. Epub 2013/11/21. doi: 10.1016/j.prp.2013.08.013. PubMed PMID: 24252309.

143. Kawanishi H, Matsui Y, Ito M, Watanabe J, Takahashi T, Nishizawa K, et al. Secreted CXCL1 is a potential mediator and marker of the tumor invasion of bladder cancer. Clinical cancer research : an official journal of the American Association for Cancer Research. 2008;14(9):2579-87. Epub 2008/05/03. doi: 10.1158/1078-0432.CCR-07-1922. PubMed PMID: 18451219.

144. Datto MB, Frederick JP, Pan L, Borton AJ, Zhuang Y, Wang XF. Targeted disruption of Smad3 reveals an essential role in transforming growth factor beta-mediated signal transduction. Molecular and cellular biology. 1999;19(4):2495-504. Epub 1999/03/19. PubMed PMID: 10082515; PubMed Central PMCID: PMC84042.

145. Inman GJ, Hill CS. Stoichiometry of active smad-transcription factor complexes on DNA. The Journal of biological chemistry. 2002;277(52):51008-16. Epub 2002/10/11. doi: 10.1074/jbc.M208532200. PubMed PMID: 12374795.

146. Jayaraman L, Massague J. Distinct oligomeric states of SMAD proteins in the transforming growth factor-beta pathway. The Journal of biological chemistry. 2000;275(52):40710-7. Epub 2000/10/06. doi: 10.1074/jbc.M005799200. PubMed PMID: 11018029.

147. Wu JW, Fairman R, Penry J, Shi Y. Formation of a stable heterodimer between Smad2 and Smad4. The Journal of biological chemistry. 2001;276(23):20688-94. Epub 2001/03/29. doi: 10.1074/jbc.M100174200. PubMed PMID: 11274206.

148. Son DS, Roby KF. Interleukin-1alpha-induced chemokines in mouse granulosa cells: impact on keratinocyte chemoattractant chemokine, a CXC subfamily. Mol Endocrinol. 2006;20(11):2999-3013. Epub 2006/07/11. doi: 10.1210/me.2006-0001. PubMed PMID: 16825293.

149. Suzuki H, Yagi K, Kondo M, Kato M, Miyazono K, Miyazawa K. c-Ski inhibits the TGF-beta signaling pathway through stabilization of inactive Smad complexes on Smad-binding elements. Oncogene. 2004;23(29):5068-76. Epub 2004/04/27. doi: 10.1038/sj.onc.1207690. PubMed PMID: 15107821.

150. Frederick JP, Liberati NT, Waddell DS, Shi Y, Wang XF. Transforming growth factor beta-mediated transcriptional repression of c-myc is dependent on direct binding of Smad3 to a novel repressive Smad binding element. Molecular and cellular biology. 2004;24(6):2546-59. Epub 2004/03/03. PubMed PMID: 14993291; PubMed Central PMCID: PMC355825.

151. Heldin CH, Moustakas A. Role of Smads in TGFbeta signaling. Cell and tissue research. 2012;347(1):21-36. Epub 2011/06/07. doi: 10.1007/s00441-011-1190-x. PubMed PMID: 21643690.

152. Shi Y, Wang YF, Jayaraman L, Yang H, Massague J, Pavletich NP. Crystal structure of a Smad MH1 domain bound to DNA: insights on DNA binding in TGF-beta signaling. Cell. 1998;94(5):585-94. Epub 1998/09/19. PubMed PMID: 9741623.

153. Zawel L, Dai JL, Buckhaults P, Zhou S, Kinzler KW, Vogelstein B, et al. Human Smad3 and Smad4 are sequence-specific transcription activators. Molecular cell. 1998;1(4):611-7. Epub 1998/07/14. PubMed PMID: 9660945.

154. Stroschein SL, Wang W, Luo K. Cooperative binding of Smad proteins to two adjacent DNA elements in the plasminogen activator inhibitor-1 promoter mediates transforming growth factor beta-induced smad-dependent transcriptional activation. The Journal of biological chemistry. 1999;274(14):9431-41. Epub 1999/03/27. PubMed PMID: 10092624.

155. Keeton MR, Curriden SA, van Zonneveld AJ, Loskutoff DJ. Identification of regulatory sequences in the type 1 plasminogen activator inhibitor gene responsive to transforming growth factor beta. The Journal of biological chemistry. 1991;266(34):23048-52. Epub 1991/12/05. PubMed PMID: 1744101.

156. Lau MT, Lin SW, Ge W. Identification of Smad Response Elements in the Promoter of Goldfish FSHbeta Gene and Evidence for Their Mediation of Activin and GnRH Stimulation of FSHbeta Expression. Frontiers in endocrinology. 2012;3:47. Epub 2012/05/31. doi: 10.3389/fendo.2012.00047. PubMed PMID: 22645522; PubMed Central PMCID: PMC3355844.

157. Choy L, Derynck R. Transforming growth factor-beta inhibits adipocyte differentiation by Smad3 interacting with CCAAT/enhancer-binding protein (C/EBP) and repressing C/EBP transactivation function. The Journal of biological chemistry. 2003;278(11):9609-19. Epub 2003/01/14. doi: 10.1074/jbc.M212259200. PubMed PMID: 12524424.

158. Coyle-Rink J, Sweet T, Abraham S, Sawaya B, Batuman O, Khalili K, et al. Interaction between TGFbeta signaling proteins and C/EBP controls basal and Tat-mediated transcription of HIV-1 LTR in astrocytes. Virology. 2002;299(2):240-7. Epub 2002/08/31. PubMed PMID: 12202226.

159. Mueller KL, Madden JM, Zoratti GL, Kuperwasser C, List K, Boerner JL. Fibroblast-secreted hepatocyte growth factor mediates epidermal growth factor receptor tyrosine kinase inhibitor resistance in triple-negative breast cancers through paracrine activation of Met. Breast cancer research : BCR. 2012;14(4):R104. Epub 2012/07/14. doi: 10.1186/bcr3224. PubMed PMID: 22788954; PubMed Central PMCID: PMC3680928.

160. Cheng N, Chytil A, Shyr Y, Joly A, Moses HL. Transforming growth factor-beta signaling-deficient fibroblasts enhance hepatocyte growth factor signaling in mammary carcinoma cells to promote scattering and invasion. Molecular cancer research : MCR. 2008;6(10):1521-33. Epub 2008/10/17. doi: 10.1158/1541-7786.MCR-07-2203. PubMed PMID: 18922968; PubMed Central PMCID: PMC2740918.

161. Comoglio PM, Giordano S, Trusolino L. Drug development of MET inhibitors: targeting oncogene addiction and expedience. Nature reviews Drug discovery. 2008;7(6):504-16. Epub 2008/05/31. doi: 10.1038/nrd2530. PubMed PMID: 18511928.

162. Eder JP, Vande Woude GF, Boerner SA, LoRusso PM. Novel therapeutic inhibitors of the c-Met signaling pathway in cancer. Clinical cancer research : an official journal of the American Association for Cancer Research. 2009;15(7):2207-14. Epub 2009/03/26. doi: 10.1158/1078-0432.CCR-08-1306. PubMed PMID: 19318488.

163. Kawaguchi Y, Harigai M, Hara M, Fukasawa C, Takagi K, Tanaka M, et al. Expression of hepatocyte growth factor and its receptor (c-met) in skin fibroblasts from patients with systemic sclerosis. The Journal of rheumatology. 2002;29(9):1877-83. Epub 2002/09/18. PubMed PMID: 12233882.

164. Lin YM, Huang YL, Fong YC, Tsai CH, Chou MC, Tang CH. Hepatocyte growth factor increases vascular endothelial growth factor-A production in human synovial fibroblasts through c-Met receptor pathway. PloS one. 2012;7(11):e50924. Epub 2012/12/05. doi: 10.1371/journal.pone.0050924. PubMed PMID: 23209838; PubMed Central PMCID: PMC3508989.

165. Longati P, Bardelli A, Ponzetto C, Naldini L, Comoglio PM. Tyrosines1234-1235 are critical for activation of the tyrosine kinase encoded by the MET proto-oncogene (HGF receptor). Oncogene. 1994;9(1):49-57. Epub 1994/01/01. PubMed PMID: 8302603.

166. Puri N, Khramtsov A, Ahmed S, Nallasura V, Hetzel JT, Jagadeeswaran R, et al. A selective small molecule inhibitor of c-Met, PHA665752, inhibits tumorigenicity and angiogenesis in mouse lung cancer xenografts. Cancer research. 2007;67(8):3529-34. Epub 2007/04/19. doi: 10.1158/0008-5472.CAN-06-4416. PubMed PMID: 17440059.

167. Christensen JG, Schreck R, Burrows J, Kuruganti P, Chan E, Le P, et al. A selective small molecule inhibitor of c-Met kinase inhibits c-Met-dependent phenotypes in vitro and exhibits cytoreductive antitumor activity in vivo. Cancer research. 2003;63(21):7345-55. Epub 2003/11/13. PubMed PMID: 14612533.

168. Tacchini L, De Ponti C, Matteucci E, Follis R, Desiderio MA. Hepatocyte growth factor-activated NF-kappaB regulates HIF-1 activity and ODC expression, implicated in survival, differently in different carcinoma cell lines. Carcinogenesis. 2004;25(11):2089-100. Epub 2004/07/09. doi: 10.1093/carcin/bgh227. PubMed PMID: 15240510.

169. Esencay M, Newcomb EW, Zagzag D. HGF upregulates CXCR4 expression in gliomas via NF-kappaB: implications for glioma cell migration. Journal of neuro-oncology.

2010;99(1):33-40. Epub 2010/02/17. doi: 10.1007/s11060-010-0111-2. PubMed PMID: 20157762.

170. Lin YZ, Yao SY, Veach RA, Torgerson TR, Hawiger J. Inhibition of nuclear translocation of transcription factor NF-kappa B by a synthetic peptide containing a cell membrane-permeable motif and nuclear localization sequence. The Journal of biological chemistry. 1995;270(24):14255-8. Epub 1995/06/16. PubMed PMID: 7782278.

171. Si J, Fu X, Behar J, Wands J, Beer DG, Souza RF, et al. NADPH oxidase NOX5-S mediates acid-induced cyclooxygenase-2 expression via activation of NF-kappaB in Barrett's esophageal adenocarcinoma cells. The Journal of biological chemistry. 2007;282(22):16244-55. Epub 2007/04/04. doi: 10.1074/jbc.M700297200. PubMed PMID: 17403674.

172. Lo HM, Lai TH, Li CH, Wu WB. TNF-alpha induces CXCL1 chemokine expression and release in human vascular endothelial cells in vitro via two distinct signaling pathways. Acta pharmacologica Sinica. 2014;35(3):339-50. Epub 2014/02/04. doi: 10.1038/aps.2013.182. PubMed PMID: 24487964.

173. Pollard JW. Tumour-stromal interactions. Transforming growth factor-beta isoforms and hepatocyte growth factor/scatter factor in mammary gland ductal morphogenesis. Breast cancer research : BCR. 2001;3(4):230-7. Epub 2001/07/04. PubMed PMID: 11434874; PubMed Central PMCID: PMC138687.

174. Dunn NR, Koonce CH, Anderson DC, Islam A, Bikoff EK, Robertson EJ. Mice exclusively expressing the short isoform of Smad2 develop normally and are viable and fertile. Genes & development. 2005;19(1):152-63. Epub 2005/01/05. doi: 10.1101/gad.1243205. PubMed PMID: 15630024; PubMed Central PMCID: PMC540233.

175. Yagi K, Goto D, Hamamoto T, Takenoshita S, Kato M, Miyazono K. Alternatively spliced variant of Smad2 lacking exon 3. Comparison with wild-type Smad2 and Smad3. The Journal of biological chemistry. 1999;274(2):703-9. Epub 1999/01/05. PubMed PMID: 9873005.

176. Randall RA, Germain S, Inman GJ, Bates PA, Hill CS. Different Smad2 partners bind a common hydrophobic pocket in Smad2 via a defined proline-rich motif. The EMBO journal. 2002;21(1-2):145-56. Epub 2002/01/10. doi: 10.1093/emboj/21.1.145. PubMed PMID: 11782434; PubMed Central PMCID: PMC125817.

177. Feng XH, Lin X, Derynck R. Smad2, Smad3 and Smad4 cooperate with Sp1 to induce p15(Ink4B) transcription in response to TGF-beta. The EMBO journal. 2000;19(19):5178-93. Epub 2000/10/03. doi: 10.1093/emboj/19.19.5178. PubMed PMID: 11013220; PubMed Central PMCID: PMC302105.

178. Bonni S, Wang HR, Causing CG, Kavsak P, Stroschein SL, Luo K, et al. TGF-beta induces assembly of a Smad2-Smurf2 ubiquitin ligase complex that targets SnoN

for degradation. Nature cell biology. 2001;3(6):587-95. Epub 2001/06/05. doi: 10.1038/35078562. PubMed PMID: 11389444.

179. Dean RA, Cox JH, Bellac CL, Doucet A, Starr AE, Overall CM. Macrophage-specific metalloelastase (MMP-12) truncates and inactivates ELR+ CXC chemokines and generates CCL2, -7, -8, and -13 antagonists: potential role of the macrophage in terminating polymorphonuclear leukocyte influx. Blood. 2008;112(8):3455-64. Epub 2008/07/29. doi: 10.1182/blood-2007-12-129080. PubMed PMID: 18660381.

180. Schmid I, Uittenbogaart CH, Giorgi JV. A gentle fixation and permeabilization method for combined cell surface and intracellular staining with improved precision in DNA quantification. Cytometry. 1991;12(3):279-85. Epub 1991/01/01. doi: 10.1002/cyto.990120312. PubMed PMID: 1709845.

181. Cheng WL, Wang CS, Huang YH, Tsai MM, Liang Y, Lin KH. Overexpression of CXCL1 and its receptor CXCR2 promote tumor invasion in gastric cancer. Annals of oncology : official journal of the European Society for Medical Oncology / ESMO. 2011;22(10):2267-76. Epub 2011/02/24. doi: 10.1093/annonc/mdq739. PubMed PMID: 21343381.

182. Bolitho C, Hahn MA, Baxter RC, Marsh DJ. The chemokine CXCL1 induces proliferation in epithelial ovarian cancer cells by transactivation of the epidermal growth factor receptor. Endocrine-related cancer. 2010;17(4):929-40. Epub 2010/08/13. doi: 10.1677/ERC-10-0107. PubMed PMID: 20702723.

183. Zlotnik A, Yoshie O. The chemokine superfamily revisited. Immunity. 2012;36(5):705-16. Epub 2012/05/29. doi: 10.1016/j.immuni.2012.05.008. PubMed PMID: 22633458; PubMed Central PMCID: PMC3396424.

184. Fresno Vara JA, Casado E, de Castro J, Cejas P, Belda-Iniesta C, Gonzalez-Baron M. PI3K/Akt signalling pathway and cancer. Cancer treatment reviews. 2004;30(2):193-204. Epub 2004/03/17. doi: 10.1016/j.ctrv.2003.07.007. PubMed PMID: 15023437.

185. Wu Y, Zhou BP. TNF-alpha/NF-kappaB/Snail pathway in cancer cell migration and invasion. British journal of cancer. 2010;102(4):639-44. Epub 2010/01/21. doi: 10.1038/sj.bjc.6605530. PubMed PMID: 20087353; PubMed Central PMCID: PMC2837572.

186. Bours V, Bentires-Alj M, Hellin AC, Viatour P, Robe P, Delhalle S, et al. Nuclear factor-kappa B, cancer, and apoptosis. Biochemical pharmacology. 2000;60(8):1085-9. Epub 2000/09/29. PubMed PMID: 11007945.

187. Demuth T, Reavie LB, Rennert JL, Nakada M, Nakada S, Hoelzinger DB, et al. MAP-ing glioma invasion: mitogen-activated protein kinase kinase 3 and p38 drive glioma invasion and progression and predict patient survival. Molecular cancer

therapeutics. 2007;6(4):1212-22. Epub 2007/04/05. doi: 10.1158/1535-7163.MCT-06-0711. PubMed PMID: 17406030.

188. Miyake M, Goodison S, Urquidi V, Gomes Giacoia E, Rosser CJ. Expression of CXCL1 in human endothelial cells induces angiogenesis through the CXCR2 receptor and the ERK1/2 and EGF pathways. Laboratory investigation; a journal of technical methods and pathology. 2013;93(7):768-78. Epub 2013/06/05. doi: 10.1038/labinvest.2013.71. PubMed PMID: 23732813.

189. Kim D, Kim S, Koh H, Yoon SO, Chung AS, Cho KS, et al. Akt/PKB promotes cancer cell invasion via increased motility and metalloproteinase production. FASEB journal : official publication of the Federation of American Societies for Experimental Biology. 2001;15(11):1953-62. Epub 2001/09/05. doi: 10.1096/fj.01-0198com. PubMed PMID: 11532975.

190. Dan HC, Cooper MJ, Cogswell PC, Duncan JA, Ting JP, Baldwin AS. Akt-dependent regulation of NF-{kappa}B is controlled by mTOR and Raptor in association with IKK. Genes & development. 2008;22(11):1490-500. Epub 2008/06/04. doi: 10.1101/gad.1662308. PubMed PMID: 18519641; PubMed Central PMCID: PMC2418585.

191. Datta SR, Dudek H, Tao X, Masters S, Fu H, Gotoh Y, et al. Akt phosphorylation of BAD couples survival signals to the cell-intrinsic death machinery. Cell. 1997;91(2):231-41. Epub 1997/11/05. PubMed PMID: 9346240.

192. Nannuru KC, Sharma B, Varney ML, Singh RK. Role of chemokine receptor CXCR2 expression in mammary tumor growth, angiogenesis and metastasis. Journal of carcinogenesis. 2011;10:40. Epub 2012/03/01. doi: 10.4103/1477-3163.92308. PubMed PMID: 22368515; PubMed Central PMCID: PMC3284109.

193. Bevers TB, Anderson BO, Bonaccio E, Buys S, Daly MB, Dempsey PJ, et al. NCCN clinical practice guidelines in oncology: breast cancer screening and diagnosis. Journal of the National Comprehensive Cancer Network : JNCCN. 2009;7(10):1060-96. Epub 2009/11/26. PubMed PMID: 19930975.

194. Yehiely F, Moyano JV, Evans JR, Nielsen TO, Cryns VL. Deconstructing the molecular portrait of basal-like breast cancer. Trends in molecular medicine. 2006;12(11):537-44. Epub 2006/10/03. doi: 10.1016/j.molmed.2006.09.004. PubMed PMID: 17011236.

195. Masuda H, Zhang D, Bartholomeusz C, Doihara H, Hortobagyi GN, Ueno NT. Role of epidermal growth factor receptor in breast cancer. Breast cancer research and treatment. 2012;136(2):331-45. Epub 2012/10/18. doi: 10.1007/s10549-012-2289-9. PubMed PMID: 23073759; PubMed Central PMCID: PMC3832208.

196. Cui JJ. Targeting receptor tyrosine kinase MET in cancer: small molecule inhibitors and clinical progress. Journal of medicinal chemistry. 2014;57(11):4427-53. Epub 2013/12/11. doi: 10.1021/jm401427c. PubMed PMID: 24320965.

197. White JR, Lee JM, Young PR, Hertzberg RP, Jurewicz AJ, Chaikin MA, et al. Identification of a potent, selective non-peptide CXCR2 antagonist that inhibits interleukin-8-induced neutrophil migration. The Journal of biological chemistry. 1998;273(17):10095-8. Epub 1998/05/30. PubMed PMID: 9553055.

Appendix A: List of Publications and Accomplishments

Publications

An Zou, Diana L Lambert, Henry Yeh, Ken Yasukawa, Fariba Behbod, Fang Fan, **Nikki Cheng** (2014) Elevated CXCL1 expression in breast cancer stroma predicts poor prognosis and is inversely associated with expression of TGF-beta signaling proteins *(manuscript submitted for BMC Cancer)*

An Zou*, **Wei Bin Fang***, Diana Lambert, Min Yao, Benford Mafuvadze, Mike Portsche, **Nikki Cheng** (2014) TGF-beta Negatively Regulates CXCL1 Expression in Mammary Carcinoma Associated Fibroblasts by Activation of Smad2/3 and Inhibition of HGF/c-Met Autocrine Signaling. *(manuscript in preparation for Plos One, *equal contributors)*

Fang WB, Jokar I, **Zou A**, Lambert D, Dendukuri P, **Nikki Cheng** (2012) CCL2/CCR2 chemokine signaling coordinates survival and motility of breast cancer cells through Smad3 protein- and p42/44 mitogen-activated protein kinase (MAPK)-dependent mechanisms. *J Biol. Chem. 287(43), 36593-608.*

Abstracts and Posters Published

An Zou, Diana Lambert, **Nikki Cheng**. De-regulated CXCL1 secretion from tumor stromal cells promotes mammary tumor cell invasion. *(KUCC Research Symposium. Kansas City. November 2013. Poster Presentation)*

An Zou, Diana Lambert, Henry Yeh, Wei Bin Fang, **Nikki Cheng**. TGF-β regulates CXCL1 expression in mammary carcinoma associated fibroblasts through novel Smad2/3- and HGF/c-Met-dependent mechanisms. *(Cellular Heterogeneity in the Tumor Microenvironment, AACR. San Diego. February 2014. Poster Presentation)*

An Zou, Diana Lambert, **Nikki Cheng**. TGF-β regulates CXCL1 expression in mammary carcinoma-associated fibroblasts through novel Smad2/3- and HGF/c-Met-dependent mechanisms. *(KU Student Research Forum, Kansas City. April 2014. Oral Presentation)*

An Zou, Diana Lambert, **Nikki Cheng**. TGF-β regulates CXCL1 expression in mammary carcinoma-associated fibroblasts through novel Smad2/3- and HGF/c-Met-dependent mechanisms. *(KU Student Research Forum, Kansas City. April 2013. Oral Presentation)*

An Zou, **Nikki Cheng**. Role of CXCL1 signaling in breast cancer progression. *(KUCC Research Symposium. Kansas City. November 2012. Poster Presentation)*

An Zou, Diana Lambert, **Nikki Cheng**. Role of CXCL1 signaling in mammary tumor progression. *(KU Student Research Forum, Kansas City. March 2012. Oral Presentation)*

An Zou, **Nikki Cheng**. Role of CXCL1 signaling in mammary tumor progression. *(KUCC Research Symposium. Kansas City. November 2011. Poster Presentation)*

An Zou, **Nikki Cheng**. Role of CXCL1 signaling in breast cancer progression. *(KUCC Research Symposium. Kansas City. November 2010. Poster Presentation)*

Awards

An Zou, mentor: **Nikki Cheng**. Honorable Mentions *(KU Student Research Forum, Kansas City. April 2014. Oral Presentation)*

An Zou, mentor: **Nikki Cheng**. Certificate of Excellence *(Graduate Studies Program, Department of Pathology and Laboratory Medicine, Kansas City. May 2013.)*